الجمهورية الجزائرية الديمقراطية الشعبية
وزارة التعليم العالي والبحث العلمي

BADJI MOKHTAR- ANNABA UNIVERSITY
UNIVERSITE BADJI MOKHTAR - ANNABA

جامعة باجي مختار-عنابة

Faculté : Sciences de l'ingéniorat **Année : 2021**
Département : Electronique

THÈSE

Présentée en vue de l'obtention du diplôme de Doctorat en sciences

Intitulé

Méthodologie pour la séparation de mélanges de signaux OFDM

Option : Télécommunications

Par : ATOUI Sakina

DEVANT Le JURY :

PRESIDENT :	**FEZARI Mohamed**	**Pr. Univ. Annaba**
DIRECTEUR DE THÈSE :	**DOGHMANE Noureddine**	**Pr. Univ. Annaba**
CO-DIRECTEUR DE THÈSE :	**LAFIFI Sadek**	**Pr. Univ. Annaba**
EXAMINATEURS :	**BENATIA Djamel**	**Pr. Univ. Batna**
	BAARIR Zine-Eddine	**Pr. Univ. Biskra**
	BOUDEN Toufik	**Pr. Univ. Jijel**

الجمهورية الجزائرية الديمقراطية الشعبية
وزارة التعليم العالي والبحث العلمي

BADJI MOKHTAR- ANNABA UNIVERSITY
UNIVERSITÉ BADJI MOKHTAR- ANNABA

جامعة باجي مختار -عنابة

Faculty: Sciences of Engineering
Department: Electronics

Year: 2021

THESIS

Presented in order to obtain the diploma of Doctorate in science

Entitled

Methodology for OFDM Mixture Signals Separation

Option: Telecommunications

By: ATOUI Sakina

COMMITTEE MEMBERS :

PRESIDENT :	**FEZARI Mohamed**	**Pr.Univ. Annaba**
SUPERVISOR :	**DOGHMANE Noureddine**	**Pr. Univ. Annaba**
CO-SUPERVISOR :	**LAFIFI Saddek**	**Pr. Univ. Annaba**
REVIEWERS :	**BENATIA Djamel**	**Pr.Univ.Batna**
	BAARIR Zine-Eddine	**Pr. Univ. Biskra**
	BOUDEN Toufik	**Pr. Univ. Jijel**

Dedications

To the memory of my brother Atoui Zoheir (1977-2018)

To my father Saifi and to my mother Fatima.

To my husband fodil and my brothers: Mounir, Sofiane, Hicham, Halim, Ala-eddine.

To my sister Karima.

To my loving children: AbdErraouf, Asma, Amina.

To my husband' father and to my husband's mother.

To my loving nephews: Wassim, Anes, Adam, Ayoubzoheir.

To my loving nieces: Maria, Assile, Meriem, Marame.

To my friends: Hanane, Fatiha, Nadia, Ghania, Zahra, Imane, Houda, Fathia, Chamia, Amina, Wassila …

To all my Family…

Acknowledgements

First, I would like to give the most sincere thanks to my supervisor **Pr Doghmane Noureddine** and my co-supervisor **Pr Lafifi Saddek** for their support and advice throughout the duration of my research work and the preparation of this thesis. I am extremely grateful to my supervisor for all kinds of support and guidance.

I would like to acknowledge the committee members for their interest in my work:

- The president of the committee **Pr FEZARI Mohamed** from the University of Annaba.
- The reviewer **Pr BENATIA Djamel** from the University of Batna.
- The reviewer **Pr BAARIR Zine-Eddine** from the University of Biskra.
- The reviewer **Pr BOUDEN Toufik** from the University of Jijel.

I would also like to thank all my friends and colleagues at Unit of development of solar equipment UDES (EPST/CDER) Tipaza, Algeria.

I would like to express my deepest gratitude to my brothers Hicham, Halim and Ala-Eddine for their helps.

Finally, I would like to thank my husband and my parents. Without your unconditional support, your kind words, I would not accomplish my work.

ملخص

في هذه الأطروحة، تمت دراسة تقنية التجميع التعامدي بتقسيم التردد OFDM المرتقب استعمالها في شبكات الجيل الخامس اللاسلكية. يمكن لهذه التقنية الواعدة التغلب على التداخل بين الرموز(ISI) الذي ينتج عن الطبيعة التشتتية للوقت للقنوات اللاسلكية. أولاً ، يتم شرح المبادئ الأساسية لهذه التقنية على سبيل المثال التجميع التعامدي، والبادئة الدورية ، وتحول فوريه السريع Fast Fourier Transform FFT ، ووتحول فورييه السريع المعاكسInverse Fast Fourier Transform IFFT.كذلك تقديم المخطط الصندوقي الدى يوصف تقنية عملOFDM. يتم تقديم عيوب OFDM وتحليل تأثير إزاحة تردد الموجة الحاملة بالتفصيل. تمت مناقشة العديد من التقنيات التي تخفف التداخل بين تردد الموجات الحاملةInter Carrier Interference ICIمع العرض الجيد لبعض الطرق الأساسية الموجودة. على وجه الخصوص ، تتم مراجعة طريقة الإمكانية القصوى للتشابه (ML)بالتفاصيل.

نقترح مقدّر تخالف التردد الأعمى الذي يستخدم الارتباطات بين التتابع المعاد تشكيله في جانب المستقبل والرمز المستقبِل التقليدي ، ويستخلص حل لتأثير إزاحة تردد الموجة الحاملة . يتم اشتقاق المقدّر المقترح ضمن فترة زمنية قصيرة عندما يكون الارتباط عاليًا ، لذلك يكون تعقيدها لحسابي منخفض. تستخدم مقدرات لين Lin وبيك Beek للمقارنة. تُظهر المحاكاة فعالية المقدّر المقترح ضمن قناة خفوترايلي Rayleigh fading channel . يمكن تنفيذ المقدّر المقترح بكفاءة باستخدام نظام OFDM. تحت نفس تكوين النظام ، توضح نتائج المحاكاة الأداء الممتاز للمقدر المقترح عند مقارنته بأداء التقنيات الأخرى لأي قيمة SNR.

كلمات البحث: إزاحة تردد الموجة الحاملة (CFO) ؛ مضاعفة تقسيم التردد المتعامد (OFDM) ؛ التداخل بين الموجات الحاملة (ICI) ؛ قناة AWGN ؛ قناة خفوترايلي.

Résumé

Dans cette thèse, la technique OFDM (Orthogonal Frequency Division Multiplexing) de multiplexage en fréquence multi porteuses envisagée pour les réseaux sans fil de cinquième génération est étudiée. Cette technique prometteuse peut surmonter l'interférence inter-symboles (ISI) qui résulte de la nature dispersive dans le temps des canaux sans fil. Tout d'abord, les principes de base de cette technique sont expliqués comme l'orthogonalité, le préfixe cyclique, la transformée de Fourier rapide (FFT) et l'inverse de la transformée de Fourier rapide (IFFT). Une implémentation efficace d'OFDM est également décrite. Les dégradations de l'OFDM sont présentées et l'effet de décalage de fréquence de la porteuse est analysé en détail. Plusieurs techniques qui atténuent les interférences inter-porteuses (ICI) sont discutées et certaines méthodes de base sont bien présentées. En particulier, l'estimation du maximum de vraisemblance est examinée en détail.

Un estimateur de décalage de fréquence aveugle qui utilise les corrélations entre la séquence remodulée du côté récepteur et le symbole reçu conventionnel est présenté et une solution sous forme fermée est dérivée. L'estimateur proposé est dérivé sous un court intervalle lorsque la corrélation est élevée, il a donc une faible complexité de calcul. Les estimateurs de Lin et Beek sont utilisés pour la comparaison. Les simulations démontrent l'efficacité de l'estimateur proposé sous le canal d'évanouissement de Rayleigh. L'estimateur proposé peut être mis en œuvre efficacement en utilisant le système OFDM. Sous la même configuration de système, les résultats de simulation démontrent l'excellente performance de l'estimateur proposé par rapport à la performance d'autres techniques pour n'importe quelle valeur de SNR.

Mots-clefs : Décalage de fréquence porteuse (CFO); Multiplexage par répartition orthogonale de fréquence (OFDM); Interférence entre porteuses (ICI); Canal AWGN; Rayleigh fading channel.

Abstract

In this thesis, the orthogonal frequency division multiplexing (OFDM) technique envisioned for fifth-generation wireless networks is studied. This promising technique can overcome the intersymbol interference (ISI) which results from the time-dispersive nature of wireless channels. First, the basic principles of this technique—orthogonality, cyclic prefix (CP), fast Fourier transform (FFT) and inverse fast Fourier transform (IFFT)—are explained. An efficient implementation of the OFDM technique is also described. The OFDM impairments are presented, and the carrier frequency offset (CFO) effect is analyzed in detail. Several techniques that mitigate intercarrier interference (ICI) are discussed and some basic methods are presented. In particular, the maximum likelihood estimation (MLE) is reviewed in detail.

A blind frequency offset estimator that uses the correlations between the remodulated sequence on the receiver side and the conventional received symbol is presented, and a closed form solution is derived. The proposed estimator is derived under short intervals when the correlation is high, so it has low computational complexity. Lin and Beek's estimators are used for comparison. Simulations demonstrate the effectiveness of the proposed estimator under a Rayleigh fading channel. The proposed estimator can be implemented efficiently using the OFDM system. Under the same system configuration, simulation results demonstrate the excellent performance of the proposed estimator when compared to the performance of other techniques for any signal-to-noise (SNR) value.

Keywords: Carrier frequency offset (CFO); Orthogonal frequency division multiplexing (OFDM); Inter-carriers interference (ICI); AWGN channel; Rayleigh fading channel.

Contents

List of figures

List of tables

Nomenclature

1G	First Generation
3G	Third Generation
4G	Fourth Generation
5G	Fifth Generation
AMPS	Advanced Mobile Phone System
AWGN	Additive White Gaussian Noise
BER	Bit Error Rate
BEM	Basis Expansion Model
BPSK	Binary Phase Shift Keying
BSS	Blind Source Separation
CDMA	Code Division Multiple Access
CE-BEM	Complex Exponential Basis Expansion Model

CIR	Carrier to Interference power Ratio
CFO	Carrier Frequency Offset
CP	Cyclic Prefix
CPE	Common Phase Error
CRB	Cramer-Rao Bound
DAC	Digital –to-Analog Converter
DAB	Digital Audio Broadcasting
DFT	Discret Fourier Transform
DMIMO	Distributed Multiple Input Multiple Output
DSP	Digital Signal Processing
DVB	Digital Video Broadcasting
ECM	Expectation Conditional Maximization
EDGE	Enhanced Data Rates for GSM Evolution

eMBB	Enhanced Mobile Broadband
FDM	Frequency Division Multiplexing
FDMA	Frequency Division Multiple Access
FFT	Fast Fourier Transform
FFO	Fractional Frequency Offset
GPRS	General Packet Radio Service
GSM	Global System for Mobile Communications
HPA	High Power Amplifier
ICI	Inter Carrier Interference
IFFT	Inverse Fast Fourier Transform
IDFT	Inverse Discret Fourier Transform
IFO	Integer Frequency Offset
IMT	International Mobile Telecommunication

IP	Internet Protocol
ISI	Inter Symbol Interference
L-BEM	Legendre Basis Expansion Model
LTE	Long Term Evolution
LTV	Linear Time Varying channel
MCFO	Multiple Carrier Frequency Offset
ML	Maximum Likelihood
MSE	Mean Squared Error
MTO	Multiple Time Offset
OFDM	Orthogonal Frequency Division Multiplexing
PAPR	Peak-to- Average Power Ratio
PDF	Probability Density Function
PHN	Phase Noise

PLL	Phase-Locked Loop
PSK	Phase Shift Keying
PSD	Power Spectral Density
QAM	Quadrature Amplitude Modulation
QPSK	Quadrature Phase Shift Keying
RF	Radio Frequency
SAGE	Space Alternating Generalized Expectation
SNR	Signal to Noise Ratio
TD-SCDMA	Time Division Synchronous Code Division Multiple Access
Ts	Symbol duration
UMTS	Universal Mobile Telecommunication System
URLLC	Ultra-Reliable Low Latency Communication
VCO	Voltage-Controlled Oscillator

WCDMA	Wideband Code Division Multiple Access
WSSUS	Wide-Sense Stationary Uncorrelated Scattering

INTRODUCTION

In the communication protocol, signals are always affected by distortion and mixture. So, separating the signals mixture is a big challenge. Having a prior information about the received data is advantageous but this diminish the bandwidth of the signal which decrease the data rates. However, high data rates is very required for the fifth generation wireless communication and the future generations, so theories of blind source or signal separation are necessary to overcome this lack and recover unobserved signals or sources from several observed mixtures when no prior information is available about the transfer.

The adjective "blind" emphasizes that the source signals are not observed or no information is available about the mixture. The shortage of prior information about the mixture is compensated by a statistical strong but often physically plausible assumption of independence between the source signals. The downside of using the prior information is the decrease in bandwidth length which is precisely the strength of the blind source separation (BSS) model. Since training or pilot data sequences are not required by blind schemes higher effective data rates are expected to be delivered. Semi-blind schemes are developed to overcome some of the drawbacks of blind schemes with reduced amount of training or pilot data in order to increase the performance. Principal components analysis, singular value decomposition, independent component analysis, dependent component analysis, non-negative matrix factorization, low-complexity coding and decoding and stationary subspace analysis can be introduced as the key categories or branches of BSS [1].

The applicability of blind source separation (BSS) principles to wireless communication systems is one of the main lines of research. Some studies are used BSS in algorithms in communications, signal processing and neural networks can be noted in [2]. These BSS algorithms are supported by energy criterion functions. The use of these types of approaches is efficient to improve the performance of well established most demanded systems based on the techniques like orthogonal frequency division multiplexing (OFDM). This is part of the attempt to meet the ever increasing demand for higher capacity communication systems.

Cellular communications have changed over years to meet human communication needs. Analog cellular network communication was developed in 1980s. Based on the Advanced Mobile Phone System (AMPS), it used frequency division multiple access (FDMA) with a channel capacity of 30 KHz and frequency band of 824-894MHz. The main drawbacks of this technology were low capacity, poor security and unreliable handoff coverage. To overcome those limitations, the second

generation mobile network, called the global system for mobile communications (GSM), was launched in 1991[3]. Based on digital technology, it provided better quality and capacity, but required stronger digital signals. The GSM technology was improved, and the general packet radio service (GPRS) (2.5G) was invented with speeds of up to 160kbps. These offered high data rates, which allowed the internet and packed-based services to be used. The GSM evolution continued and enhanced data rates for GSM evolution (EDGE) (2.75G) was developed which increased the data rate to 500kbps. The third generation (3G) air interfaces were standardized in 1999 to comply with the ITU (International Telecommunication Union) international mobile telecommunication (IMT-2000) standards [4]. 3G has been applied in wireless voice telephony, mobile internet access, fixed wireless internet access, video calls and mobile TV. It operates at a range of 2100MHz and has a bandwidth of 15-20MHz used for high-speed internet service and video chatting [5]. In Europe, the 3G mobile system is known as UMTS (universal mobile telecommunication system), while CDMA2000 (code division multiple access) is the name of the American variant. In March 2001, the IMT-2000 approved TD-SCDMA (time division-synchronous code division multiple access) developed and deployed exclusively in China as a new 3G standard, while WCDMA (wideband code division multiple access) was developed as the air-interface technology for UMTS [6-7]. 4G, the fourth generation offers the same features as 3G, but also provides additional services like multimedia newspapers, allowing viewers to watch TV programs with more clarity at speeds up to 100Mbps [8]. It presents an all internet protocol (IP) based network system. The first release of the LTE (long term evolution) standard was commercially deployed in Oslo, Norway and Stockholm, Sweden in 2009[9-10]. 4G networks integrate several radio access networks with fixed internet networks [10].

The fifth generation 5G wireless accesses have been improved beyond previous generations of mobile communication. 5G technologies were developed to accommodate the increasing demands for mobile data (i.e., more people using more data on more devices). They include very high data rates, very low latency, ultra-high reliability, energy efficiency and extreme device densities, and are being realized by the development of LTE in combination with new radio-access technologies. Key technology components include extension to higher frequency bands, access/backhaul integration, device-to-device communication, flexible duplex, flexible spectrum usage, multi-antenna transmission, ultra-lean design, and user/control separation [11].

The fifth generation has the capacity to make life easier, in any given society, for everyone: students, government, industries, individuals…. It can make the use of the internet easier. The

ultra-high speed of the fifth generation has enough potential to make the cell phone usability parallel to the laptop.

5G is more advanced than 4G in terms of [12]:

- Increased bit rates
- Increased peak bit rate
- Larger data volume per unit area (i.e. high system spectral efficiency)
- Higher capacity, allowing increased concurrent and instantaneous device connectivity
- Lower battery consumption
- Better connectivity irrespective of the geographic region, in which you are
- Larger number of supporting devices
- Reduced cost of infrastructure development
- Increased communication reliability

Figure 1 shows the difference between 4G/LTE and 5G.

Like all technologies, 5G presents major challenges that we can categorize as follows:

1. Technological challenges:
    - Inter-cell interference
    - Efficient medium access control
    - Traffic management
2. Common challenges:
    - Multiple servicesInfrastructure
    - Communication
    - Navigation and sensing
    - Security and privacy
    - Cyber security legislation

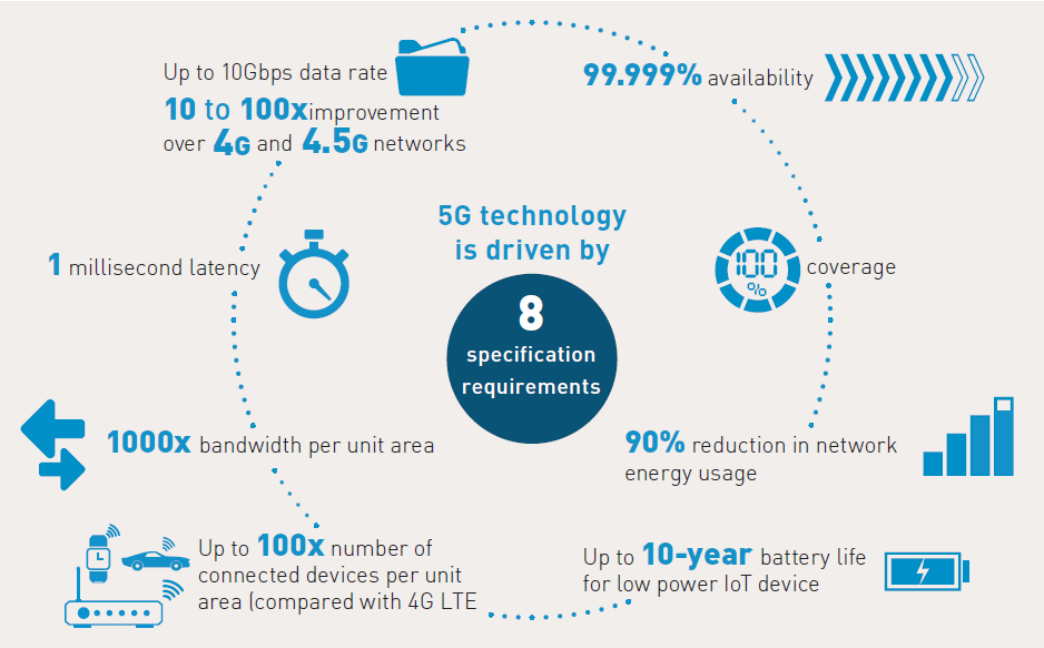

Figure 1. The difference between 4G/LTE and 5G [13]

Advantages of 5G Technology

5G overall is more effective and efficient than previous technologies and has several advantages, including higher resolution and bi-directional large bandwidth shaping, and facilitation of subscriber supervision tools for higher speeds. Other advantages are:

- All networks can be collected on one platform
- Potentially provides huge broadcasting data capacities (in Gigabits), which can support more than 60,000 connections
- Compatible with previous generation technologies
- Technologically sound to support heterogeneous services (including private networks)
- Allows uniform, uninterrupted and consistent global connectivity

Disadvantages of 5G Technology

Although 5G technology has been thoroughly researched and conceptualized to solve all radio signal problems and hardships of the mobile world, because of some security issues and lack of technological advancements in most geographic regions, it has following shortcomings:

- Technology is still a work in progress, and research on its viability is ongoing

- The potential speeds of this technology, which may be attainable in the future, currently seem difficult to achieve in practice because of insufficient technological infrastructure in most parts of the world
- Many of the old devices would not be compatible with 5G; hence, all of them would need to be replaced with new ones: an expensive undertaking
- Developing adequate infrastructure comes with a high cost
- Security and privacy issues are yet to be resolved

An excellent choice for the fourth generation, and of great interest for the fifth generation, is orthogonal frequency division multiplexing (OFDM) techniques, which play a prominent role in the sphere of multicarrier communication. OFDM technique is the most widespread multi-carrier modulation and it is used in many wireless communication systems such as WiFi IEEE 802.11, WiMax IEEE 802.16, LTE, ... ect.

Frequency offsets in OFDM, which remain the main drawbacks of the OFDM system, introduce inter carrier interference (ICI). This thesis focuses on the frequency offset estimation for OFDM-based systems using a blind source separation (BSS) algorithm. This latter is the first mechanism used in extracting unobserved signals from observed mixtures in signal processing. Our work is based on the elimination of inter carrier and inter symbol interference by minimizing the loss of bandwidth in order to overcome the drawbacks of OFDM to be used in the fifth generation. The mean squared error (MSE) and the bit error rate (BER) are approximated for additive white Gaussian noise (AWGN) and multipath channels.

In this thesis, the OFDM (Orthogonal Frequency Division Multiplexing) technique of multi-carrier frequency multiplexing envisaged for fifth generation wireless networks is studied. This promising technique can overcome inter-symbol interference (ISI) that results from the time-dispersive nature of wireless channels. First, the basic principles of this technique are explained such as orthogonality, cyclic prefix, fast Fourier transform (FFT) and inverse fast Fourier transform (IFFT). An efficient implementation of OFDM is also described. The degradations of OFDM are presented and the effect of frequency shifting of the carrier is analyzed in detail. Several techniques that mitigate inter-carrier interference (ICI) are discussed and some basic methods are well presented. In particular, the estimation of maximum likelihood is discussed in detail.

A blind frequency offset estimator which uses the correlations between the remodulated sequence on the receiver side and the conventional received symbol is presented and a closed form solution is derived. The proposed estimator is derived within a short interval when the correlation is high, so it

has low computational complexity. The Lin and Beek estimators are used for the comparison. The simulations demonstrate the efficiency of the estimator proposed under the Rayleigh fading channel. The proposed estimator can be implemented efficiently using OFDM system. Under the same system configuration, the simulation results demonstrate the excellent performance of the proposed estimator compared to the performance of other techniques for any SNR value.

The thesis starts with a general introduction where the development of wireless communication is presented, from 1G to the future fifth generation. The first chapter describes the principle of the OFDM system and its impairments. The main subject in this thesis is the CFO mitigation techniques which are detailed in Chapter 2. The proposed CFO estimator is presented in Chapter 3. The evaluation of the proposed estimator is discussed in Chapter 4.

The details of each of the chapters are described below:

In chapter 1 we have presented and treated the essential properties of the OFDM system. The property of orthogonality between sub-carriers, as well as the concept of orthogonality in the OFDM system are discussed. In order to make the implementation of OFDM possible, the IFFT and the FFT are used in the multiplexing of the transmit and receive OFDM data respectively. We explain the process and operation of IFFT and FFT in more detail. In addition, to attenuate inter-symbol interference and maintain orthogonality, the cyclic prefix, as explained in this chapter, must be longer than the impulse response of the channel. One of the inevitable problems of the OFDM system is its sensitivity to the CFO carrier frequency offset; therefore the effect of CFO is also discussed in detail. Additionally, this chapter highlights other OFDM related issues that affect its performance such as PAPR, phase noise, time varying channel, and timing offset.

Chapter 2 presents methods that mitigate the effect of the CFO carrier frequency offset. First, CFO estimation and compensation techniques are described. An overview of the maximum likelihood (ML) carrier frequency offset estimate is given. The algorithms of the Moose estimator, the Beek estimator, the Classen estimator and the Schmidl Cox estimator are explained in detail. Frequency domain equalization is included. Windowing in the time domain is also discussed in this chapter. However, this method does not address Doppler shift and frequency mismatch between transmitter and receiver. The Kalman filter and self-canceling ICI are well presented. However, the Kalman filter method is limited because it requires linearization of the system. Even though ICI self-cancellation works well, the bandwidth efficiency is reduced by the half.

In Chapter 3 we proposed a new blind frequency offset estimator for the OFDM system. First, the mathematical model and the design parameters of the OFDM system were presented. The effect of

frequency and time offsets are introduced. Next, the multipath channel is described. A carrier frequency offset estimator for OFDM systems on the Rayleigh channel is proposed. This estimator is based on the maximum likelihood method and it uses the correlation between the samples remodulated and received on the receiving side. In addition, the mathematical development of the proposed frequency offset estimator has been described in detail.

Chapter 4 presents the simulation results which prove the efficiency of the proposed estimator compared to Lin and Beek estimators. In addition, the proposed estimator can achieve a much lower MSE using a short guard interval with lower computational complexity. Although the results indicate an improvement in terms of reducing the length of the cyclic prefix and increasing OFDM performance; further research is needed to further reduce the length of the cyclic prefix, eliminate ICI completely and thus be able to increase the performance of OFDM systems.

Finally, this thesis is brought to a close with a general conclusion.

Chapter 1

ORTHOGONAL FREQUENCY DIVISION MULTIPLEXING OFDM

1.1. Introduction

The development of high-speed wireless communications requires high bandwidth efficiency. Hence, large amounts of data transmission happen in shared channels simultaneously. Orthogonal frequency division multiplexing (OFDM) is one kind of such communication modulation that has wide bandwidth efficiency on one side and robustness against multipath channels on the other. It is a multicarrier transmission technique which divides the bandwidth into many carriers; each one modulated by a low rate data stream [14-16]. OFDM prevents interference between the closely spaced carriers by making all of them orthogonal to one another. Thus, OFDM uses the spectrum much more efficiently. In this chapter we present the principal notions of the OFDM system and its impairments.

1.2. Concepts of Orthogonal Frequency Division Multiplexing OFDM

1.2.1. Orthogonality

The orthogonality of the subcarriers is the principal concept in OFDM; each subcarrier is orthogonal to the other subcarriers. Two signals x(t) and y(t) are orthogonal if their dot product is zero. Orthogonality can be achieved by carefully selecting carrier spacing at multiples of 1/Ts, Ts being the symbol duration. As the subcarriers are orthogonal, the spectrum of each carrier has a null at the center frequency of each of the other carriers in the system. This results in no interference between the carriers, allowing them to be spaced as close as theoretically possible. The orthogonality allows simultaneous transmission on a lot of subcarriers in a tight frequency space without interference from each other as shown in Figure 1.1.

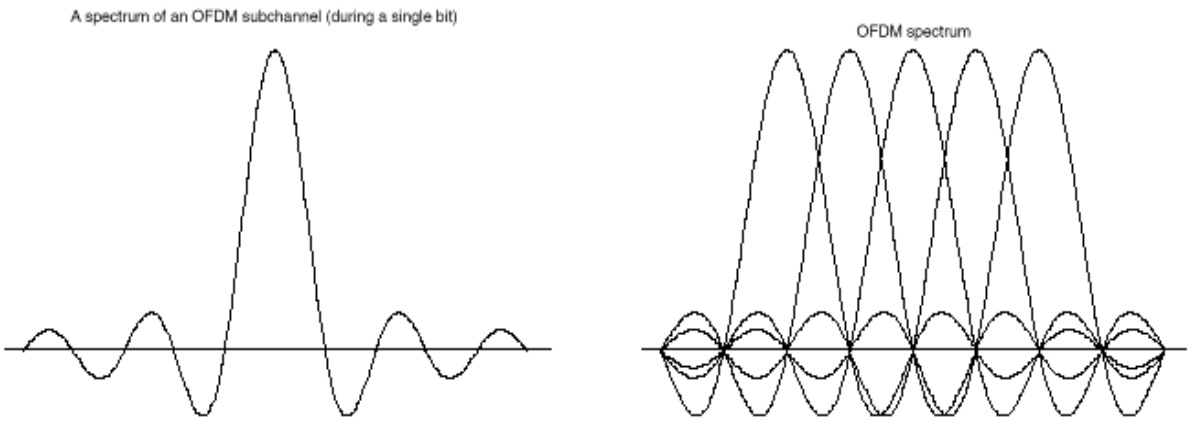

Figure1.1. Examples of OFDM spectrum: (a) a single subchannel, (b) 5 carriers at the central frequency of each subchannel, with no crosstalk from other subchannels

An OFDM signal consists of N orthogonal subcarriers modulated by N parallel data streams. Each baseband subcarrier $\Phi_k(t)$ is of the form

$$\Phi_k(t) = \exp(j2\pi f_k t), \quad \text{k=1,2,3,...,N.} \tag{1.1}$$

Where f_k is the frequency of the k[th] subcarrier. The subcarrier frequencies f_k are equally spaced as follows:

$f_k = k / NT.$

This makes the subcarriers $\Phi_k(t)$ on $0 \le t \le NT$ orthogonal on each other

$$\{\Phi_k(t), \Phi_i(t)\} = \begin{cases} NT & \text{i=k} \\ 0 & \text{i} \neq \text{k} \end{cases} \tag{1.2}$$

1.2.2. Fast Fourier Transform FFT

The fast Fourier transform (FFT), first published in 1965 by J.W. Cooley and J.W. Tuckey, is an algorithm for calculation of the discrete Fourier transform (DFT). It has revolutionized modern experimental mechanics, signal and system analysis, and acoustics, and has paved the way for the introduction of modal analysis. The FFT algorithm applies only to signals comprising a number of elements which are equal to 2^m (e.g. 2^8 = 256, 2^{10}=1024 etc.). Its main advantage is that it significantly reduces the computation time by a factor of the order m/log2m, i.e. more than 100 times for a sample of 1024 elements. FFT, a fast algorithm for computing DFT, can further reduce the number of arithmetic operations from N^2 to NlogN (where N number of symbols).

OFDM transmits a large number of narrowband carriers, closely spaced in the frequency domain. In order to avoid a large number of modulators and filters at the transmitter and complementary filters and demodulators at the receiver, it is desirable to be able to use modern digital signal processing techniques, such as fast Fourier transform (FFT). In the OFDM system, inverse fast Fourier transform/fast Fourier transform (IFFT /FFT) algorithms are used in the modulation and demodulation of the signal. The length of the IFFT/FFT vector determines the resistance of the system to errors caused by the multipath channel.

The use of the FFT technique to implement modulation and demodulation functions makes it computationally more efficient. The reason is that the computation algorithm of DFT needs N^2, however the FFT needs only N log2 N [17], [18]. See Table 1.1.

Table 1.1. Number of operation between DFT and FFT

Bits OFDM Symbol	N	DFT	FFT
1	2	4	2
2	4	16	8
3	8	64	24
4	16	256	64
5	32	1024	160
6	64	4096	384
7	128	16384	896
8	256	65536	2048
9	512	262144	4608
10	1024	1048576	10240

OFDM as a viable modulation scheme came into commercial use with the advancements made in DSP and, more specifically, the inexpensive implementation of the discrete Fourier transform (DFT). DFT is defined as:

$$X(k) = \sum_{n=0}^{N-1} x(n) e^{-j2\pi k \frac{n}{N}} \text{ for } k = 0, \ldots, N-1. \quad (1.3)$$

where $x(n)$ is a sequence of complex numbers, and the inverse DFT (IDFT) is defined as

$$x(n) = \frac{1}{N} \sum_{k=0}^{N-1} X(k) e^{j2\pi k \frac{n}{N}} \text{ for } n = 0, \ldots, N-1. \quad (1.4)$$

The inverse fast Fourier transform (IFFT) performs the same operations as an IDFT, except that it is much more computationally efficient, and so is used in all practical systems. In order to transmit the OFDM signal the calculated time domain signal is then upconverted to the required frequency.

The IFFT and the FFT are complementary functions and the most appropriate term depends on whether the signal is being received or generated. In cases where the signal is independent of this distinction then the terms FFT and IFFT are used interchangeably. The receiver performs the reverse operation of the transmitter, mixing the RF (radio frequency) signal to baseband for processing, using FFT to analyze the signal in the frequency domain. The amplitude and phase of the subcarriers is determined and the signal is then converted back to digital data.

1.2.3. Cyclic Prefix (CP)

In real wireless communication, the transmitted signal passes through the multipath fading channel, in which intersymbol interference (ISI) occurs at the receiver due to the channel delay spread. In order to mitigate ISI, at first researchers proposed to use null guards between OFDM symbols. In 1980, Peled and Ruiz solved the problem of orthogonality and replaced the null guards with cyclic extensions in their OFDM scheme, referred to as cyclic prefix (CP). This CP is the copy of the end of the OFDM symbol added at the beginning of the symbol as shown in Figure 1.2. The cyclic extension converts the linear convoluted channel to simulate a channel performing cyclic convolution, thus ensuring orthogonality over a time-dispersive channel, and eliminating ISI completely between subcarriers as long as the cyclic extension remains longer than the delay spread of the channel. The disadvantage of the CP is the waste of energy.

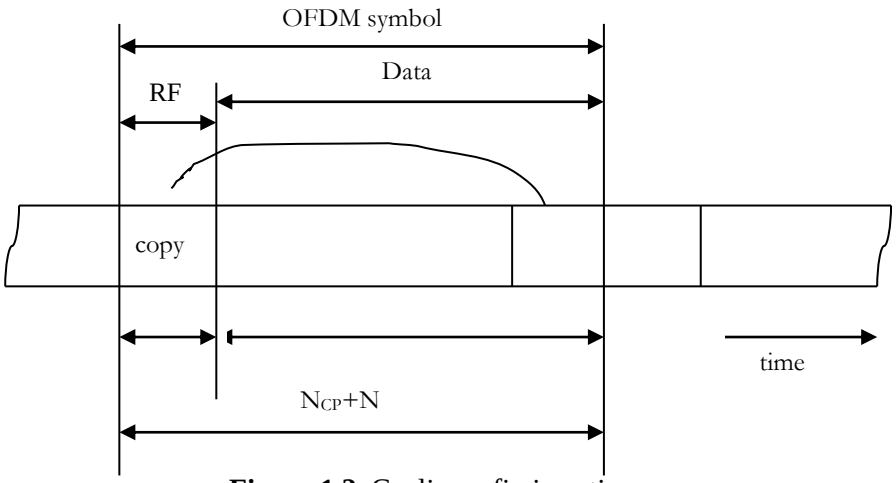

Figure 1.2. Cyclic prefix insertion

After passing by IDFT, the CP is added. Thus, the frame structure of the transmitted OFDM $x(k)$, consisting of $\left(N+N_{CP}\right)$ samples, is given by:

$$x(k)=\left[x_{N-N_{CP}}(k),....,x_{N-1}(k),x_0(k),....,x_{N-1}(k)\right]^T \tag{1.5}$$

The resulting OFDM block length $\left(N+N_{CP}\right)$ samples are upconverted to a radio frequency (RF) centered at f_c and then transmitted through the antenna. [19]

1.2.4. OFDM System Model

The modulation of the set of *K* OFDM subcarriers using an inverse fast Fourier transform (IFFT) is equivalent to modulating each subcarrier individually with a rectangular baseband pulse shaper. The receiver samples the transmitted waveform to obtain *K* samples on which a fast Fourier transform (FFT) is then performed. The FFT modulation is equivalent to performing an integral and dump on each subcarrier using a matched filter of the rectangular baseband waveform. The OFDM system plays a primary role to transform frequency selective channels to narrow band flat fading channels, and generally OFDM makes optimum use of frequency selective channels and eliminates the need for high complexity receivers.

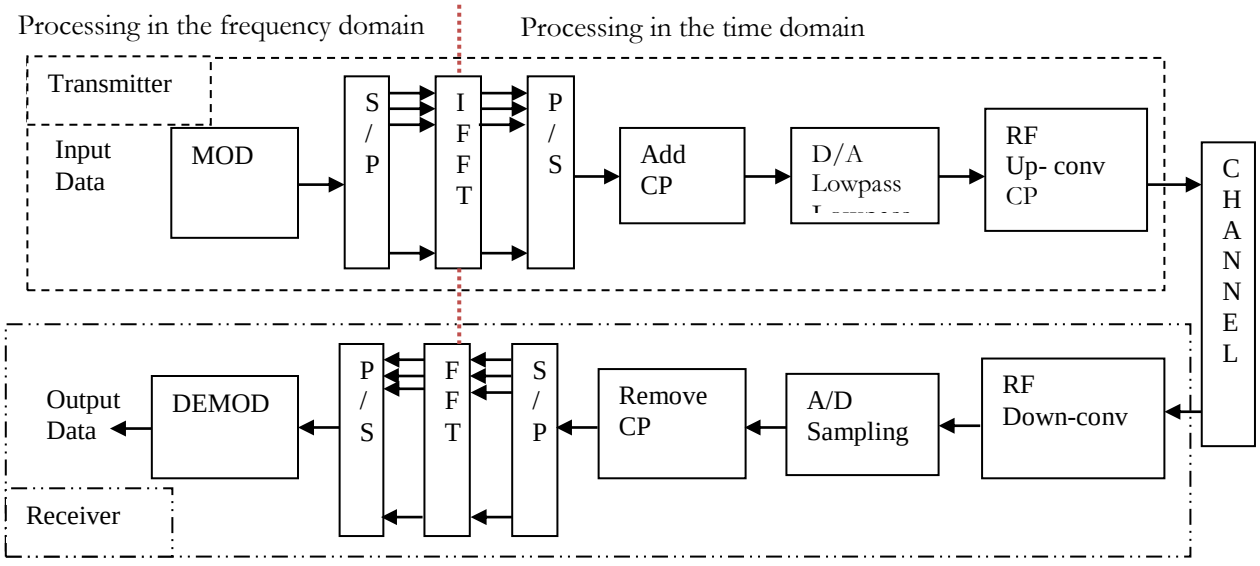

Figure 1.3. Block diagram of an OFDM transceiver

OFDM is a particular type of FDM modulation. Figure 1.3 presents a block diagram of an OFDM transceiver. The first step in the OFDM system is to convert a serial data stream into a parallel stream and then modulate the symbols, using the quadrature amplitude modulation (QAM) or the phase shift keying (PSK) modulation. The transmitter and receiver can be implemented by means of the IDFT and DFT respectively. After the symbols are modulated, the data stream is converted to time domain by means of an IFFT. The chosen length N_{FFT} of the FFT function should be significantly larger than the number of useful subchannels N to ensure that the edge effects are negligible at half the sampling frequency (Nyquist creterion). Also to ensure that the shape of the reconstruction filter, of the digital-to-analog converter (DAC) does not affect a significant part of the spectrum. The OFDM modulated signal can be expressed as:

$$x(t) = \int_{n=0}^{N-1} X_n e^{j2\pi f_n t}, \qquad (0 < t < T_s) \tag{1.6}$$

where *Ts* is the duration of an OFDM symbol, and 1/*Ts* is the distance between subcarriers (or subchannel space) in frequency domain. Each subcarrier is located at:

$$f_n = \frac{n}{T_s} \qquad (0< n <N-1) \tag{1.7}$$

In order to maintain the orthogonality between the OFDM symbols, the symbol duration and subchannel space must meet the condition $Ts.f = 1$. When x(*t*) is sampled, every *Ts/N* [20] OFDM transmits a large number of modulated orthogonal subcarriers in parallel. Each subcarrier is modulated using BPSK, QPSK or QAM modulations.

Let's {X(0), X(1), X(2), …, X(N-1)} be a bloc of N data symbols after the serial-to-parallel conversion. The IDFT of data symbols can be:

$$s_n = \sum_{k=0}^{N-1} X(k) e^{\frac{j2\pi nk}{N}}, \quad n = 0,1,...,N-1, \tag{1.8}$$

$\{s_n,\ n = 0,1,...,N-1\}$ The latter is the time domain OFDM symbol.

The tail of each OFDM symbol is copied in the beginning to form the cyclic prefix (CP). This latter is introduced to deal with inter symbol interference (ISI). The length of CP N_{cp} is chosen at least equal to channel order L. Thus, the linear convolution between the symbol and the channel is transformed to a circular convolution.

The output of the DFT demodulation is the multiplication of the frequency domain OFDM symbol X (X(0), X(1), X(2), …, X(N-1))^T and the channel response in the frequency domain.

Then $$y = HX + W \tag{1.9}$$

where W is an additive white Gaussian noise (AWGN) vector, and

$$\text{H=diag}\left\{H[0],...,H[N-1]\right\},\ H[n]=\sum_{l=0}^{L-1}h(l)e^{-\frac{j2\pi nl}{N}} \tag{1.10}$$

is the complex channel frequency response at subcarrier n. [21]

The n^{th} element of y is given by:

$$y[n] = H[n]X(n) + w[n]\ , \quad 0 \le n \le N-1 \tag{1.11}$$

The data transmission over N parallel subchannels is done without taking into consideration the CFO.

1.3. OFDM Impairments

The OFDM system has some impairments that affect its performance.

1.3.1. Sensitivity to Frequency Offset [22]

The carrier frequency offset (CFO) is the cause of the ICI, which is the main drawback in an OFDM system. It degrades the orthogonality between subcarriers. This carrier frequency offset is occurred from two principal sources. The first is the mismatch between the transmitter and the receiver oscillators. The second is from Doppler spread.

Let ε denote the normalized carrier frequency offset and Δf_o be the carrier frequency offset, so,

$$\varepsilon = \frac{\Delta f_o}{\Delta f} \tag{1.12}$$

Where Δf is the subcarrier spacing.

The data sample x[k] is transmitted over a multipath channel h[k] with L taps.

The n^{th} received symbol is given by:

$$y[n] = \frac{1}{N}\sum_{k=0}^{N-1}\left(\sum_{l=0}^{L-1}h[l]x[k-l]\right)e^{-j2\pi\frac{nk}{N}}e^{j2\pi\frac{k\varepsilon}{N}}, \tag{1.13}$$

where $e^{-j2\pi\frac{nk}{N}}$ performs the demodulation via FFT. $e^{j2\pi\frac{k\varepsilon}{N}}$ is the normalized CFO.

$$y[n]=\frac{1}{N}\sum_{k=0}^{N-1}\sum_{l=0}^{L-1}h[l]\sum_{m=0}^{N-1}X[m]e^{-j2\pi m\frac{k-l}{N}}e^{-j2\pi\frac{nk}{N}}e^{j2\pi\frac{k\varepsilon}{N}}$$

$$y[n]=\frac{1}{N}\sum_{k=0}^{N-1}e^{j2\pi\frac{k\varepsilon}{N}}\sum_{l=0}^{L-1}h[l]\sum_{m=0}^{N-1}X[m]e^{-j2\pi k\frac{n-m}{N}}e^{-j2\pi\frac{ml}{N}}$$

$$y[n]=\frac{1}{N}\sum_{k=0}^{N-1}e^{j2\pi\frac{k\varepsilon}{N}}\sum_{m=0}^{N-1}X[m]e^{-j2\pi k\frac{n-m}{N}}\sum_{l=0}^{L-1}h[l]e^{-j2\pi\frac{ml}{N}}$$

$$y[n]=\frac{1}{N}\sum_{k=0}^{N-1}e^{j2\pi\frac{k\varepsilon}{N}}\sum_{m=0}^{N-1}X[m]H[m]e^{-j2\pi k\frac{n-m}{N}}$$

$$y[n]=\sum_{m=0}^{N-1}X[m]H[m]\frac{1}{N}\sum_{k=0}^{N-1}e^{j2\pi k\frac{(m-n+\varepsilon)}{N}} \tag{1.14}$$

$$y[n]=X[n]H[n]\frac{1}{N}\sum_{k=0}^{N-1}e^{j2\pi k\frac{\varepsilon}{N}}+\frac{1}{N}\sum_{m=0,m\neq n}^{N-1}X[m]H[m]\sum_{k=0}^{N-1}e^{j2\pi k\frac{(m-n+\varepsilon)}{N}}$$

$$y[n]=X[n]H[n]\frac{1}{N}\left(\frac{1-e^{j2\pi\varepsilon}}{1-e^{j2\pi\frac{\varepsilon}{N}}}\right)+\frac{1}{N}\sum_{m=0,m\neq n}^{N-1}X[m]H[m]\left(\frac{1-e^{j2\pi(m-n+\varepsilon)}}{1-e^{j2\pi\frac{(m-n+\varepsilon)}{N}}}\right)$$

$$y[n]=X[n]H[n]\frac{1}{N}\frac{e^{j\pi\varepsilon}}{e^{j\pi\frac{\varepsilon}{N}}}\left(\frac{e^{-j\pi\varepsilon}-e^{j\pi\varepsilon}}{e^{j\pi\frac{\varepsilon}{N}}-e^{j\pi\frac{\varepsilon}{N}}}\right)+\frac{1}{N}\sum_{m=0,m\neq n}^{N-1}X[m]H[m]\frac{e^{j\pi(m-n+\varepsilon)}}{e^{j\pi\frac{(m-n+\varepsilon)}{N}}}\left(\frac{e^{-j\pi(m-n+\varepsilon)}-e^{j\pi(m-n+\varepsilon)}}{e^{-j\pi\frac{(m-n+\varepsilon)}{N}}-e^{j\pi\frac{(m-n+\varepsilon)}{N}}}\right)$$

$$y[n]=X[n]H[n]\frac{e^{j\pi\varepsilon(1+\frac{1}{N})}}{N}\left(\frac{\sin(\pi\varepsilon)}{\sin(\pi\frac{\varepsilon}{N})}\right)+\sum_{m=0,m\neq n}^{N-1}X[m]H[m]\frac{e^{j\pi(m-n+\varepsilon)(1+\frac{1}{N})}}{N}\left(\frac{\sin(\pi(m-n+\varepsilon))}{\sin\left(\pi\frac{(m-n+\varepsilon)}{N}\right)}\right)$$

$$y[n]=\underbrace{X[n]H[n]}_{\text{the desired demodulated symbol}}\underbrace{\frac{e^{j\pi\varepsilon(1+\frac{1}{N})}}{N}}_{\text{phase rotation}}\underbrace{\left(\frac{\sin(\pi\varepsilon)}{\sin(\pi\frac{\varepsilon}{N})}\right)}_{\text{attenuation}}$$
$$+\underbrace{\sum_{m=0,m\neq n}^{N-1}X[m]H[m]}_{\text{the effect of the remaining sub-carriers}}\underbrace{\frac{e^{j\pi(m-n+\varepsilon)(1+\frac{1}{N})}}{N}}_{\text{with phase rotation}}\underbrace{\left(\frac{\sin(\pi(m-n+\varepsilon))}{\sin\left(\pi\frac{(m-n+\varepsilon)}{N}\right)}\right)}_{\text{attenuation}} \tag{1.15}$$

The effect of the remaining subcarriers is called inter carriers interference (ICI).

Lets m-n=k.

The ICI coefficient for the k[th] subcarrier is given by:

$$ICI_N(k) = \frac{e^{j\pi(k+\varepsilon)(1+\frac{1}{N})}}{N}\left(\frac{\sin(\pi(k+\varepsilon))}{\sin(\pi\frac{(k+\varepsilon)}{N})}\right) \tag{1.16}$$

1.3.1.1. Carrier-to-Interference Power Ratio (CIR)

The carrier-to-interference ratio (CIR) is similar to the signal-to-noise ratio (SNR) and is given by:

$$CIR = \frac{\left|ICI_N(0)\right|^2}{\sum_{k=1}^{N-1}\left|ICI_N(k)\right|^2} \tag{1.17}$$

where $\sum_{k=1}^{N-1}\left|ICI_N(k)\right|^2$ is the power of the ICI.

The figure below describes the carrier-to-interference ratio (CIR) versus the normalized frequency offset. It is clear that as the normalized frequency offset increases, the CIR decreases.

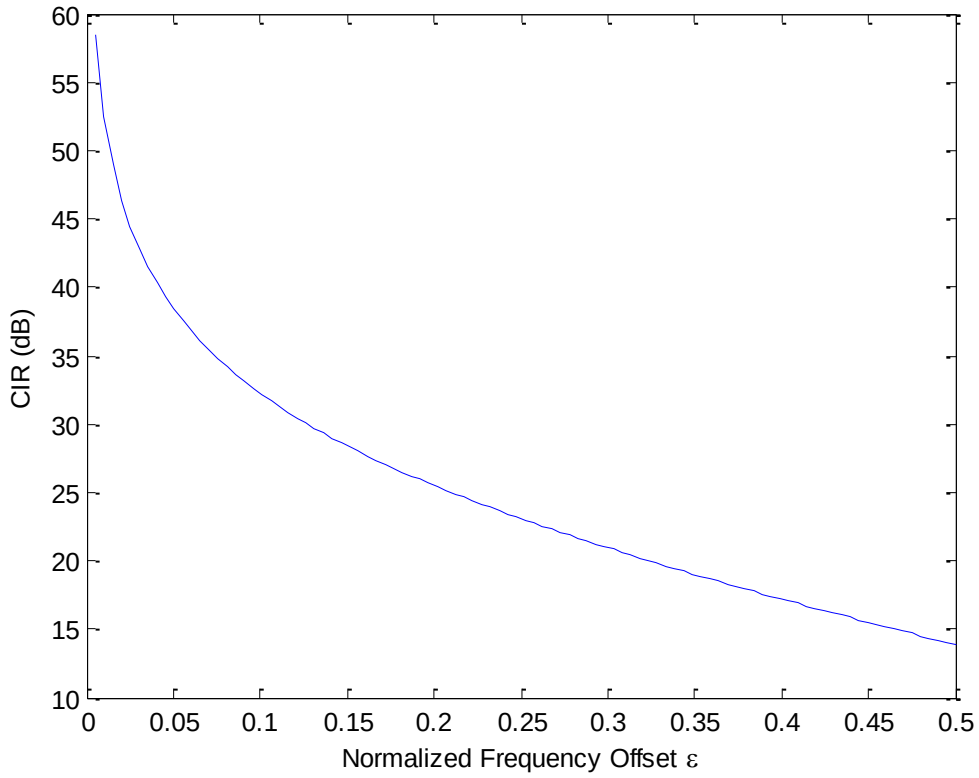

Figure 1.4. Carrier-to-interference ratio (CIR)

Figure 1.5 presents the power of inter carrier interference (ICI).

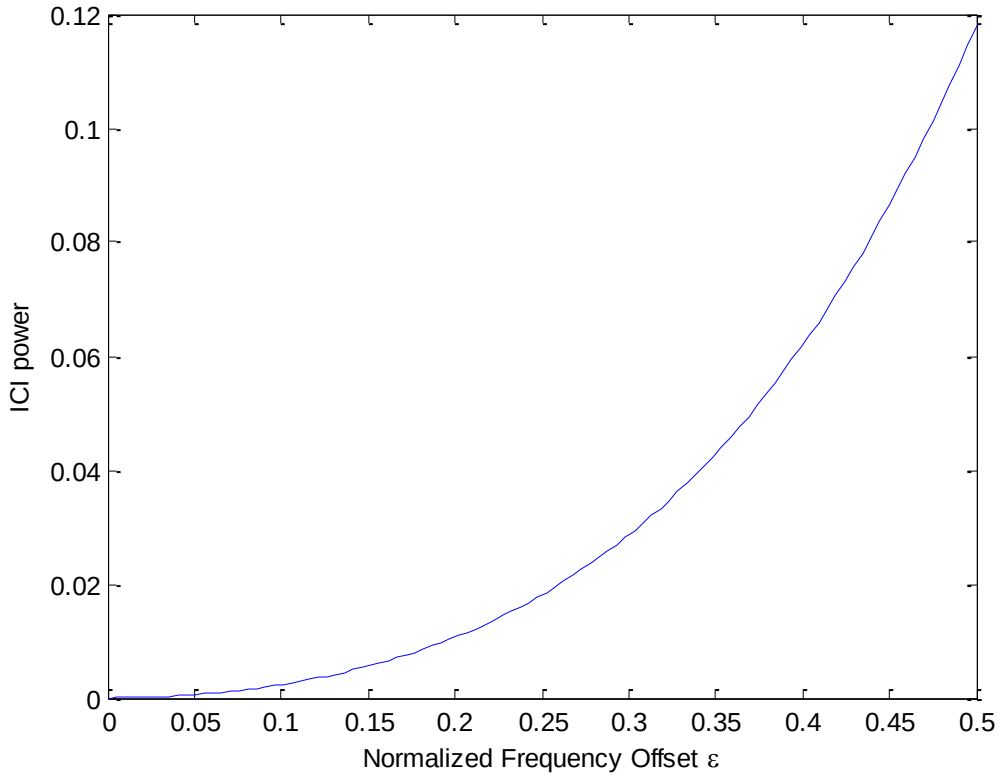

Figure 1.5. Relation between intercarrier interference (ICI) power and normalized frequency offset

As shown in the figure above, the normalized frequency offset increases as the ICI increases. The pace has an exponential shape but when we take the negative and positive normalized frequency offset, the pace becomes parabolic.

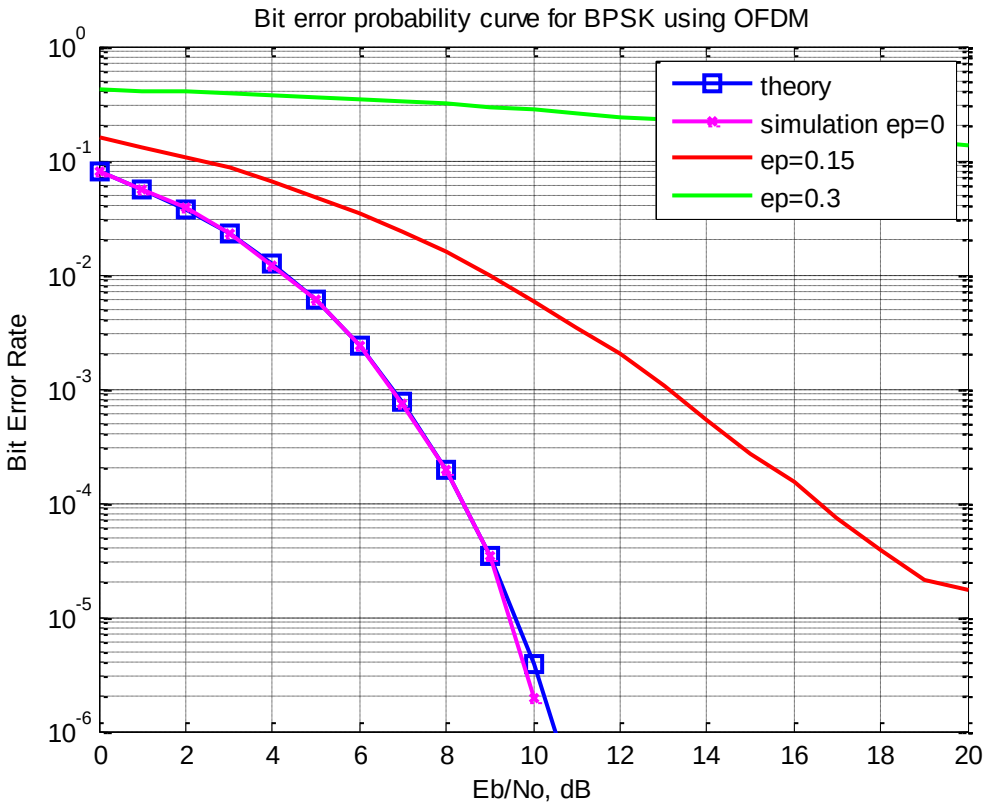

Figure 1.6. The bit error rate for different values of frequency offset

The figure above shows the influence of carrier frequency offset on the OFDM system. The bit error rate (BER) is increasing as the CFO is increasing.

The theoretical BER is given by :

$$\text{TheoryBER} = \frac{1}{2} \times erfc\sqrt{10^{\frac{E_b N_0}{10}}} \tag{1.18}$$

Where erfc is complementary error function and E_b N_0 is bit to noise ratio.

1.3.2. Peak-to-Average Power Ratio (PAPR)

One of the most serious problems of the transmitted OFDM signal is the high peak-to-average-power ratio (PAPR), since this large peak introduces a serious degradation in performance when the signal passes through a nonlinear high power amplifier (HPA). The PAPR is the relation between the maximum powers of a sample in a given OFDM transmit symbol divided by the average power of that OFDM symbol [23].

When the OFDM signal is transformed to time domain, the resulting signal is the sum of all the subcarriers, and when the different subcarriers are out of phase with each other, the PAPR occurs. At each instance, they are different with respect to each other at different phase values. When all the

points achieve the maximum value simultaneously; this causes the output envelope to suddenly shoot up which causes a 'peak' in the output envelope. Due to the presence of a large number of independently modulated subcarriers in an OFDM system, the peak value of the system can be very high as compared to the average of the whole system. This ratio of the peak-to-average-power value is termed peak-to-average-power ratio (PAPR). So an OFDM signal has a very large PAPR, which degrades the performance of OFDM signals by forcing the analog amplifier to work in a nonlinear region. As a result, the signal is distorted and the amplifier consumes more power.

The OFDM signal is given as:

$$x(t) = \sum_{n=0}^{N-1} X_k e^{j2\pi f_k t}, \qquad 0 \le t \le NT \tag{1.19}$$

PAPR is calculated as:

$$PAPR = \frac{\max \left| x(t) \right|^2}{E\left[\left| x(t) \right|^2 \right]} \tag{1.20}$$

$E[.]$ denotes the expected value.

A major obstacle is that the OFDM signal exhibits a very high PAPR. Thus, RF power amplifiers should be operated in a very large linear region, otherwise the signal peaks get into a non-linear region of the power amplifier causing signal distortions. These signal distortions introduce intermodulation among the subcarriers and out-of-band radiation. Therefore, the power amplifiers should be operated with large power backups. However, this leads to very inefficient amplification and expensive transmitters. In addition, these large peaks cause saturation in power amplifiers, leading to intermodulation products among the subcarriers and disturbing out-of-band energy. Thus, it is desirable to reduce the PAPR.

1.3.2.1. PAPR Reduction Techniques

Several methods have been proposed in the literature to decrease the PAPR [24-26]. There are various factors that influence the choice of the PAPR reduction techniques, such as: increase in transmit signal power, loss in data rate, PAPR spectral efficiency, reduction capacity, complexity of computation and increase in the bit-error rate (BER) at the receiver end. The PAPR reduction techniques [27] are divided into two sets: signal scrambling techniques and signal distortion techniques.

1.3.2.2. Signal Scrambling Techniques [28]

- Block coding techniques
- Block coding scheme with error correction
- Selected mapping (SLM)
- Partial transmit sequence (PTS)
- Interleaving technique
- Tone reservation (TR)
- Tone injection (TI)

1.3.2.3. Signal Distortion Techniques

- Peak windowing
- Envelope scaling
- Peak reduction carrier
- Clipping and filtering

1.3.3. Phase noise

Phase noise is produced by local oscillators as a parasitic phase modulation at the receiver. Several works are proposed in the literature for both phase-locked-loop (PLL) based and free-running oscillators [29-31].

An oscillator is an autonomous electronic circuit, which ideally produces a periodic oscillating electric signal at a precise frequency. This frequency is commonly used to provide clock signals for timing and frequency synchronization, and carrier signals for pass band transmission and reception in communication systems. Oscillators used in communication transceivers are imperfect in that their output signals are affected by random amplitude and phase instabilities. The signal at the output is written as[32]:

$$v(t) = (1 + a(t))\cos(2\pi f_{osc} t + \theta(t)) \tag{1.21}$$

where:

f_{osc} denotes the center frequency of the oscillator,

$a(t)$ is the random amplitude variation, where

$\theta(t)$ represents the random phase variation.

The random amplitude variation can be ignored; however the random phase variation causes distortion on the transmitted signals.

1.3.3.1. Noise Sources in an Oscillator

The phase of the oscillator signal is affected by three main sources:

- Short-term instabilities caused by thermal and colored noises
- Deterministic instabilities caused by power supply feed-through and other interfering sources and spurious signals
- Long-term instabilities occur in oscillators due to aging of the constituent resonator material

1.3.3.2. Phase Noise Model

Two different models of phase noise (PHN) are available:

- For free-running oscillators at the receiver, a non-stationary Gaussian process, called *Wiener PHN* is employed.
- For oscillators controlled by a phase-locked loop (PLL), we assume a zero-mean colored Gaussian process, called *Gaussian PHN*.

The prior statistics of both types of PHN can be modeled as a multivariate Gaussian distribution:

$$p(\theta) = N(0, \phi) \tag{1.22}$$

where the covariance matrix ϕ can be determined from the power spectral density (PSD) of the voltage-controlled oscillator (VCO) output.

Assuming that the received signal is only affected by the phase noise and the channel is flat, then the received signal in time domain is given by:

$$y(n) = x(n)e^{j\phi(n)} \tag{1.23}$$

After removing the CP and taking the DFT on the remaining samples, the demodulated OFDM signal is given as [18]:

$$\begin{aligned} Y_k &\approx \mathrm{X(k)}+\frac{j}{N}\sum_{r=0}^{N-1}X(r)\sum_{n=0}^{N-1}\phi(n)e^{j(2\pi/N)(r-k)n} \\ &\approx \mathrm{X(k)}+\underbrace{\mathrm{jX(k)}\frac{1}{N}\sum_{n=0}^{N-1}\phi(n)}_{jX(k)\phi}+\underbrace{\frac{j}{N}\sum_{r=0,r\neq k}^{N-1}X(r)\sum_{n=0}^{N-1}\phi(n)e^{j(2\pi/N)(r-k)n}}_{ICI\ term} \end{aligned} \tag{1.24}$$

Assuming that the phase noise is small, then $e^{j\phi(n)} \approx 1+ j\phi(n)$.

In equation 1.23, the term $jX(k)\phi$ acts on all subcarriers as a common phase error (CPE). The value $j\phi$ is a rotation of the constellation. This rotation is the same for all subcarriers, so it must be corrected to obtain a good performance by using a phase rotation equal to the average of the phase noise.

$$\phi = \frac{1}{N}\sum_{n=0}^{N-1}\phi(n) \tag{1.25}$$

The ICI term indicates the intercarrier interference. In this term, both the phase offset and the input data sequence are random, so it cannot be easily corrected.

1.3.4. Time-Varying Channel

In OFDM transmission, the channels are generally assumed to be linear time-invariant frequency selective. These channels avoid ICI among the data symbols of the same OFDM block, which allows for easy channel equalization. However, the channel experiences a non-negligible time variation, so ICI is produced by the effect of Doppler spread. Thus, the performances of the OFDM systems will degrade. To overcome this, the shortening method is proposed to shorten the OFDM block duration in order to make the channel almost stationary over each block. However, this method is capacity inefficient [33].

In rapidly time-varying scenarios, the channel estimation task is difficult because the CIR is not constant within the OFDM block. As a consequence, multiple parameter estimation is necessary for each channel path, and the estimation has to be updated for each OFDM block. Several techniques are proposed to estimate a linear time-varying channel (LTV) such as a basis expansion model (BEM), Legendre basis expansion model (L-BEM) and complex exponential BEM (CE-BEM)...etc.

1.3.5. Timing Offset

The symbol timing offset can disturb the amplitude and the phase of the received symbol. It also introduces intersymbol interference (ISI). The starting point of the OFDM symbol must be

determined before doing the FFT demodulation. Incorrect synchronization may lead to the loss of the first samples of the OFDM symbol. Thus, the OFDM signal is attenuated and not all of the transmitted energy can be recovered. So, the orthogonality between subcarriers is lost, causing intercarrier interference (ICI). However, the addition of the cyclic prefix N_{CP} such that the timing offset θ is in the interval $-N_{CP} \le \theta \le 0$, preserves the orthogonality. Thus, the received signal is only affected by the specific rotation.

1.4. Conclusion

This chapter has dealt with essential properties of the OFDM system. The principal property of an OFDM signal is orthogonality between subcarriers; thus, the concept of orthogonality in OFDM is discussed. In order to make the implementation of OFDM possible, IFFT and FFT are used in the multiplexing of transmitting and receiving OFDM data respectively. Thus, the IFFT and FFT process and operation are included in this chapter. Furthermore, to mitigate ISI and maintain the orthogonality, the CP, as explained in this chapter, has to be longer than the channel impulse response. One of inevitable problems in an OFDM system is its sensitivity to carrier frequency offset (CFO). This problem brings disadvantage to an OFDM system, thus, the details of CFO is also discussed. In addition, this chapter highlights other OFDM-related issues that affect its performance such as PAPR, phase noise, time-varying channels, and timing offset.

Chapter 02

FREQUENCY OFFSET MITIGATION TECHNIQUES

2.1. Introduction

Intercarrier interference (ICI) is the biggest drawback of OFDM systems. This is due to the mismatch between transmitter and receiver sampling clocks, the misalignment between the reference frequency of transmitter and receiver stations, or the Doppler shift. Many techniques have been developed to deal with this problem and avoid ICI. Several frequency offset mitigation techniques have been proposed in the literature. These methods can be categorized as:

- Carrier frequency offset (CFO) estimators
- Frequency domain equalization
- Time domain windowing
- Pulse shaping
- Kalman filter
- ICI self-cancellation

In this chapter we discuss these methods in detail.

2.2. Carrier Frequency Offset (CFO) Estimators

Carrier frequency offset (CFO) has a significant influence on the orthogonal frequency division multiplexing (OFDM) efficiency. It causes the intercarrier interference (ICI) that destroys the orthogonality between subcarriers and degrades the performance of the OFDM system. In the literature, several techniques have been used to estimate and compensate for the CFO. They can be categorized into three major types:

- Training-based CFO estimators
- Blind CFO estimators
- Semi-blind CFO estimators

Looking at them in another way, they can be categorized as data-aided, non-data-aided and hybrid techniques. Several data-aided frequencies offset correction techniques have been proposed to avoid ICI [34-35]. They employ one or more OFDM symbols as a preamble before the actual data transmission or a set of known pilot signals integrated within the data. Although these algorithms can effectively estimate frequency offset, they reduce the bandwidth efficiency. To eliminate this reduction, non-data-aided algorithms that exploit the redundancy of the cyclic prefix (CP) have been developed [36-39]. These blind estimators do not depend on training sequences or pilot symbols for estimating frequency offset. Although these techniques have high bandwidth efficiency, they have lower estimation accuracy compared to data-aided techniques. Hence a hybrid approach is proposed to overcome these shortcomings and give a good tradeoff between data-aided approaches and blind approaches. This category of CFO estimator uses the intrinsic virtual carrier present at the band edges of OFDM symbols or deliberately introduced null subcarriers in the data carriers.

2.2.1. Maximum Likelihood (ML) Carrier Frequency Offset (CFO) Estimation (An Overview)

Maximum likelihood (ML) frequency offset estimation is of great interest and gives good tradeoff among performances, computational complexity and bandwidth efficiency. Because an ML scheme has fast convergence and achieves high accurate estimation, it has been used in many research projects in the literature. It can be used in data-aided, non-data-aided and hybrid approaches..

The ML method selects the set of values of the model parameters that maximizes the likelihood function. Intuitively, this maximizes the "agreement" of the selected model with the observed data. It gives an unified approach to estimation.

The ML carrier frequency offset scheme can be classified as:

- Blind ML CFO Estimation
- Data-aided ML CFO Estimation
- Semi-blind (hybrid) ML CFO Estimation

2.2.1.1. Blind ML CFO Estimation

The demodulation of received OFDM signals with an offset in carrier frequency will produce a high bit error rate and decrease the performances of OFDM systems. OFDM symbols already have cyclic prefix (CP) to avoid intersymbol interferences (ISI). Beek 1997[36] exploits the redundant information in the CP and develops a joint ML estimator of time and frequency offset in OFDM systems. Beek's purpose is to reduce the need for pilots by using CP in the ML estimation of time and frequency offset.

Beek notices that two quantities can affect the LL function: the length of CP L and the correlation coefficient. As L increases over a certain threshold, only the performance of a frequency offset will appear to be continuously increasing. This estimator has an efficient bandwidth. Simulations show performance improvement of the scheme through the AWGN channel; however, it shows degradation of the performances through dispersive channels due to a simple correlation structure that has been designed for AWGN channels. Signals passed through dispersive channels have more complex correlations.

Two other synchronization parameters are not accounted for in this model: an offset in the carrier phase may affect the symbol error rate in coherent modulation, and an offset in the sampling frequency will also affect the system performance.

Further work is needed considering the offset in the carrier phase and the offset in the sampling frequency. Also, the hybrid approach that uses pilots and CP needs further work.

In order to mitigate CFO that introduces severe ICI over time dispersive channels, Biao Chen and Hao Wang 2002 [40] have proposed an accurate ML estimator of frequency offset on the presence of virtual subcarriers. ML estimation is calculated to estimate frequency offset. In order to maximize the log likelihood function, they minimize the cost function. The proposed method is similar to the method proposed by Liu and Tureli [41]. Simulation results show the performance improvements of the estimator compared to the estimator of Liu and Tureli [41].

Jia et al. [42] proposed a novel blind maximum-likelihood (ML) technique for frame timing instant and frequency offset estimation in an orthogonal frequency-division multiplexing system over a fast Rayleigh fading channel, which is more desirable when dealing with a carrier frequency offset and to avoid reducing bandwidth efficiency. The method based on ML criterion that estimates timing offset is first done without knowledge of the frequency offset, then it estimates frequency offset over a fast Rayleigh-fading channel.

Simulation experiments demonstrate the effectiveness of the method in terms of low estimation errors in frame timing and frequency offset. The proposed frequency offset estimator is similar to that derived by Beek [36].

Differently from previous works [36], the frame timing is calculated first in a manner independent of frequency offset; then, frequency offset can be accurately derived. The proposed technique can outperform that of previous works [36]. It has been noticed that the proposed method can obtain good estimated rates without increasing the computational complexity.

Authors use the fast Rayleigh fading channel in order to stimulate real wireless channel communication. However, they estimate that the channel is time varying not time dispersive, which is not the case of a real channel. Developing CFO and timing offset estimators over a multipath fading channel in order to assimilate the real channel needs further work.

Because a fast time-varying multipath channel model is the best model for simulating real wireless OFDM communications systems, Lv et al. [43] proposed an approach to jointly estimate both symbol timing and CFOs over fast time-varying multipath channels. The estimation process is divided between a coarse and a fine synchronization. The coarse synchronization is an LS estimation based on cyclic autocorrelation and it has low computational complexity. It is used to decrease the complexity of the fine synchronization by finding a rough offset. The fine synchronization is based on ML estimation to obtain accurate frequency and timing offsets.

The ML estimation is divided into three cases, depending on the timing offset range. In each case, a likelihood function is calculated and, by maximizing the log likelihood function, the estimation of frequency and timing offsets can be obtained.

Simulations demonstrate that the coarse synchronization can rapidly give rough estimates. The fine synchronization can get the accurate estimates of frequency offset and timing offset but with high computational complexity. By combining coarse and fine synchronization, Lv et al. provide a good tradeoff between estimation accuracy and implementation complexity.

Lv et al. give accurate estimates of frequency and timing offsets in real mobile communications environments. Also the intervals of correlation are determined with precision.

If the rough timing offset is not optimal then the estimation of the fine synchronization is not accurate. Wang overcomes the weakness of the coarse synchronization and the computational complexity of the fine synchronization by developing reduced complexity alternative (RCE).

Wen-Long Chin [44] also tries to simulate frequency offset through real channel conditions. He publishes a paper that examines the problem of the synchronization of OFDM over-dispersive fading channels based on the ML criteria.

The new approach uses distinctive correlation characteristics of the CP at each sampling time without requiring additional pilot symbols, and fully utilizes the delay spread of dispersive fading channels. A suboptimal approach with closed form solution is derived. The proposed CFO depends on the channel's length. Simulations demonstrate that the new approach gives good results. Also, the Cramer–Rao lower bound (CRLB) is discussed.

The purpose of this paper is to explore a method based on the redundancy of the CP to jointly estimate CFO and symbol timing over dispersive channels with low complexity like AWGN method [36]. Channel length is used to enhance the estimation.

In this approach, the correlations between m^{th} OFDM symbol and its neighbors $(m-1)^{th}$ and $(m+1)^{th}$ are calculated. Using these correlations, the likelihood function is derived. Then the log likelihood function is computed and the CFO is estimated.

The performances of the proposed method are approved by simulations. The CFO estimation is comparable to CRLB over AWGN and dispersive channels. The proposed symbol timing emulates that of the ML estimator [36] over an AWGN channel. It is found that the ML function depends on the channel length, symbol timing and CFO, as well as the correlation coefficient. The delay diversity of dispersive channels is fully utilized.

The ML estimation needs high computational complexity, hence it is not practical. An approximate ML estimator is introduced to implement the proposed method. So, the accurate method is not valuable. By reformulating the LL function, an accurate CFO and symbol timing will be developed but will require further work to simplify the computations.

Liu et al.2014 [45] developed a new blind FFO estimator using ML criterion to overcome the low estimation of fractional CFO estimation accuracy over multipath channels—a non-cooperation communication system, which derived a blind FFO estimator over multipath channels. First the timing offset was estimated using the relativity in the CP and then an FFO estimator was developed based on ML criterion. They proposed two cases of FFO estimation: assuming that the max time delay of the channel is known, in one case, and unknown, in the other.

Simulation results demonstrate that the proposed method resists in multipath channels and noise, and outperforms existing methods [36], [46]. Also, it can be used for non-cooperative communication systems. The proposed estimators give better results than existing ones over

multipath channels and in high SNR regions. However, they presume that timing offset has been estimated accurately, where this is not the case in real applications. Also, they ignore the effect of the sampling clock, symbol perfect synchronization and integer frequency offset. Similar studies should be undertaken which taking into consideration timing offsets.

The repetitive structure of a training preamble is used for most pilot-based synchronization algorithms for multicarrier transmissions. However, this structure is not convenient for a WiMAX cellular network for two reasons [47]: one is that it is a non-perfectly periodic structure in the time domain and the other is that the MT has only partial knowledge of the received preamble waveform.

In order to avoid the high complexity and the impractical implementation of joint ML estimation of the timing error, the FFO, the IFO and the preamble index, Morelli et al 2014 [48] propose a realistic approach based on a two-stage procedure. In the first stage, the timing offset and FFO is estimated using a blind estimation based on the redundant information in the cyclic prefix. In the second stage, the IFO and the preamble index recovery are accomplished in a joint ML estimation. Suboptimal algorithms are also developed.

However, as there is a certain increase of the system complexity, this approach gives a more accurate estimation than existing ones and it is insensitive to residual timing errors.

A novel expression of the CRB for CFO recovery applicable to the WiMAX preamble is presented. Also, a low-complexity algorithm for WiMAX applications is derived by combining the FFO recovery scheme illustrated in [49] with the ML estimator. Finally, a novel ML-based approach for a joint IFO and preamble index is developed.

The joint ML estimation of the CFO and preamble index in multicarrier systems that employ a training sequence composed of some correlated but non-identical parts is derived. Although the CFO can be derived by the ML metric, they show that it is convenient to decompose the frequency errors into fractional and integer parts. As the exact ML estimation is very complex, FFO is estimated by using an ad-hoc frequency estimation method that attains the relevant CRB at all SINR values of practical interest. An approximated ML approach that resists to timing offset is used to jointly estimate the integer part IFO and the preamble index. This method outperforms the existing methods suited for the WiMAX preamble; this approach offers the opportunity of reaching the desired trade-off between complexity and system performance. Also, the simulation results attain CRB at all SINR values of practical interest.

Qi Zhan and Hlaing Minn [50] show that the existing CFO estimators are derived from incomplete signal models without considering energy loss and distortion induced by CFO and sampling offsets,

and channel tap energy dispersions due to timing and sampling offsets. Qi Zhan and Hlaing Minn incorporate timing offsets and sampling offsets to the exact signal model [51] with CFO. They examine the effect of them on the CFO estimation. Also, pilot-aided estimators and blind estimators for integer normalized CFO (ICFO) are established under the new accurate signal model.

Simulation results confirm the analytical performances and the accurate estimation of the new estimators. In addition, these estimators can be applied to both PSK and QAM modulations and they are not influenced by the number of cyclic prefixe.

Qi Zhan and Hlaing Minn generalize the existing signal model [51] by taking in consideration timing offsets and sampling offsets and using only one OFDM symbol.

Q. Zhan et al. demonstrate the influence of timing offsets and sampling offsets on the channel gains. They observe that the (integer) timing offset will shift the channel, while the sampling offset will cause the spreading of each channel tap energy to adjacent taps cyclically (most of the leaked energy is on the two (cyclically) adjacent taps). In contrast, fractional CFO estimation is insensitive to timing and sampling offsets. They develop PAE and BE estimators. They use only one OFDM symbol. In addition, these estimators can be applied to both PSK and QAM modulation and they are not influenced by the number of cyclic prefix.

Although they proposed a new accurate signal model different from the existing ones by taking the effect of sampling offsets, they confirm that the effect of a sampling offset is not significant and neglected it.

Wang et al. [52] studied again the issue of synchronization in OFDM. They noticed that there is a lack of accurate studies on blind OFDM synchronization methods for multipath fading channels in the literature. As a result, Wang et al. use a more complete signal correlation model involving triplet structure. Based on this model, an exact likelihood function is derived. It is found that the ML CFO estimate is the solution of a quartic equation rather than the phase angle of a complex number as obtained in many previously derived methods. As a truly ML synchronizer (abbreviated MLE below) is very complicated, Wang et al. also derive a reduced-complexity alternative (dubbed RCE below) which claims a much lower computational complexity than MLE as well as a slightly lower complexity than LLCE. They present deep analysis and comparison of the performance of various methods. Simulations indicate the robustness of the performance in modeling errors of the fading rate and the channel power-delay profile (PDP). It is shown that the RCE has lower computational complexity than MLE while they have close performances. The objective of their work is to jointly estimate the STO and the CFO under accurate system models over wide sense stationary

uncorrelated scattering (WSSUS) channels. Wang et al. use complete signal correlations and they have found a solution to a quartic equation (not closed form); they derive the truly ML synchronizer and a reduced-complexity alternative (dubbed RCE).

The proposed methods yield rather robust performances in modeling errors of the fading rate and the channel power-delay profile (PDP). The RCE showed an insignificant performance difference in comparison to the MLE. A lot of papers include triplet correlation structure [43, 46, 53] but they don't find the truly ML synchronizer for multipath fading channels that uses triplet correlation structure. Also the paper derives a solution for an arbitrary-sized observation window.

The paper gives a detailed performance analysis while there is a lack of such performance analyses on blind OFDM synchronization methods in the literature.

The estimator presents a bad tradeoff. On the one hand, it has high complexity to calculate MLE, which uses triplet structure. On the other hand, there is no significant performance difference from LLCE [43] results. The truly ML estimator derived is not practical nor is it implementable; it has high complexity to implement it, and there is only a small performance difference between RCE and LLCE. In addition, similar to Wang, LLCE also uses triplet correlation r(n-N), r(n) and r(n+N). However, LLCE divides the problem into three cases and gives the solution to each case separately; Wang gives a more general solution to the problem.

Tzu-Chiao Lin and See-May Phoong [54] develop a solution to exploit the repetitive structure of CP samples in multipath channels by using the so-called remodulated received vectors in [55]. The purpose of the paper is to develop a blind estimator for fractional CFO and derive the closed-form formula. A new CP-based algorithm for blind CFO estimation in OFDM systems is proposed. Both the Cramer-Rao bound (CRB) on MSE and a closed-form formula for the theoretical MSE is derived for multipath channels. Using the remodulated received signal in the presence of CFO for a blind estimation; coarse and fine CFO estimators are derived.

This CFO estimator outperforms the main existing estimators over multipath channels and is very robust with regards to the symbol timing synchronization error. Also, it has low complexity and its performance is independent of modulation symbols and virtual carriers. Simulation results show that the proposed estimator achieves higher estimation accuracy than other CP-based methods.

Over Rayleigh block fading channels, for a=1, the performances of the estimator degrade significantly. Also in the case when the object speed increases, the performances of the estimator decreases gradually. The developments of the CFO estimator that resist to the Rayleigh block fading channels and to the object speed need further study.

2.2.1.2. Data-aided ML CFO Estimation

The main problem with CFO is that it introduces interference among the multiplicity of carriers in OFDM signals. To deal with ICI, Moose [35] presents a method to estimate frequency offset using a repeated data symbol and investigates the effect of offset errors on the signal-to-noise ratio of the OFDM carriers. A maximum likelihood estimation (MLE) is also proposed and evaluated by computer simulations. Moose found that the bound for SNR is quite accurate for small offsets, but about 3 dB too pessimistic as the offset approaches 1/2 the carrier spacing.

The ML frequency offset estimation is derived based on two repeated data symbols. If the channel impulse response is constant for a period of two symbols, the frequency offset will be well estimated in multipath spread channels because the estimation error depends only on total symbol energy. Simulations demonstrate that an accurate CFO estimate can be found even when the frequency offset is too high.

The effect of frequency offset is examined in detail and the performance analysis is precisely investigated. The paper summarizes the effect of frequency offset in OFDM systems. They assume that the multipath channel should be constant for a period of two symbols and that's not realistic. Moose notices that it may be advantageous to use shortened repeated symbols for tracking offset variations too, instead of an AFC (automatic frequency control) loop, because this reduces the time during which the channel must be stable. He assumes that the symbol timing is known, so he just has to find the CFO. The limit of the acquisition range for the carrier frequency offset is the subcarrier spacing. He also describes how to increase this range by using shorter training symbols to find the CFO. For example shortening the training symbols by a factor of two would double the range of carrier frequency acquisition. This approach will work to a point, but the estimates get worse as the symbols get shorter because there are fewer samples to average over, and the training symbols need to be kept longer than the guard interval so that the channel impulse response does not cause distortion when estimating the frequency offset.

A new joint CFO and SFO maximum-likelihood (ML) estimation scheme is proposed by Yong-Hwa Kim, and Jong-Ho Lee [56]. This method is a generalization of Moose's estimation scheme using two long training symbols in the frequency domain. Simulation results show that the proposed method outperforms existing ones. Cramer-Rao bounds (CRBs) for the mean square errors (MSEs) of the CFO and SFO estimation are developed.

The purpose of this paper is to develop joint fractional CFO and SFO estimators in frequency domains using two identical training symbols in which the phase shift between the two training symbols is exploited.

The proposed ML scheme outperforms Nguyen-Le's ML and Moose schemes. The FD CRB is proposed in order to examine the performance of the FD joint CFO and SFO estimators.

The FD CRBs are derived by CFO and SFO estimations. More accurate CFO and SFO estimators are developed.

Because conventional maximum-likelihood (ML) methods demand high computational complexity, Xu Wang et al. [34] develop a low-complexity closed-form ML estimator that achieves almost the same performance as existing ML methods without an exhaustive search.

In this article, Xu and Bo overcome the exhaustive search of CFO ML estimation in [56]. Using two long training symbols in the preamble, they find the closed-form solution of the CFO; as a result only a one-dimensional search is needed to estimate the SFO. They rewrite the cost function in some what they can find the exact estimation of the CFO. Because the value of the SFO is usually much smaller than unity, it can be estimated by using the second-order Taylor series expansion.

Xu and Bo's algorithm obtain the same performance as a two-dimensional ML estimation and with low computational complexity. They find closed-form solutions to frequency offset estimations which are very suitable in real implementation. Xu and Bo assume that timing offset is well compensated but that is not the case. Their estimation depends on well-known timing offsets.

2.2.1.3. Semi-blind (hybrid) ML CFO Estimation

In order to improve the performance of a blind estimation and to reduce the overhead of a data-aided estimation, a semi-blind approach is proposed.

Fusco et al. [57] present a semi-blind joint carrier phase and CFO synchronization scheme based on the insertion of pilot tones and exploiting the statistical redundancy of the OFDM signal due to the CP and virtual subcarriers.

They supposed that the OFDM is transmitted through an AWGN channel and the number of subcarriers is sufficiently large, the received signal is modeled as a circular complex Gaussian random vector (C-CGRV) with nonzero mean.

To overcome the limitations of previous blind and data-aided estimators, a hybrid approach is studied in detail, and the performance improvements are assessed by computer simulations. The results outperform the ones presented in [36-41] for both AWGN and multipath channels where

[36] has a limitation. Further studies are still needed to overcome the drawbacks in multipath channels using a hybrid approach.

Sameer et al. proposed another hybrid approach to overcome the requirements of an accurate estimation of CFO in OFDM systems. This approach is based on a CP and a few null subcarriers. They also propose a novel null subcarrier allocation scheme based on the Fibonacci series.

This hybrid approach outperforms existing ones in terms of BER performance, an estimation range equal to the full OFDM bandwidth, bandwidth overhead and receiver complexity.

The purpose of this paper is to develop a bandwidth efficient hybrid CFO estimation for OFDM systems using a CP to estimate the FFO in a time domain and using null subcarriers to estimate IFO in a frequency domain. A novel null subcarrier allocation technique based on Fibonacci series is proposed and the results are evaluated by simulations.

The proposed study assumes that the timing synchronization is done separately and perfectly through other means.

FFO and IFO estimators based on CP and null subcarriers in beacon symbols, respectively, are proposed. Simulations show that the proposed estimators give good performance with extremely low overheads.

2.2.1.4. Maximum likelihood Estimate of Differential Phase using Moose method

Moose develops an ML estimate of frequency offset as presented below

Let M complex values $\{X_k\}$ be represented by a length 2M row vector

$$\begin{aligned} \mathrm{X} &= [X_{1R}\ X_{2R} \ldots X_{MR}\ X_{1I}\ X_{2I} \ldots X_{MI}] \\ \mathrm{X} &= [X_R\ X_I]. \end{aligned} \tag{2.1}$$

Consider the random vectors

$$\begin{aligned} Y_1 &= R_1 + W_1 \\ Y_2 &= R_1 T(\alpha) + W_2 \end{aligned} \tag{2.2}$$

where

$$T(\alpha) = \begin{bmatrix} t_1 & t_2 \\ t_1 & t_2 \end{bmatrix} \tag{2.3}$$

$$t_1 = \cos(\alpha) I \quad \& \quad t_2 = \sin(\alpha) I \tag{2.4}$$

and T is the rotation matrix of size $2M \times 2M$. Given the observations Y_1 and Y_2, the maximum likelihood estimate of the parameter α is the value of α that maximizes the conditional joint density function of the observations. That is

$$\hat{\alpha} = \max_{\alpha}\left[f(Y_1, Y_2 | \alpha \right] \tag{2.5}$$

$$\begin{aligned} \hat{\alpha} &= \max_{\alpha}\left[f(Y_1, Y_2 | \alpha \right] \\ &= \max_{\alpha}\left[f(Y_2 | \alpha, Y_1) f(Y_1 | \alpha) \right] \end{aligned} \tag{2.6}$$

Because α and Y_1 are independent, so:

$$\hat{\alpha} = \max_{\alpha}\left[f(Y_2 | \alpha, Y_1) \right]. \tag{2.7}$$

Using equation (2.2), therefore:

$$Y_2 = (Y_1 - W_1)H(\alpha) + W_2 \tag{2.8}$$

Then

$$Y_2 = Y_1 H(\alpha) + W_2 - W_1 H(\alpha). \tag{2.9}$$

$$\hat{\alpha} = \max_{\alpha}\left[f(Y_2 | \alpha, Y_1) \right] = \min_{\alpha}\left[J(\alpha) \right]. \tag{2.10}$$

Where $$(\alpha) = (Y_2 - Y_1 H(\alpha))(Y_2 - Y_1 H(\alpha))^t. \tag{2.11}$$

using the fact that

$$H(\alpha)\left[dH(\alpha)/d\alpha \right]^t + \left[dH(\alpha)/d\alpha \right] H^t(\alpha) = 0 \tag{2.12}$$

$$dJ(\alpha)/d\alpha = -Y_2\left[dH(\alpha)/d\alpha \right]^t Y_1^t - Y_1\left[dH(\alpha)/d\alpha \right] Y_2^t. \tag{2. 13}$$

when $\hat{\alpha} = \alpha$, $dJ(\alpha)/d\alpha = 0$.

$$\sin(\hat{\alpha})\left[Y_{2R}Y_{1R}^t + Y_{2I}Y_{1I}^t \right] = \cos(\hat{\alpha})\left[Y_{2I}Y_{1R}^t - Y_{2R}Y_{1I}^t \right]. \tag{2.14}$$

Therefore,

$$\begin{aligned} \hat{\alpha} &= \tan^{-1}\left[(Y_{2I}Y_{1R}^t - Y_{2R}Y_{1I}^t)/(Y_{2R}Y_{1R}^t + Y_{2I}Y_{1I}^t) \right] \\ &= \tan^{-1}\left\{ \left(\sum_{k=1}^{M} \mathrm{Im}\left[Y_{2k}Y_{1k}^* \right] \right) \left(\sum_{k=1}^{M} \mathrm{Re}\left[Y_{2k}Y_{1k}^* \right] \right) \right\} \end{aligned} \tag{2.15}$$

is the maximum likelihood estimate (MLE) of α.

The range of CFO estimation given by Moose is $|\alpha| \le 0.5$.

2.2.1.5. Frequency Offset Estimator (CFO) using the Beek Method

Beek's estimator in [36], which is a blind estimator, is used later in Chapter 4 for the sake of comparison. It is based on the maximum likelihood criteria. A rough estimate of the frequency offset estimation has been done in [36], and is briefly given below:

The joint ML estimation of time offset θ and frequency offset ε are:

$$\hat{\theta}_{ML} = \arg\max_{\theta} \left\{ |\gamma(\theta)| - \rho\Phi(\theta) \right\} \tag{2.16}$$

$$\hat{\varepsilon}_{ML} = -\frac{1}{2\pi} \angle\gamma\left(\hat{\theta}_{ML}\right) \tag{2.17}$$

where

$$\rho = \frac{SNR}{SNR+1} \tag{2.18}$$

$$\gamma(m) \triangleq \sum_{k=m}^{m+L-1} r(k) r^*(k+N), \tag{2.19}$$

$$\Phi(m) \triangleq \frac{1}{2} \sum_{k=m}^{m+L-1} |r(k)|^2 + |r(k+N)|^2 \tag{2.20}$$

ρ is the correlation coefficient between $r(k)$ and $r(k+N)$. $\gamma(m)$ is a sum of L consecutive correlations between pairs of samples spaced N samples apart. $\Phi(m)$ is an energy term which is independent of θ and ε.

2.2.2. Carrier Frequency Offset (CFO) using the Classen Method

Another approach is proposed by Classen [59], where the CFO is estimated by using the pilot tones inserted in the frequency domain and transmitted in every OFDM symbol. In this process, two different estimation modes for CFO estimation are implemented: acquisition and tracking modes. In the acquisition mode, a large range of CFO including an integer CFO is estimated. In the tracking mode, only a fine CFO is estimated. The integer CFO is estimated by [60]:

$$\hat{\varepsilon}_{acq} = \frac{1}{2\pi T_{sub}} \max \left\{ \left| \sum_{j=0}^{L-1} Y_{l+D}\left[p[j], \varepsilon\right] Y_l^*\left[p[j], \varepsilon\right] X_{l+D}^*\left[p[j] X_l\left[p[j]\right]\right] \right| \right\} \tag{2.21}$$

where L, $p[j]$ and $X_l\left[p[j]\right]$ denote the number of pilot tones, the location of the j[th] pilot tone, and the pilot tone located at.

$$\hat{\varepsilon}_f = \frac{1}{2\pi T_{sub^D}} \arg\left\{\left|\sum_{j=0}^{L-1} Y_{l+D}\left[p[j], \hat{\varepsilon}_{acq}\right] Y_l^*\left[p[j], \hat{\varepsilon}_{acq}\right] X_{l+D}^*\left[p[j] X_l\left[p[j]\right]\right]\right|\right\} \quad (2.22)$$

In the acquisition mode, $\hat{\varepsilon}_{acq}$ and $\hat{\varepsilon}_f$ are estimated and then, the CFO is compensated by their sum. In the tracking mode, only $\hat{\varepsilon}_f$ is estimated and then compensated.

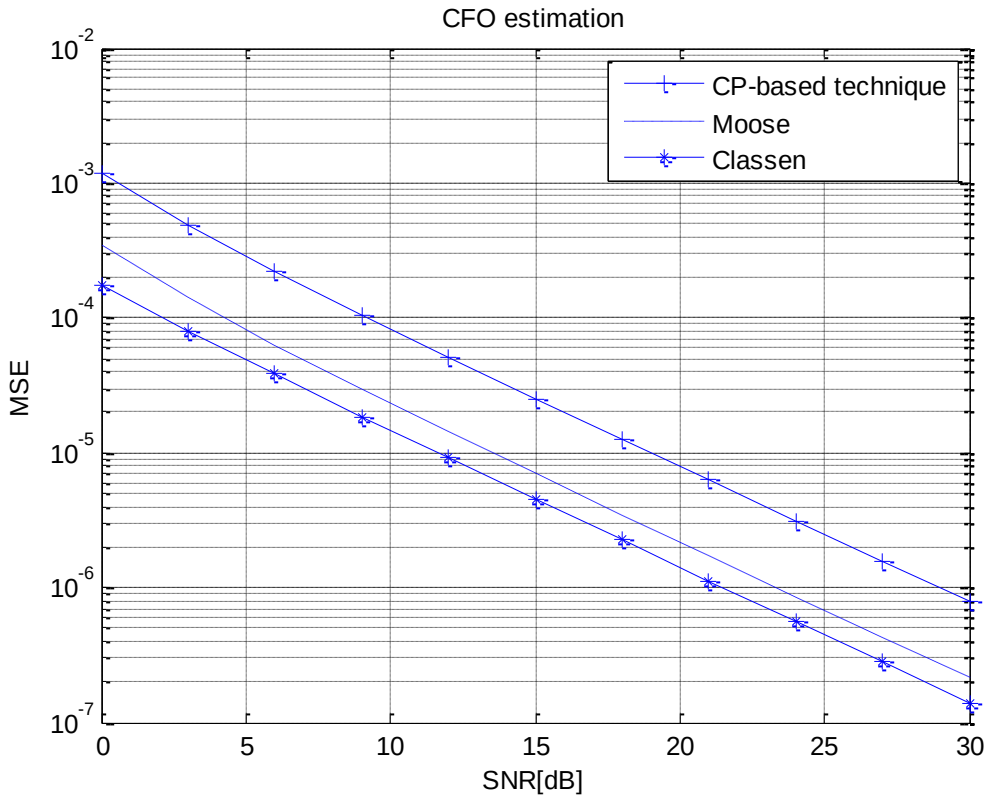

Figure 2.1. Frequency offset estimation for the Moose, Classen and CP-based techniques

Figure 2.1 presents a comparison between the CFO estimator given by the Moose, Classen and CP-based techniques. It is clear that the mean squared CFO estimation errors decrease as the SNR of received signal increases. The performance of these techniques depends upon the number of samples in CP, the number of samples in the preamble and the number of pilot tones.

Even though Classen's method gives better results, it is very computationally complex which makes it impractical.

2.2.3. Frequency Offset Estimator (CFO) using the Schmidl Cox Method

Dr. T.M. Schmidl and Dr. D.C. Cox [61] proposed a time and frequency synchronization algorithm for OFDM systems. They introduce some modifications to Classen's method which greatly simplify the computation necessary for synchronization and extend the range for the acquisition. They used a specially generated preamble as a pilot in the OFDM transmission. At the receiver side, the necessary information is extracted from the pilot for synchronization. They solve the acquisition problem by using a two-symbol training sequence placed at the beginning of the frame. The first symbol (the first half being identical to the second half in the time domain) is used to find the timing, and the second symbol is used to find the carrier frequency offset.

This method avoids the extra overhead of using a null symbol, while allowing for a large acquisition range for the CFO.

At the receiver, the sum of the pairs of products of the training symbol is given by:

$$P(d) = \sum_{m=0}^{L-1} \left(r_{d+m}^{*} r_{d+m+L} \right) \tag{2.23}$$

where

L is the number of complex samples in one-half of the first training symbol (excluding the CP).

d is a time index corresponding to the first sample in a window of $2L$ samples.

The phase difference between the two halves of the first training symbol is given by:

$$\varphi = \pi T \Delta f \tag{2.24}$$

It can be estimated using the following formula:

$$\hat{\varphi} = angle(P(d)) \tag{2.25}$$

Then, the frequency offset estimate is given by:

$$\Delta f' = \hat{\varphi} / (\pi T) \tag{2.26}$$

2.3. Frequency Domain Equalization

This technique is used to reduce only the ICI caused by the fading distortion in the channel. Frequency domain equalization process is addressed for mitigating ICI by using suitable equalization techniques. By inserting frequency domain pilot symbols in each frame, the ICI can be estimated for each frame. This method is appropriate for flat fading channels; however, in mobile communication the channels experience frequency-selective fading.

2.4. Time Domain Windowing

Time domain windowing [62] is a technique that is used to reduce both the spectral side lobes and the effect of ICI in OFDM systems. Several windows that fulfill the Nyquist criterion could reach this purpose, such as hanning, hamming, and Kaiser. Due to the tapered and smooth edges, the raised cosine (RC) window is generally used to reduce the effect of ICI in OFDM systems. It has a slow spectrum roll off. It is used in time domains before FFT where each subcarrier of OFDM gets multiplied by a window function. In order to receive the same transmitted signal, the same window is used on both the transmitter and the receiver sides.

However, this intuitive window is shown to be sub-optimum and a closed solution for optimum window coefficients. A condition for orthogonality of windowing schemes in terms of the FFT of the windowing function is derived. The FFT can be considered as a filter bank with N filters where N is the FFT size.

Even though the windowing before the FFT reduces the side lobes of the OFDM spectrum, it can lead to a loss of orthogonality between subcarriers [62]. However, Nyquist windowing can reduce the side lobes and conserve the orthogonality.

2.4.1.Nyquist criteria

Nyquist introduced criteria for dealing with ISI.

The criterion was that each pulse is zero at the sampling time of the other pulses.

$$p(t)=\begin{cases}1 & \text{t=0}\\ 0 & t=\pm kT_b,\ k=\pm 1,\pm 2,...\end{cases} \tag{2.27}$$

The Nyquist criterion in the spectral domain leads to the condition below:

$$\Gamma\left(\tfrac{1}{2T_s}+\Delta f\right)+\Gamma\left(\tfrac{1}{2T_s}-\Delta f\right)=\Gamma(0) \tag{2.28}$$

where Δf is the occupied channel bandwidth.

2.4.2. The Raised Cosine Pulse

The raised cosine filters are a generalized case of a Nyquist filter. It is a realistic and frequently used filter in telecommunication systems because of its ability to minimize the intersymbol interference (ISI). Unlike the rectangular pulse, the raised cosine pulse takes the shape of a sinc pulse, as indicated by the left-most term of $p(t)$, in equation (2.30). Unfortunately, the name "raised cosine" is misleading. It actually refers to the pulse's frequency spectrum, $P(\omega)$, not to its time domain shape, $p(t)$. The precise shape of the raised cosine spectrum is determined by the parameter, α, where $0 \leq \alpha \leq 1$. Specifically, α governs the bandwidth occupied by the pulse and the rate at which the tails of the pulse decay. A value of $\alpha = 0$ offers the narrowest bandwidth, but the slowest rate of decay in the time domain. When $\alpha = 1$, the bandwidth is $1/\tau$, but the time domain tails decay rapidly. Figures (2.2), (2.3) present the time domain waveform and frequency domain representation of raised cosine pulse shaping filters respectively for $\alpha = 0, 0.5, 1$.

The magnitude spectrum of the raised cosine pulse is given by [52]

$$P(w) = \begin{cases} \tau & 0 \leq \omega \leq \frac{\pi(1-\alpha)}{\tau} \\ \frac{\tau}{2}\left(1-\sin\left(\left(\frac{\tau}{2\alpha}\right)\left(\omega-\frac{\pi}{\tau}\right)\right)\right) & \frac{\pi(1-\alpha)}{\tau} \leq \omega \leq \frac{\pi(1+\alpha)}{\tau} \\ 0 & \omega \geq \frac{\pi(1+\alpha)}{\tau} \end{cases} \quad (2.29)$$

The time domain response is given by:

$$p(t) = \frac{\left(\sin c\,\frac{t}{\tau}\right)\left(\cos\frac{\alpha\pi t}{\tau}\right)}{1-\left(\frac{2\alpha t}{\tau}\right)^2} \quad (2.30)$$

$$p(t) = \begin{cases} \left(\frac{\pi}{4}\right)\sin c\left(\frac{t}{\tau}\right) & \frac{\alpha t}{\tau} = \pm\frac{1}{2} \\ \dfrac{\left(\sin c\,\frac{t}{\tau}\right)\left(\cos\frac{\alpha\pi t}{\tau}\right)}{1-\left(\frac{2\alpha t}{\tau}\right)^2} & \text{elsewhere} \end{cases} \quad (2.31)$$

The precise shape of the raised cosine spectrum is determined by the roll-off factor, α, where $0 \leq \alpha \leq 1$.

When a value of the roll off-factor increases, the side lobes of OFDM spectrum decrease. This reduction in side-lobe level power leads to the reduction in ICI power.

Windowing can only reduce the ICI if the channel is band limited and avoids the propagation of errors in the demodulation process. However, this method does not take into consideration the Doppler shift and the frequency mismatch between the transmitter and the receiver.

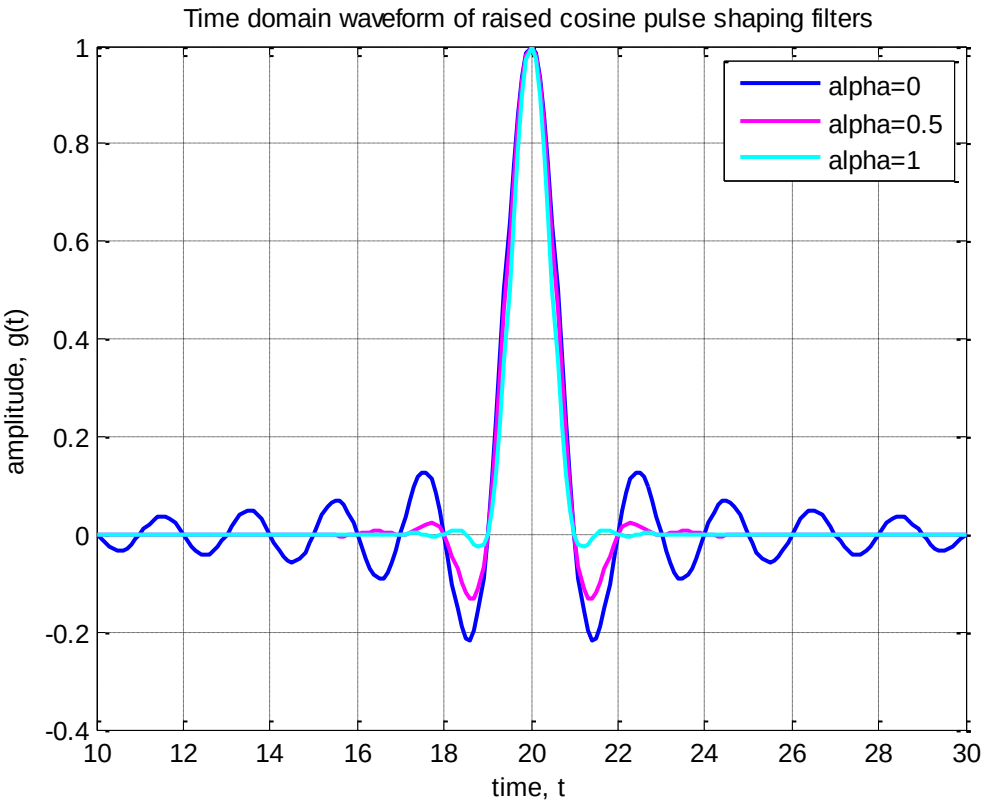

Figure 2.2. Time domain waveform of raised cosine pulse shaping filters

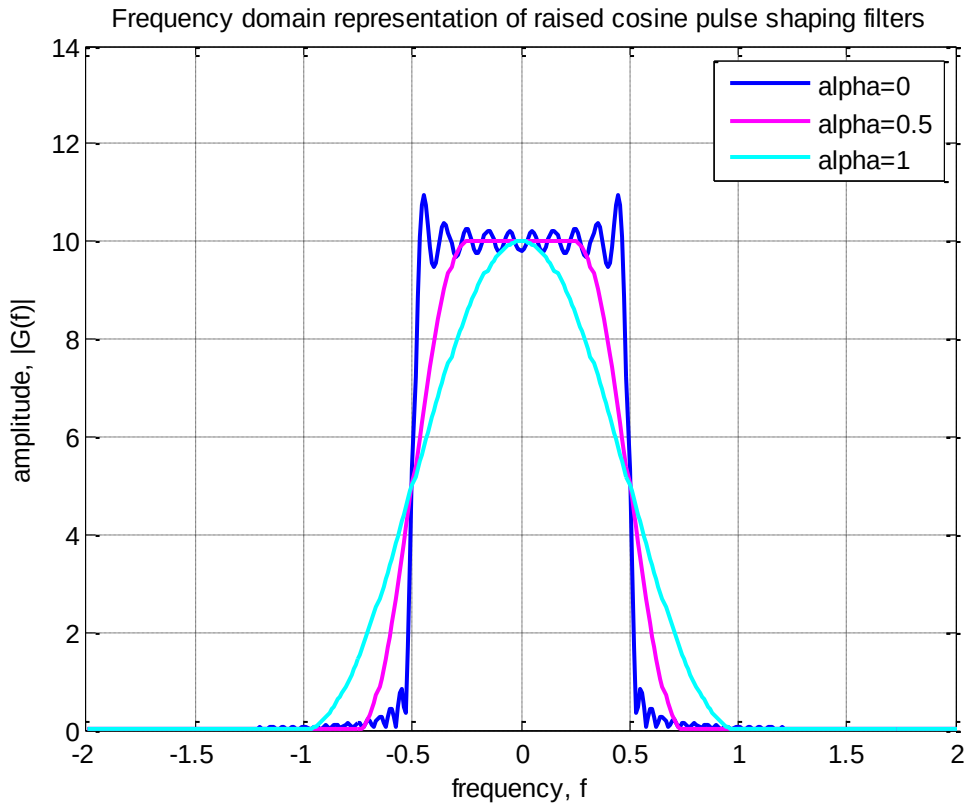

Figure 2.3. Frequency domain representation of raised cosine pulse shaping filters

2.5. Kalman Filter

Kalman filtering has gained huge attention in the field of optical communication systems [64], wireless sensor networks [65] and in the estimation process. The Kalman filter is minimum variance unbiased linear filter. It provides an efficient computational (recursive) means to estimate the state for a discrete-time process described by a linear difference stochastic equation. It estimates a process by using a form of feedback control: the filter estimates the process state at some time and then obtains feedback in the form of (noisy) measurements. As such, the equations for the Kalman filter fall into two groups: time update equations and measurement update equations. The time update equations are responsible for projecting forward (in time) the current state and error covariance estimates to obtain the a priori estimates for the next time step. The measurement update equations are responsible for the feedback for incorporating a new measurement into the a priori estimate to obtain an improved a posteriori estimate. The time update equations can also be thought of as predictor equations, while the measurement update equations can be thought of as corrector equations. Indeed the final estimation algorithm resembles that of a predictor-corrector algorithm for solving numerical problems.

A state-space model of the discrete Kalman filter is defined as

$$y(n) = x(n)d(n) + w(n) \tag{2.32}$$

In this model, the observation $y(n)$ has a linear relationship with the desired value.

However, the extended Kalman filter (EKF) gives an approximation of the optimal estimate of the state for a discrete-time process described by a non-linear difference stochastic equation. The non-linearities of the systems' dynamics are approximated by a linearized version of the non-linear system model around the last state estimate. For this approximation to be valid, this linearization should be a good approximation of the non-linear model in the entire uncertainty domain associated with the state estimate.

The EKF uses a first order Taylor expansion. So, we can linearize the estimation around the current estimate using the partial derivatives of the process and measurement functions to compute estimates even in the face of non-linear relationships.

The drawback of EKF is the error in function approximation because the EKF uses a first order Taylor series for approximating, then on linearities. So, large errors may happen when it is used in systems with higher order non-linearities. [66]

2.5.1. ICI Cancelation using the EKF Algorithm

First, we use the EKF to estimate the frequency offset. Secondly, we apply the offset correction scheme.

To estimate the frequency offset we need.

The received OFDM symbol is given by:

$$y(n) = x(n)e^{j\frac{2\pi n'\varepsilon(n)}{N}} + w(n) \tag{2.33}$$

It is clear that the received OFDM symbol has nonlinear relationships with the desired value $\varepsilon(n)$. So, we use the first-order Taylor's expansion in order to linearize the desired value.

$$y(n) = f(\varepsilon(n)) + w(n). \tag{2.34}$$

$$y(n) \approx f(\hat{\varepsilon}(n-1)) + f'(\hat{\varepsilon}(n-1))\left[\varepsilon(n) - \hat{\varepsilon}(n-1)\right] + w(n). \tag{2.35}$$

Then

$$y(n) - f(\hat{\varepsilon}(n-1)) \approx f'(\hat{\varepsilon}(n-1))\left[\varepsilon(n) - \hat{\varepsilon}(n-1)\right] + w(n) \tag{2.36}$$

where

$\hat{\varepsilon}(n-1)$ is the estimation of $\varepsilon(n-1)$.

$$f'(\hat{\varepsilon}(n-1)) = \left.\frac{\partial f(\varepsilon(n))}{\partial(\varepsilon(n))}\right|_{\varepsilon(n)=\hat{\varepsilon}(n-1)} = j\frac{2\pi n'}{N}x(n)e^{j\frac{2\pi n'\hat{\varepsilon}(n-1)}{N}} \tag{2.37}$$

$y(n) - f(\hat{\varepsilon}(n-1))$ is linearly related with the desired value $\left[\varepsilon(n) - \hat{\varepsilon}(n-1)\right]$.

2.6. ICI Self-Cancellation

Orthogonal frequency-division multiplexing (OFDM) communications systems need precise frequency synchronization to avoid intercarrier interference (ICI). However, perfect synchronization is difficult to achieve, so methods that eliminate ICI are required.

The ICI self-cancellation scheme is an easier method for suppressing ICI in OFDM. The main idea is to modulate one data symbol onto a group of subcarriers with predefined weighting coefficients [67]. Thus, the ICI signals produced within a group can be "self-cancelled" by each other. A lot of studies are using ICI self-cancellation [68-69]. Further discussions on the ICI self-cancellation scheme are presented in [70, 71], where the scheme is also called polynomial cancellation coding (PCC). In previous works, the mechanism analysis of the scheme is developed. A quantitative ICI

power analysis of the ICI self-cancellation scheme is studied in [67]. The average carrier-to-interference power ratio (CIR) [35] is used as the ICI level indicator, and a theoretical CIR expression is derived as in [67].

2.6.1. ICI Processes of Standard OFDM Systems

For OFDM systems, the received signal at subcarrier *k* can be expressed as

$$Y(k) = X(k)S(0) + \sum_{l=0,l\neq k}^{N-1} X(l)S(l-k) + n_k, \quad k = 0,1,\dots,N-1. \quad \text{..... (2.38)}$$

Where N is the total number of OFDM subcarriers, $X(k)$ is the modulated subcarrier, n_k is additive noise, and $S(l-k)$ are the complex coefficients for the ICI components in the received signal. These coefficients are given by

$$S(l-k) = \frac{\sin(\pi(l+\varepsilon-k))}{N\sin(\frac{\pi}{N}(l+\varepsilon-k))} e^{(j\pi\left(1-\frac{1}{N}\right)(l+\varepsilon-k))} \quad (2.39)$$

where ε represents the normalized frequency offset, that is, $\varepsilon = \Delta f / (1/NT)$, where Δf is the frequency difference between the transmitter and the receiver, and NT denotes the interval of an FFT period [67]. Fig. 2.4 gives an example of the $S(l-k)$ when $l=0$ and $N=16$.

The frequency offset values are $\varepsilon = 0.2$ and $\varepsilon = 0.4$. It has been shown that as ε increase, the desired part $|S(0)|$ decreases and the undesired part $|S(l-k)|$ rises.

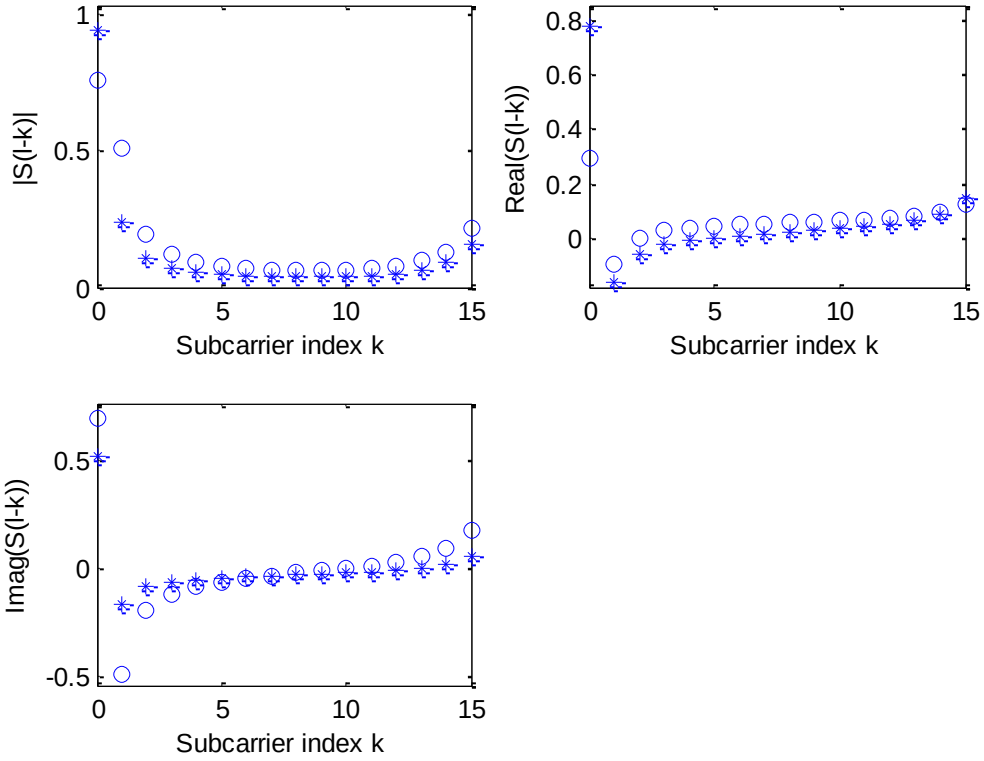

Figure 2.4. An example of $\boldsymbol{S(l-k)}$ for N = 16; l = 0. (a) Amplitude of $(\boldsymbol{l-k})$. (b) Real part of $(\boldsymbol{l-k})$. (c) Imaginary part of $\boldsymbol{S(l-k)}$.

The self-cancellation method relies on the fact that the real and imaginary parts of the ICI coefficients change gradually with respect to the subcarrier index k; therefore, the difference between consecutive ICI coefficients, *S(l-k)-S(l-k+1)*, is very small.

During modulation, one data symbol is mapped onto two consecutive subcarriers with predefined weighting coefficients. The weighting coefficients are calculated carefully such that the ICI signals within the successive subcarriers are cancelled by each other at the receiver end; hence this technique is called "self-cancellation". It is worth noting that the redundant modulation in the self-cancellation scheme reduces the bandwidth efficiency. The investigators will explore ways to compensate for that problem if possible.

The system ICI power level can be evaluated by using the CIR [35]. While deriving the theoretical CIR expression, the additive noise is omitted. The desired received signal power on the kth subcarrier can be represented as

$$E[|C(k)|^2] = E[|X(k)S(0)|^2] \tag{2.40}$$

and the ICI power is

$$E[|I(k)|^2] = E\left[\left|\sum_{l=0,\ l\neq k}^{N-1} X(l)S(l-k)\right|^2\right] \quad (2.41)$$

It is assumed that the transmitted data have zero mean and are statistically independent; therefore, the CIR expression for subcarrier $0 \leq k \leq N-1$ can be derived as

$$CIR = \frac{|S(k)|^2}{\sum_{l=0,l\neq k}^{N-1}|S(l-k)|^2} = \frac{|S(0)|^2}{\sum_{l=1}^{N-1}|S(l)|^2} \quad (2.42)$$

Equation (2.42) suggests that the CIR is a function of N and l. However, the CIR varies very little as a function of N. Analysis shows that the CIR, for a given, results in a maximum change of 0.068 dB when $N \geq 8$ [67]. Therefore, the CIR of OFDM systems only depends on the normalized frequency offset approximately.

2.6.2. ICI Cancelling Modulation

The previous conclusion explains that the only way to reduce ICI is by decreasing frequency offset. For a certain channel frequency offset, smaller values can be obtained by increasing the subcarrier separation. Consequently, the bandwidth efficiency will be reduced since the time-domain symbol length is reduced and, therefore, the guard interval will take a relatively larger portion of the useful signal [67].

It has been shown in Figure 2.4 that both real and imaginary parts of the ICI coefficient are gradually changed with respect to the subcarrier index. Often, there is little difference between $S(l-k)$ and $S(l+1-k)$. Therefore, if a data pair *(a,-a)* is modulated onto two adjacent subcarriers *(l,l+1)* where *a* there is complex data, then the ICI signals generated by the subcarrier *l* will be cancelled out significantly by the ICI generated by a subcarrier *l+1*. This is the ICI cancellation idea proposed in [68].

Assume the transmitted symbols are composed so that *X(1) = -X(0), X(3) = -X(2),…X(N-1) = -X(N-2)*, then the received signal on subcarrier becomes [56]

$$Y'(k) = \sum_{\substack{l=0 \\ l=even}}^{N-2} X(l)[S(l-k) - S(l+1-k)] + n_k \quad (2.43)$$

and on subcarrier *k+1* is

$$Y'(k+1) = \sum_{\substack{l=0 \\ l=even}}^{N-2} X(l)[S(l-k-1) - S(l-k)] + n_{k+1} \quad (2.44)$$

So, the ICI coefficient is denoted as

$$S'(l-k) = S(l-k) - S(l+1-k). \quad (2.45)$$

Figure 2.5 presents the comparison between $|S(l-k)|$ and $|S'(l-k)|$ on a logarithmic scale. For the majority of the *l-k* values, it is found that $|S'(l-k)| \ll |S(l-k)|$ Moreover, the summation in (2.43) only takes even values, and the total number of the interference signals is reduced to half, compared with that in (2.38). Thus, the ICI signals in (2.43) are much smaller than those in (2.38) since both the number of ICI signals and the amplitudes of the ICI coefficients have been minimized. This modulation method is called an ICI-cancelling modulation.

The notion of an ICI self-cancellation method and the derived coefficients was also used to the partial response signaling of OFDM systems [72].

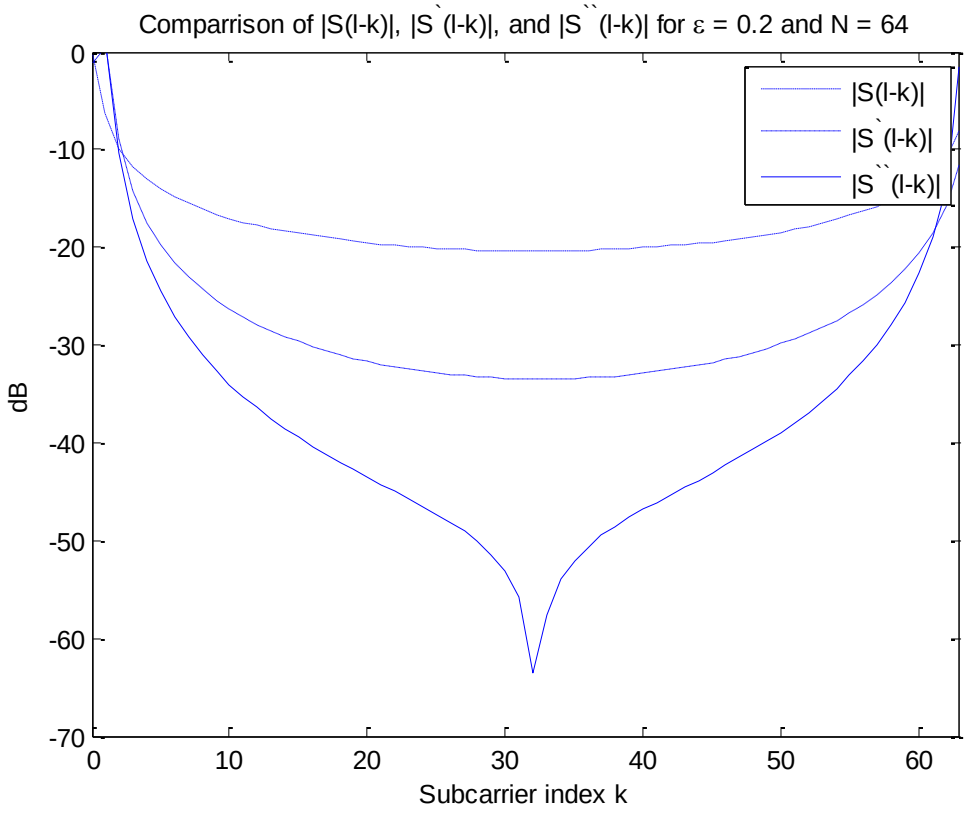

Figure 2.5. A comparison between $|S(l-k)|$; $|S'(l-k)|$and $|S''(l-k)|$; N = 64

2.6.3. ICI cancelling demodulation

The ICI-cancelling modulation allows one data symbol transmitted by each pair of subcarriers. It improves the performance of the system on the receiver side. Further reduction of ICI can be considered to be using a so-called ICI-cancelling demodulation scheme.

The demodulation is suggested to work in such a way that each signal at the k+1th subcarrier (now k denotes an even number) is multiplied by " -1" and then summed with the one at the kth

subcarrier. Then the resulting data sequence is used for making symbol decisions. It can be represented as [67]

$$Y''(k) = Y'(k) - Y'(k+1) = \\ = \sum_{\substack{l=0 \\ l=even}}^{N-2} X(l)[-S(l-k-1) + 2S(l-k) - S(l-k+1)] + n_k - n_{k+1}.$$

(2.46)

The corresponding ICI coefficient then becomes

$$S''(l-k) = -S(l-k-1) + 2S(l-k) - S(l-k+1). \quad (2.47)$$

Three types of ICI coefficients are obtained: 1) $S(l-k)$for the standard OFDM system; 2) $S'(l-k)$ for ICI cancelling modulation; and 3) $S''(l-k)$ for combined ICI-cancelling modulation and demodulation. Figure 2.5 shows the amplitude comparison of $|S(l-k)|$,$|S'(l-k)|$ and $|S''(l-k)|$ for N=64 and $\varepsilon = 0.2$. Notice the logarithmic scale on the vertical axis. For the majority of $(l-k)$ values, $|S'(l-k)|$ is much smaller than $|S(l-k)|$, and the $|S''(l-k)|$ is even smaller than $|S'(l-k)|$. Thus, the ICI signals become smaller when applying ICI-cancelling demodulation. In addition, the ICI-cancelling demodulation can further reduce the residual ICI in the received signals. This combined ICI-cancelling modulation and demodulation method is called the ICI self-cancellation scheme.

It is worth noting that the proposed ICI-cancelling demodulation also enhances the system signal-to-noise ratio. The signal level rises by a factor of 2 due to coherent addition, whereas the noise level is proportional to $\sqrt{2}$ because of noncoherent addition of the noise on different subcarriers. Using the ICI coefficient given by the equation (2.45), the theoretical CIR of the ICI self-cancellation scheme can be derived as

$$CIR = \frac{|-S(-1)+2S(0)-S(1)|^2}{\sum_{l=2,4,6,\dots}^{N-1}|-S(l-1)+2S(l)-S(l+1)|^2} \quad (2.48)$$

With this scheme, carrier-to-interference ratio (CIR) will increase, thus improving the BER at the receiver. The goal in this part of the project is to simulate different OFDM channels and use the self-cancellation scheme to determine and compare the improvements in the CIR and BER.

Simulated CIR can be calculated using Y for the received signal, X for the transmitted signal and by using equation (2.38). It can be written:

Y = X.S0 + I , so (2.49)

$$I = Y - X.S0 \tag{2.50}$$

Where I is the ICI coefficient,

Using equations (2.40), (2.41), (2.42) the simulated CIR can be written as:

$$\text{Simulated CIR}=E[|X(k)S(0)|^2]/\ E[|Y(k)-X(k)S(0)|^2]; \tag{2.51}$$

Figures (2.6), (2.7) show the simulated and theoretical CIR, respectively, versus normalized frequency offset.

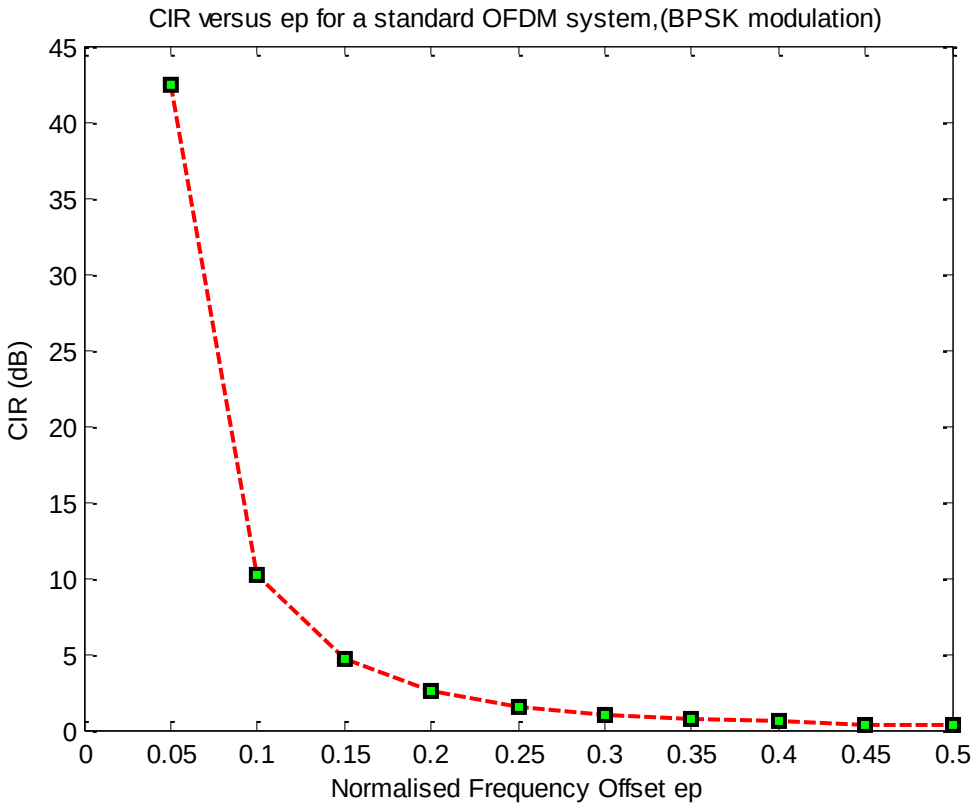

Figure 2.6. CIR (simulated) versus ep for a standard OFDM system

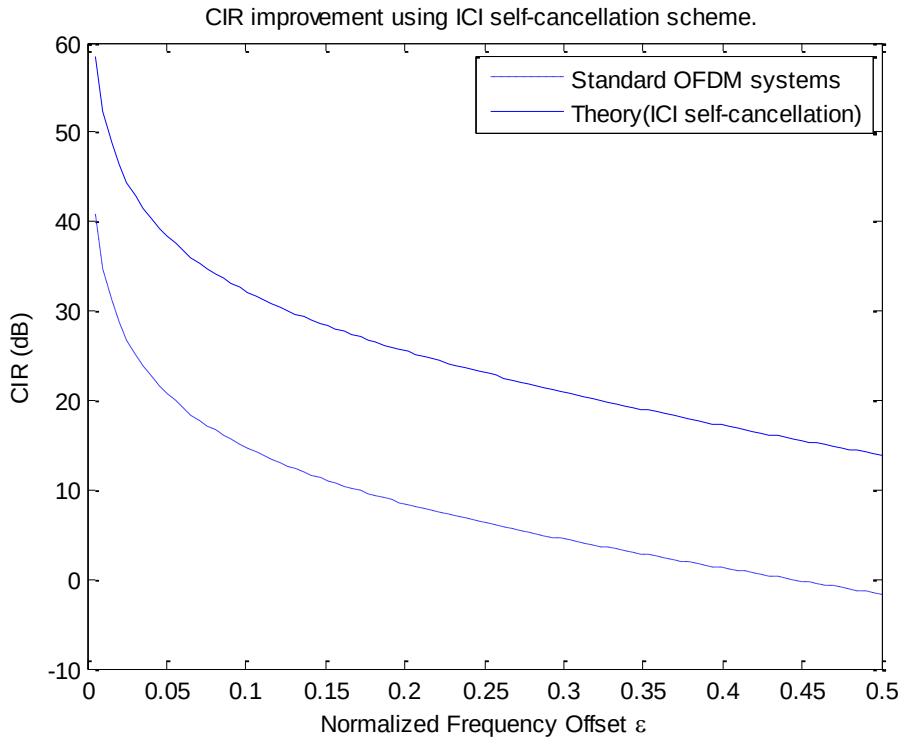

Figure 2.7. Theory CIR for a standard OFDM system and ICI self-cancellation

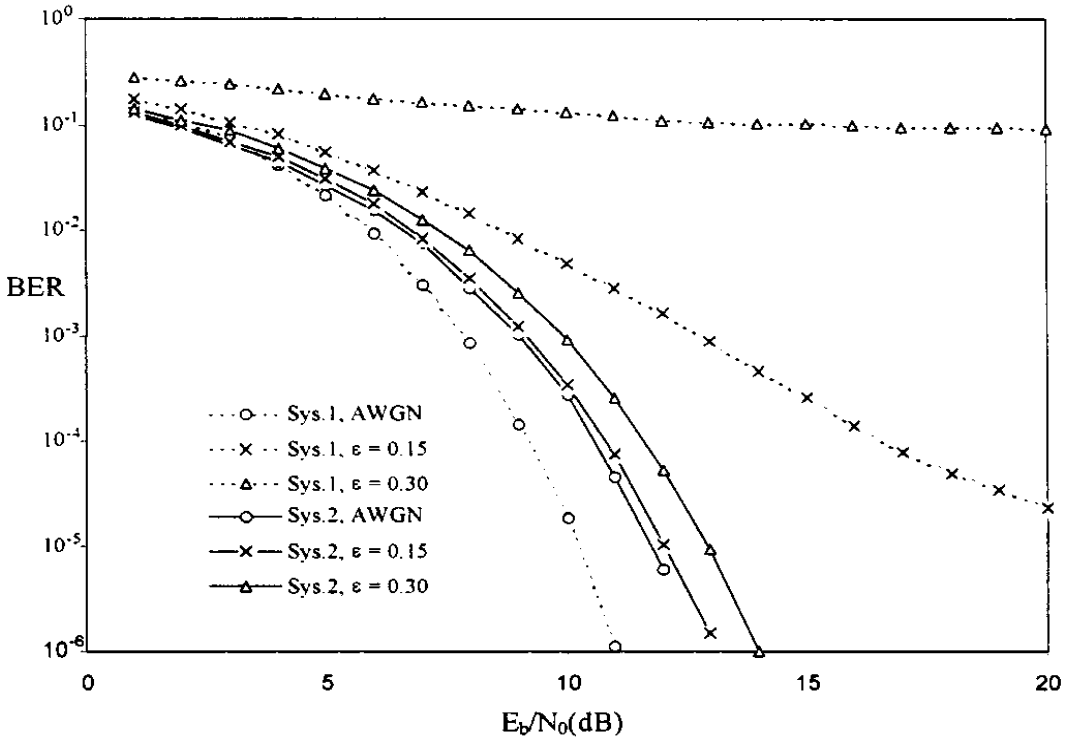

Figure 2.8. BER versus E_b/N_0 of two systems for different frequency offset values [72].

Reference [72] used two systems to evaluate the ICI self-cancellation method.

System 1: Standard BPSK modulation OFDM system without ICI self-cancellation;

System2: 4PSK modulation OFDM system with ICI self-cancellation.

The results in Figure 2.8 confirm that the system that uses ICI self-cancellation performs better than the conventional one (without ICI self-cancellation) except in the case where the frequency offset is zero. Y. Zhao et al. [72] argued that about the use of BPSK for the first system and the use of 4PSK for the second system under AWGN channel, where the BPSK modulation performs better than 4PSK modulation.

2.7. Conclusion

In this chapter, the methods that mitigate the effect of carrier frequency offset (CFO) are presented. First, the techniques that estimate and compensate CFO are described. An overview of maximum likelihood (ML) carrier frequency offset estimation is given. The algorithms of the Moose estimator, Beek estimator, Classen estimator and Schmidl Cox estimator are explained in detail. Frequency domain equalization is included. Time domain windowing is also yielded in this chapter. However, this method does not deal with either the Doppler shift or the frequency mismatch between the transmitter and the receiver. The Kalman filter and ICI self-cancellation are presented. However, the Kalman filter method is limited because it requires system linearity. Even though ICI self-cancellation has good results, bandwidth efficiency is reduced by half.

Chapter 03

PROPOSEDFREQUENCY OFFSET ESTIMATOR

3.1. Introduction

The OFDM system has the potential to be used in the development of the fifth generation standards because of its high robustness against channel dispersion and multipath channels [73]. This multicarrier modulation technique was used by several standards including enhanced mobile broadband (eMBB) and ultra-reliable low latency communication (URLLC) services at below 40 GHz [74]. However, further research is needed to define the key performance requirements on spectral efficiency, unwanted emission limits and the carrier synchronization [75-76]. Hence, several techniques that use OFDM have been developed to overcome fifth generation technological challenges.

One of the major disadvantages in the OFDM system is the intercarrier interference (ICI) caused by the carrier frequency offset (CFO) between the transmitter and the receiver or by Doppler spread [77-78]. This CFO destroys the orthogonality between subcarriers, while, due to the requirements of the speed data, orthogonality [79] needs to be maintained. Hence, the estimation of carrier frequency offsets (CFOs) is an interesting problem [80] to be addressed for OFDM systems.

Many data-aided techniques have been proposed to correct frequency offset and avoid ICI [34-35; 80-82]. Although these algorithms can effectively estimate frequency offset, they reduce the bandwidth efficiency. To eliminate this reduction, non-data-aided algorithms that exploit the redundancy of the cyclic prefix (CP) have been developed [36, 38, 39, 42-44, 52]. The joint maximum-likelihood (ML) estimation of the symbol-time and carrier frequency offset [36], referred to as VDB-MLA, is assumed in additive white Gaussian noise (AWGN) channels. However, its performance might be degraded over multipath channels. To overcome this shortage, authors in [42-44] propose a joint ML synchronization algorithm for symbol timing and CFO in OFDM systems over dispersive fading channels, based on the redundancy of the CP. In order to avoid the high complexity and the impractical implementation of joint ML estimation of the timing error, the FFO, the IFO and the preamble index, a realistic approach based on two-stage procedure is proposed in [48]. In the first stage, timing offset and FFO is estimated using blind estimation based on redundant information from the CP. In the second stage, the IFO and the preamble index recovery

are accomplished in a joint ML estimation and also suboptimal algorithms are developed. B. Xie et al. [51] studied the effects of CFO-induced spectral misalignment for OFDM systems in frequency-selective channels and generated an exact signal model. However, this exact signal model didn't include timing and sampling offsets. A generalization of reference [51] is presented in [50]. It incorporates timing and sampling offsets and studies what effects the accurate signal model brings to the CFO estimation and how to address them. P. S. Wang et al. [83] used a more complete signal correlation function over wide-sense stationary uncorrelated scattering (WSSUS) channels involving triplet structure. Based on this model, an exact likelihood function is derived. It is found that the ML CFO estimate is the solution of a quartic equation rather than the phase angle of a complex number as obtained in many previously derived methods. T. C. Lin et al. [54] developed a solution to exploit the repetitive structure of CP samples in multipath channels by using the so-called remodulated received vectors [55]. The authors developed a blind estimator for fractional CFO. They proposed a new CP-based algorithm for blind CFO estimation in OFDM systems. Both the Cramer-Rao bound (CRB) on MSE and a closed-form formula for the theoretical MSE is derived for multipath channels. Using the remodulation of the received signal in the presence of CFO for blind estimation, coarse and fine CFO estimators are derived. The distributed multiple-input multiple-output (DMIMO) system, combined with orthogonal frequency division multiplexing (OFDM), is an arising model with high data rates for the fifth generation [84]. The DMIMO-OFDM system demands rigorous synchronization and tracking because the received signal has multiple timing offsets (MTOs); multiple carriers frequency offsets (MCFOs) and frequency-selective channel gains. Thus, the reference [84] proposed two iterative estimators: expectation conditional maximization (ECM) and space-alternating generalized expectation maximization (SAGE) to mitigate these impairments. The residual time-frequency estimation errors at the relays are improved.

OFDM leads to high spectral efficiency over multipath channels, which makes its use in the fifth generation more suitable and relevant [85]. However, its sensitivity to intercarrier interference ICI is a real obstacle that prevents its use. Despite the extensive number of studies dealing with the problem of synchronization [86-88], OFDM still requires additional research to overcome this disadvantage which penalizes the use of its capabilities in the fifth generation. Hence our contribution in this chapter focuses on the problem of ICI. We develop a blind frequency offset estimator CFO based on the correlation between samples in the cyclic prefix over a Rayleigh fading channel. We use the remodulated sequence proposed in [58-59]. A closed-form solution is derived using the correlation characteristic and the log likelihood function.

Channel medium plays an essential role in wireless communications. The transmitted signal has undergone a lot of degradations on the receiver side, the main ones being path loss, shadowing, reflection and diffraction[91]. Thus, the channel wireless medium can be categorized into large-scale fading and small-scale fading [92]. Large-scale fading is due to motion over large areas. Small-scale fading is due to small changes in position. In our thesis, we focus on small-scale fading channels. We used a multipath fading channel as the medium for our transmitted signal to demonstrate the effectiveness of OFDM under these types of channels. Multipath fading in wireless communication systems is commonly modeled by Rayleigh (for the case where no line-of-sight component is present) and Rician (for the case where a line-of-sight component is present) distributions [93].

The purpose of this chapter is to develop a new algorithm that can estimate the carrier frequency offset (CFO) under different Rayleigh channel parameters. An accurate CFO is obtained by integrating the remodulated received symbols. This chapter is organized as follows: Section 2 introduces the effect of CFO in OFDM systems; Section 3 explains the effect of timing synchronization; the effect of Rayleigh fading channel is provided in section 4; the proposed CFO estimator is explained in detail in Section 5; and the chapter ends with a conclusion.

3.2. The Effect of CFO in OFDM Systems

The block diagram of an OFDM system is shown in Figure 3.1. The source bit stream may include source coding, channel coding, and bit interleaving. The transmitter maps the source bit stream to modulation symbols from a complex constellation such as phase-shift keying (PSK) or quadrature amplitude modulation (QAM). The different constellations may be used for different subcarriers, if bit loading algorithms are used [89].

Let $\{Z(0), Z(1).....Z(N-1)\}$ be a block of N data symbols after the serial to parallel conversion.

An OFDM symbol which consists of N subcarriers is given by the formula below:

$$z(n) = \sum_{k=0}^{N-1} Z(k) e^{\frac{j2\pi kn}{N}} \tag{3.1}$$

where $z(n)$ is the IDFT (inverse discrete Fourier transform) of the transmitted symbol $Z(k)$ for k=0,.. N-1. Therefore, OFDM modulation and demodulation can be efficiently implemented by using IFFT/FFT. Thus, the hardware realization is simplified as compared to the traditional implementation using the oscillators.

We assume that α_0 is the normalized frequency offset (the ratio of actual frequency offset to the intercarrier spacing) and τ_0 is the time offset. Carrier frequency offset is modulated by a phase shift of $2\pi\alpha_0 n/N$, assuming that N_{cp} is the length of the cyclic prefix which is used to avoid ISI and $h(l)$ is the multipath fading channel of length L where $L \le N_{cp}$. The observed window is assumed to be of length *$(2N+N_{cp})$.*

After going across multipath channel and an AWGN channel, the received signal is given by:

$$u(n) = \sum_{l=0}^{L-1} h(l) z(n-l-\tau_0) e^{\frac{j2\pi n\alpha_0}{N}} + w_n \tag{3.2}$$

where w_n is an additive white Gaussian noise.

Then, the k^{th} element of a DFT sequence of a received signal consisting of three components can be written as [35]:

$$U(k) = DFT(u(n)) \tag{3.3}$$

$$U(k) = Z(k)H(k)\left\{(\sin\pi\alpha_0)/(N\sin(\pi\alpha_0/N))\right\} e^{j\pi\alpha_0(N-1)/N} + I_k + W_k \tag{3.4}$$

where H is the DFT of the multipath channel h and W_k is the DFT of the additive white Gaussian noise w_n.

The data is attenuated by the term $\left\{(\sin\pi\alpha_0)/(N\sin(\pi\alpha_0/N))\right\}$ and shifted by the term $e^{j\pi\alpha_0(N-1)/N}$

I_k representing the intercarrier interference and is expressed as [35]

$$I_k = \sum_{\substack{i=0 \\ i\neq k}}^{N-1} Z_i H_i \left\{\sin\pi(i-k+\alpha_o)/(N\sin(\pi(i-k+\alpha_o)/N))\right\}.e^{j\pi\alpha_o(N-1)/N} e^{-j\pi(i-k)/N} \tag{3.5}$$

The inter carrier interference subcarrier

The frequency offset degrades the signal-to-noise ratio (SNR) as it presented in the formula below:

$$D_{freq} = \frac{10}{3\ln 10}\left(\pi\Delta f T\right)^2 \frac{E_s}{N_0} \tag{3.6}$$

Where D_{freq} is the SNR degradation, Δf is the frequency offset, T is the symbol duration and E_s is energy per bit of the OFDM signal, N_0 one-sided noise power spectrum.

The degradation of SNR is presented in the figure 3.2. It shows that the value E_s / N_0 increases as the degradation decreases. In addition, the degradation varies in proportion to the value of the frequency offset. As frequency offset rises, the degradation of SNR rises.

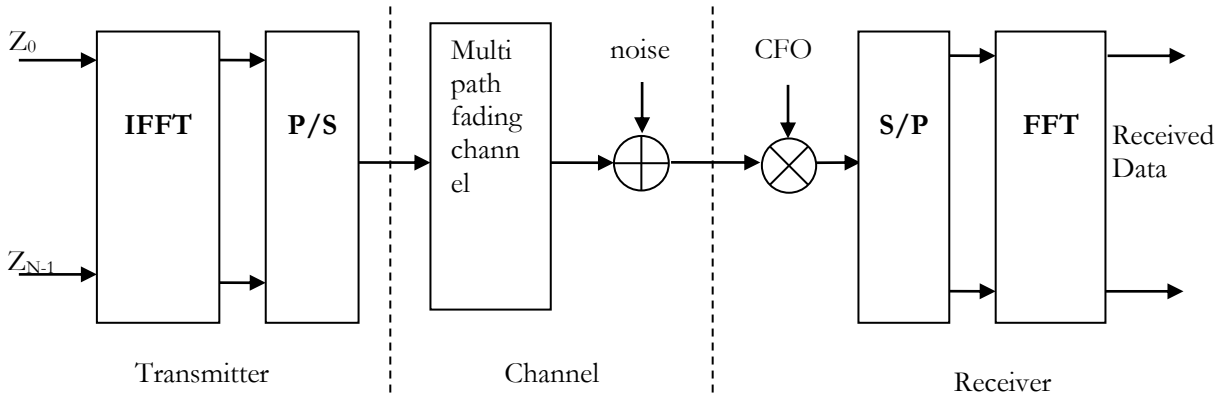

Figure 3.1.OFDM block diagram

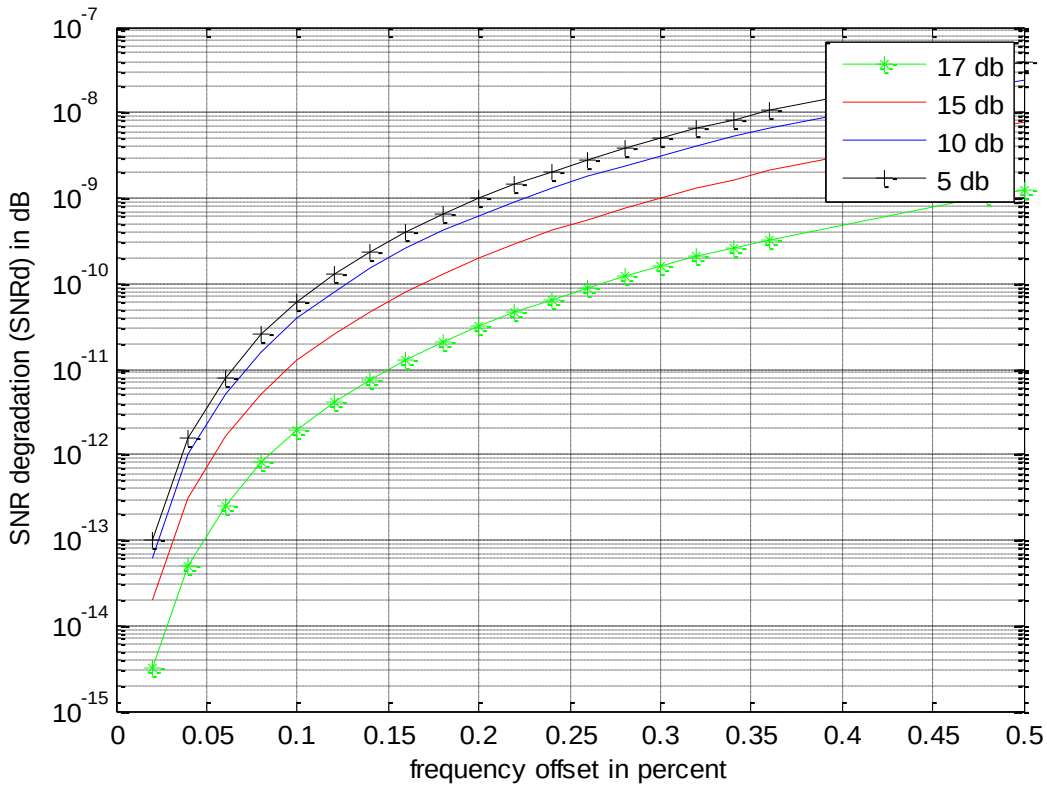

Figure 3.2. SNR degradation of frequency offset for different E_b/N_0 values (5 10 15 17dB)

The effect of carrier frequency offset (CFO) can be categorized as integer carrier frequency offset (IFO) and fractional carrier frequency offset (FFO). The IFO can cyclically shift the transmitted

signal at the receiver which causes the degradation in bit error rate (BER) performance. IFO does not destroy the orthogonality between subcarriers, while the fractional carrier frequency offset (FFO) can destroy the orthogonality between subcarriers as well as ICI.

3.3. The Effect of Timing Synchronization

The goal of symbol synchronization is to determine the correct position of the FFT window, which is the original position of OFDM symbol, and the FFT window can contain the current OFDM symbols of N, so that it can get the correct demodulation. If the timing estimation was not done properly, the original position of the FFT window would not be on the first sample point of the current OFDM symbol, and there might contain sample points of neighboring OFDM symbols. If there is no synchronization, the beginning of the FFT window will be placed too early or too late. If placed too late, some samples will be collected from the actual OFDM symbol and the others will be collected from the following OFDM symbol; if no following OFDM symbol exists, the last samples are filled up with noise. If placed too early, samples from the previous OFDM symbol will be collected. Both cases result in intersymbol interference (ISI). So symbol timing estimation is important for OFDM synchronization.

However, when the time offset is within the guard interval (GI), no ISI occurs (assuming no ICI), only a phase offset ϕ which is proportional to the time shift occurs. If the DFT is applied to the cyclically shifted time sequence $u[n-\tau_0]$, the result is:

$$DFT\left\{u[n-\tau_0]\right\} = U[k].e^{-j\frac{2\pi k}{N_{FFT}}\tau_0} \tag{3.7}$$

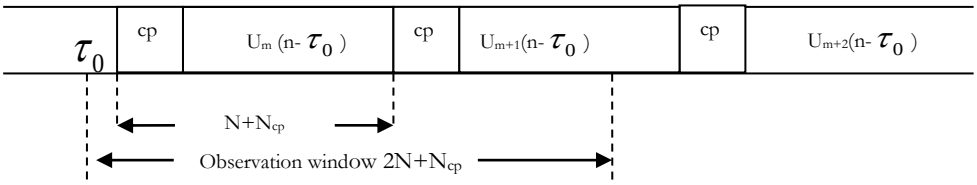

Figure 3.3. Frame structure of transmitted data (delayed by τ_0)

This shows that the offset has the formula:

$$\phi = -\frac{2\pi k}{N_{FFT}}\tau_0 \tag{3.8}$$

This is not constant for all subcarriers.

3.4. The Effect of Rayleigh Fading Channel

The transmission channel is the pathway for information to pass through from transmitters to receivers. It is the critical part because the RF signal will always be distorted when passing through a channel, and proper recovery at the receiver is needed. In addition, channels are different in various communication scenarios, which affects signal and system designs.

There are two types of fading effects that characterize mobile communications [92]:

- Large-scale fading that represents the average signal power attenuation or path loss due to motion over large areas;
- Small-scale fading, which is also called Rayleigh fading because if the multiple reflective paths are large in number and there is no line-of-sight propagation path (signal component), the envelope of the received signal is statistically described by a Rayleigh probability density function (PDF).

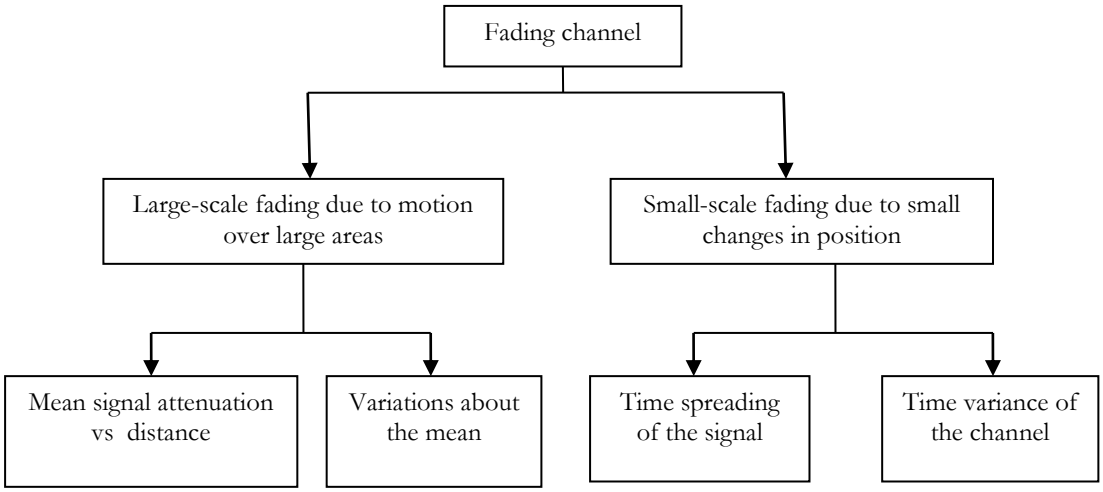

Figure 3.4. Fading channel manifestations [92]

The multipath propagation arises from the fact that the transmitted signal is reflected from objects such as buildings or mountains, scattered from smaller objects such as lamp posts, and diffracted at edges of houses and roof-tops [91] as presented in Figure 3.5.

The most harmful fading channel is the Rayleigh fading model which was first introduced by Bell Lab in the 1970s. It is a statistical model of the communication channel representing the effects of a propagation environment on a radio signal. A statistical Rayleigh fading model is the simplest fading channel model. Rayleigh fading models assume that the magnitude of a signal that has

passed through such a transmission medium (also called a communications channel) will vary randomly, or fade, according to a Rayleigh distribution — the radial component of the sum of two uncorrelated Gaussian random variables.

The Rayleigh fading model performs as a reasonable channel model when there are many objects (such as buildings and mountains) in the propagation environment which scatter the radio signal before it arrives at the receiver. The Rayleigh fading channel in mobile digital communication systems is introduced in [92, 94].

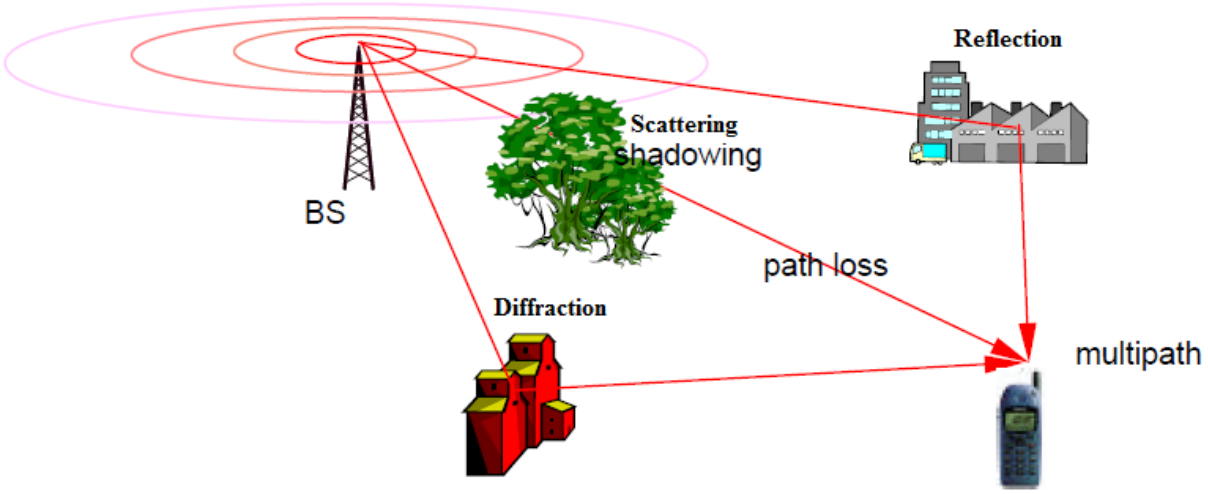

Figure 3.5. Multipath channel

In this study, the channel is assumed to exhibit Rayleigh fading. The envelope of the impulse response is Rayleigh distributed. The probability density function (PDF) of the Rayleigh distribution is given by:

$$f(x) = \frac{x}{\sigma^2} e^{-\frac{x^2}{2\sigma^2}} \tag{3.9}$$

The scale parameter σ is the root mean square (RMS) of the received signal voltage and σ^2 is the normalized average power of the multipath component. The value x is the amplitude of the received signal envelope.

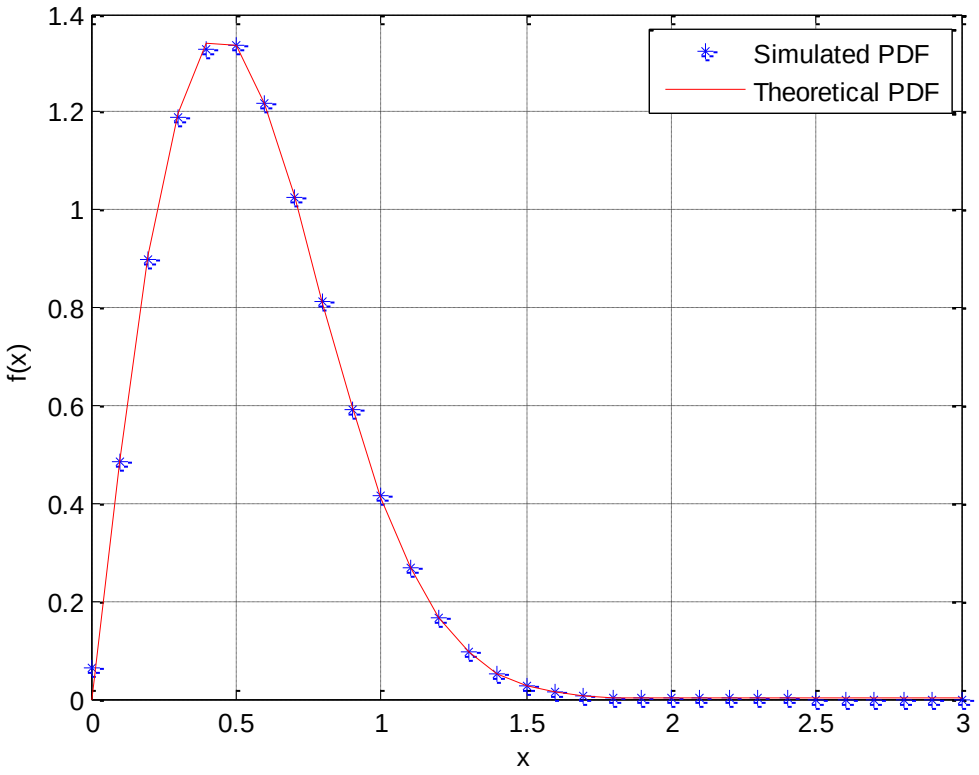

Figure 3.6. Simulated and Theoretical Rayleigh PDF for variance = 0.5

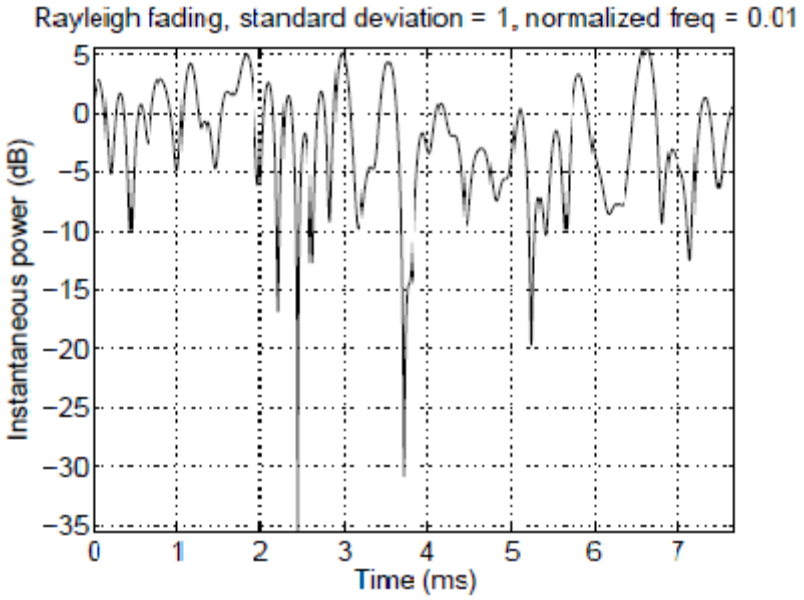

Figure 3.7. A realization of a Rayleigh fading signal with a classical Doppler spectrum.[90]

The impulse response of a multipath channel can be represented by discrete number of impulses as :

$$h(t) = \sum_{k=0}^{L-1} a_k e^{j\theta_k} \delta\left(t - \tau_k\right) \tag{3.10}$$

where k is an integer, L is the number of multipath components between transmitter and receiver, a_k is a random amplitude of the k^{th} multipath component, τ_k is the propagation delay, θ_k is the signal phase and δ is the Dirac delta function.

Figure 3.8 below describes the multipath channel model for four paths delay.

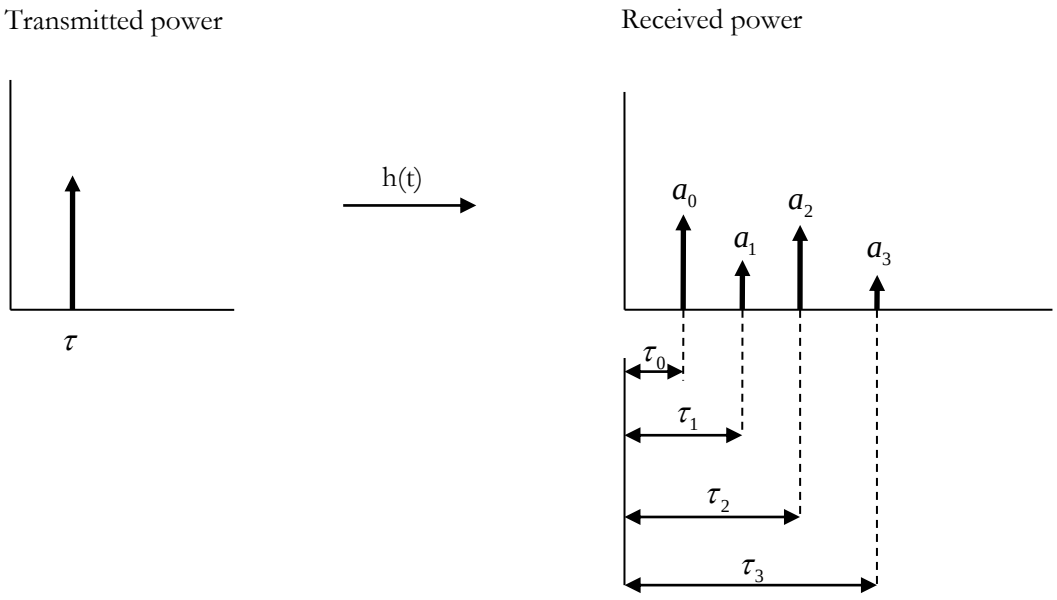

Figure 3.8. Multipath power delay profile for four paths

3.5. Proposed CFO Estimator

Utilizing the remodulated sequence [54-55]; a proposed CFO estimator is derived. Before removing the cyclic prefix (CP) on the receiver side, the received data is given by:

$$U_k = \left[u_k(\tau_0)...u_k(N_{cp}+\tau_0-1)...u_k(N+N_{cp}+\tau_0-1) \right]^T \tag{3.11}$$

The remodulated vector is formed by bringing together the last N carriers of u_{k-1} and the first N_{cp} carriers of u_k as presented below:

$$U_r = \left[u_{k-1}(N_{cp}+\tau_0)...u_{k-1}(N+N_{cp}+\tau_0-1)\ u_k(\tau_0)...u_k(N_{cp}+\tau_0-1) \right]^T \tag{3.12}$$

The calculation interval I_c is given by:

$$I_c = \left[\tau_0,...,\tau_0+N_{cp}-1, \tau_0+N,...,\tau_0+N+N_{cp}-1 \right] \tag{3.13}$$

The correlation between remodulated samples and received samples is given by:

$$\forall k \in I_c, \quad \mathrm{E}\left\{u(k)u^{r*}(k)\right\} = \sigma_u{}^2 \; e^{-j2\pi\alpha_0} \sum_{m=1}^{M} \left|h(m)\right|^2 \tag{3.14}$$

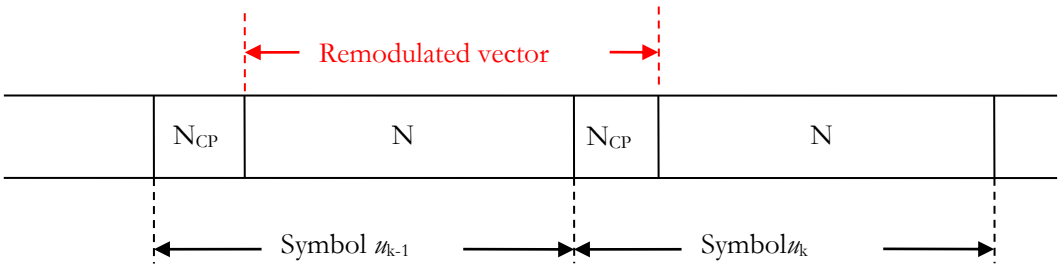

Figure 3.9. Remodulated sequence

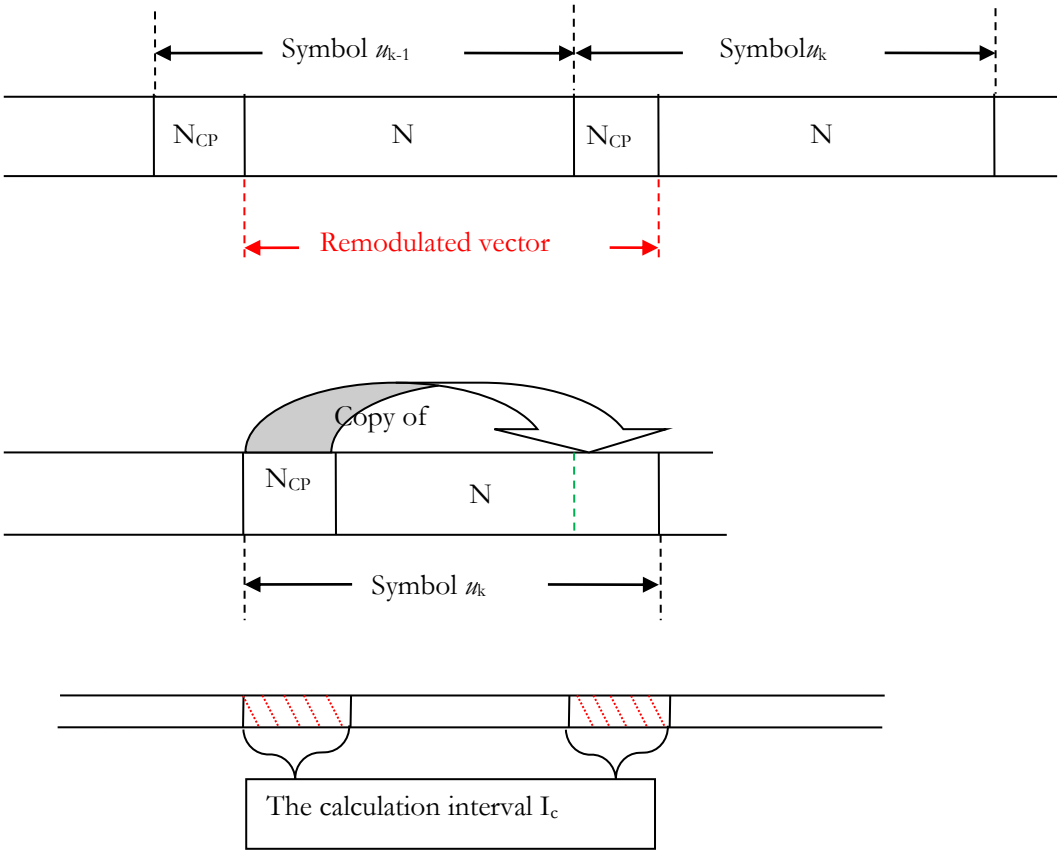

Figure 3.10. Remodulated and received samples

Assuming that the length L of the channel $h(l)$ is inferior to the length of the cyclic prefix N_{cp} and the channel taps slide into the calculation interval I_c, thus the channel effect is neglected in the manipulations.

Using the log likelihood function of the received samples and the remodulated samples as:

$$\Im(\tau_0,\alpha_0)=\log\prod_{k\in I_c}\frac{f(u(k),u^r(k))}{f(u(k))\,f(u^r(k))} \tag{3.15}$$

According to the central limit theorem, $u(k)$ can be approximated as a complex Gaussian random variable when *N* is large enough; the probability density function (PDF) is given by

$$f\left(u(k)\right)=\frac{\exp\left(-\dfrac{\left|u(k)\right|^2}{\sigma_u{}^2+\sigma_w{}^2}\right)}{\pi\left(\sigma_u{}^2+\sigma_w{}^2\right)}\ \forall k \tag{3.16}$$

In addition, the joint Gaussian PDF of received samples $u(k)$ and remodulated samples $u^r(k)$ is given by:

$$f\left(u(k),u^r(k)\right)=\frac{\exp\left(-\dfrac{\left|u(k)\right|^2-2\rho_k\,\mathrm{Re}\left\{e^{j2\pi\alpha_0}u(k)u^{r*}(k)\right\}+\left|u^r(k)\right|^2}{\left(\sigma_u{}^2+\sigma_w{}^2\right)\left(1-\rho_k^2\right)}\right)}{\pi^2\left(\sigma_u{}^2+\sigma_w{}^2\right)^2\left(1-\rho_k^2\right)} \tag{3.17}$$

where the correlation coefficient is given by

$$\rho_k=\left|\frac{E\left[u(k)u^{r*}(k)\right]}{\sqrt{E\left[\left|u(k)\right|^2\right]E\left[\left|u^r(k)\right|^2\right]}}\right|. \tag{3.18}$$

By inserting the probability density function (PDF) $f(u(k))$, $f(u^r(k))$ and the joint Gaussian PDF $f(u(k),u^r(k))$ and after some algebraic manipulations, we get:

$$\Im(\tau_0,\alpha_0)=\sum_{k\in I_0}\left\{\frac{2(\rho_k(\chi(k)-\rho_k^2\beta(k))}{(\sigma_u^2+\sigma_w^2)(1-\rho_k^2)}-\log(1-\rho_k^2)\right\} \tag{3.19}$$

where

$$\chi(k)=\sum_{k\in I_0}\mathrm{Re}\left\{E(u(k)u^{r*}(k))\right\} \tag{3.20}$$

$$\beta(k)=\sum_{k\in I_0}\frac{1}{2}\left(\left|u(k)\right|^2+\left|u^r(k)\right|^2\right) \tag{3.21}$$

$\chi(k)$ being the sum of the real consecutive correlation, $\beta(k)$ being the energy term.

The LL function $\Im$ is a function of α_0, the correlation coefficient and τ_0. It's clear that if the correlation coefficient is high ($\rho_k \cong 1$), then the LL function is high ($\Im \to +\infty$), and if the correlation coefficient is null, the LL function is also null. Thus, we derive the log likelihood function $\Im$ in the interval where the correlation coefficient is high. So, to obtain the maximum of the LL function $\Im(\tau_o, \alpha_o)$,we maximize the equation below:

$$\max \Im(\tau_o, \alpha_o) = \max\left[\chi(\tau_o, \alpha_o) - \rho_k \beta(\tau_o, \alpha_o)\right] \tag{3.22}$$

This equation depends on the frequency offset α_0 and the time offset τ_0. Then the new estimator is derived as

$$\tilde{\tau}_o = \arg\max\left[\chi(\tau_o) - \rho_k \beta(\tau_o)\right] \tag{3.23}$$

$$\tilde{\alpha}_o = -\frac{1}{2\pi} \angle \chi(\tilde{\tau}_o) \tag{3.24}$$

A similar frequency offset estimator has been proposed in [36,42]. The developed carrier frequency offset estimator is derived when the correlation coefficient is high to deal with the carrier frequency offset.

3.6. Conclusion

This chapter provided a new frequency offset estimator for OFDM systems. The mathematical model and design parameters of OFDM system were presented. The effect of frequency and time offsets were introduced. Fading channel manifestations were exhibited. Then the Rayleigh fading channel was described. Moreover the remodulated vectors were presented and the proposed frequency offset estimator was described in detail.

Chapter 04

SIMULATION AND RESULTS

4.1. Introduction

In this chapter, we assess our proposed blind carrier frequency offset (CFO) estimator for OFDM systems using computer simulations. At the beginning, the effect of CFO in OFDM systems is discussed. Then, the evaluation of the proposed CFO estimator over an additive white Gaussian noise (AWGN) channel with different parameters is highlighted. Study of the performance of the proposed estimator has been done considering three Rayleigh fading channels. Subsequently, the CFO estimation of the Lin estimator [54] for OFDM systems over Rayleigh fading channels is introduced for the sake of comparison. Monte Carlo simulation results are presented for the performance assessment of the proposed scheme for OFDM systems. To demonstrate the robustness and efficiency of the proposed synchronization techniques, different channel conditions and OFDM configurations are considered and compared with other state-of-the-art techniques.

The normalized CFO is randomly generated from -0.5 to 0.5. The computational complexity can be reduced using the proposed method. The simulation results demonstrate the improvements of the proposed scheme over other methods.

In addition, the new frequency offset estimator is evaluated for different lengths of cyclic prefix (CP) and the IFFT length. Most of our simulations in this chapter use 16-QAM (4 bit rate per OFDM symbol). One of the reasons for this is to give intermediate results between 4 and 64-QAM, 2 and 6 bit rate per OFDM symbol respectively. 16-QAM is also considered one of the standard modulation schemes in OFDM applications such as terrestrial digital video broadcasting (DVB), digital audio broadcasting (DAB) and high performance radio LAN version 2 (HIPERLAN/2).[89]

4.2. The Effect of Frequency Offset for OFDM Systems

Figure 4.1 illustrates the sensitivity of OFDM systems versus carrier frequency offset (CFO) under AWGN channels. Simulation results show the performance degradation of the OFDM system for high CFO values. For CFO=0, the simulated bit error rate (BER) is close to the theoretical one. As the CFO increases, the BER increases.

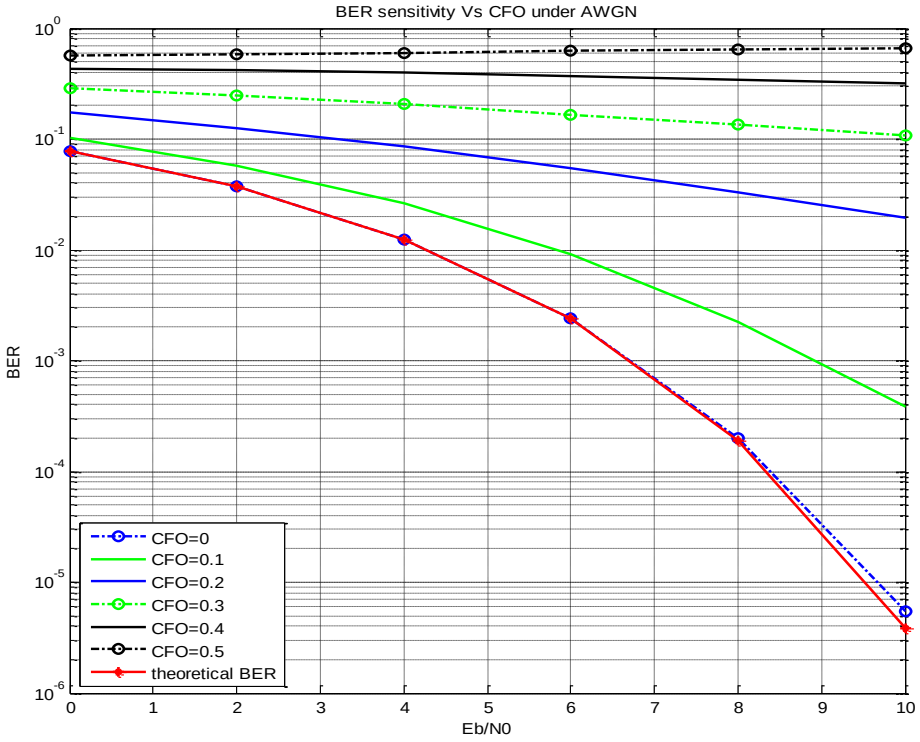

Figure 4.1. BER sensitivity versus CFO values under AWGN channels

4.3. Evaluation of the Proposed Method over AWGN Channel

The simulations are carried out in MATLAB in order to study the behavior of our proposed estimator for different carrier frequency offsets (CFOs) in additive white Gaussian noise (AWGN) channels. The parameters considered for the simulations are listed in Table 4.1.

Table 4.1. The simulation parameters

Modulation	4QAM
Number of subcarrier	64, 128
Cyclic Prefix length (Ncp)	16, 32
Number of Bits per Symbol	2
Normalized Carrier Frequency Offset (CFO)	0, 0.25, 0.295, 0.395, 0.4, 0.49
Signal to Noise Ratio (SNR)	0:30

The graph shown in Figure 4.2 presents the effect of error in estimating the CFO represented by the MSE of the proposed estimator. The Monte Carlo simulation is performed for 500 iterations, using 100 symbols for the OFDM system. For an SNR between 0 and 3dB, we have closer results for both CFO=0.295 and CFO=0.395. However, for an SNR superior to 3dB, the proposed estimator offers better results for CFO=0.295 than the results obtained for CFO=0.395. In contrast, the proposed estimator does not perform well for CFO=0.49 when the SNR is inferior to 17dB whereas its MSE

stabilizes at $6\times 10^{-5}$for an SNR superior to 17dB. It is clear that, as the CFO increases, the performance of the OFDM system decreases.

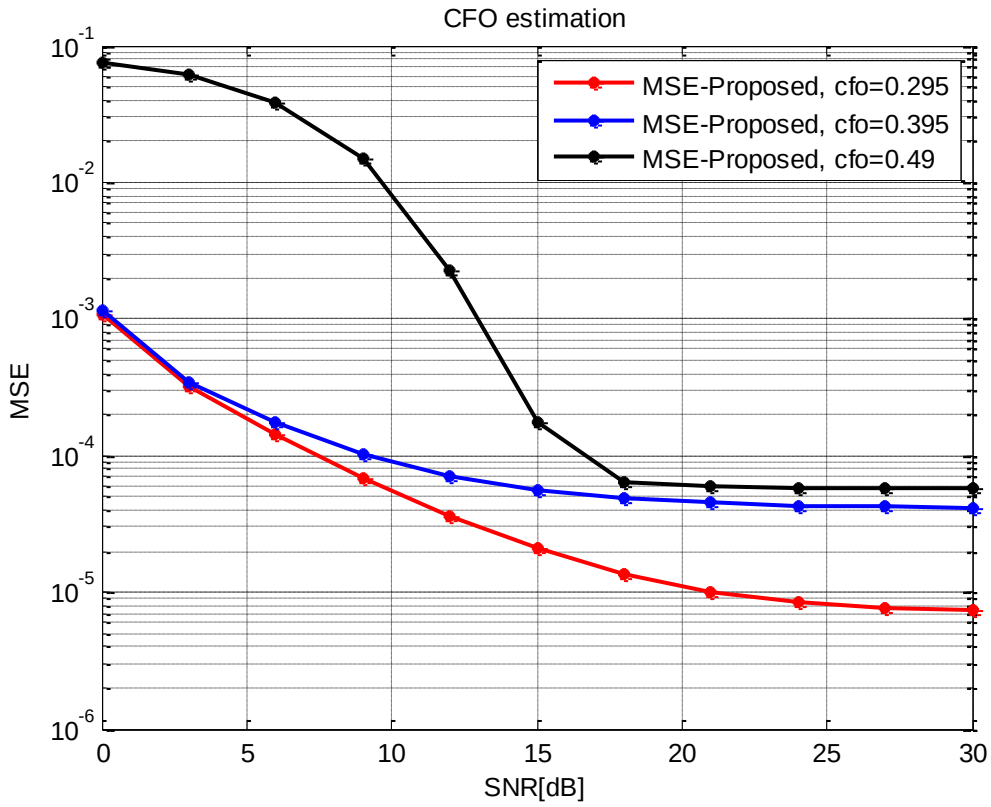

Figure 4.2. The MSE of the proposed estimator under AWGN channel for CFO=0.295, 0.395, 0.49

Figure 4.3 shows the mean squared error (MSE) of the carrier frequency offset of OFDM systems. This latter uses 128 subcarriers for the length of IFFT and 32 subcarriers for the length of the CP. For CFO=0, the MSE of the proposed estimator varies from 6×10^{-4} to 5×10^{-7} for an SNR between 0 and 30dB. In addition, the results of our estimator, obtained with CFO = 0.25, are better than those obtained with CFO = 0.4 for all ranges of SNR.

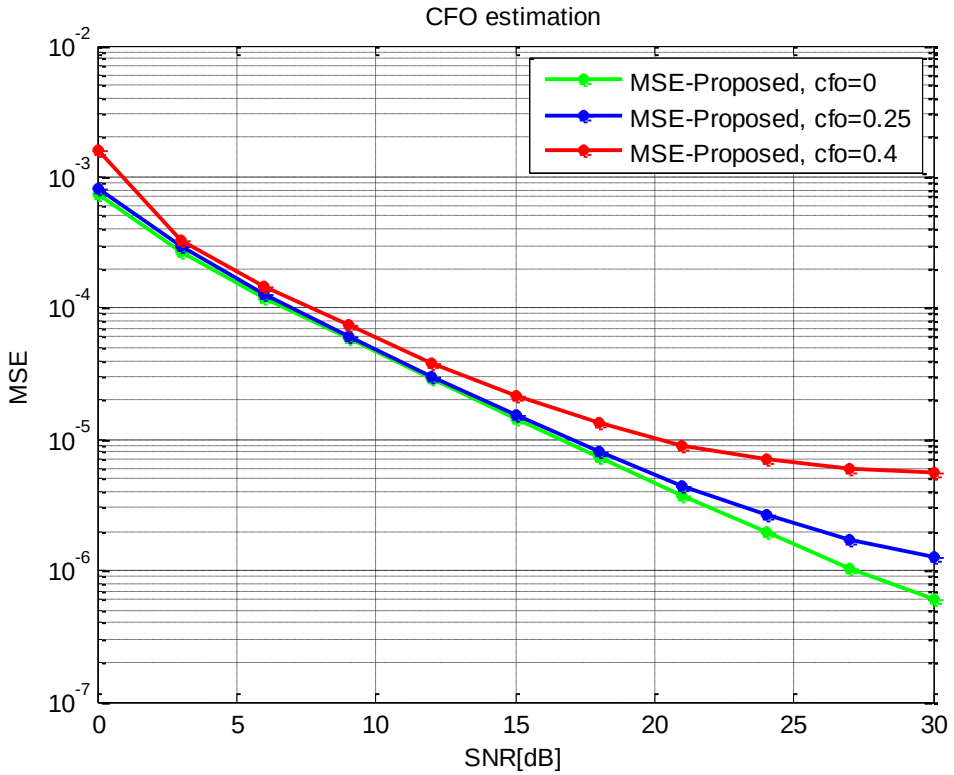

Figure 4.3. The MSE of the proposed estimator under AWGN channel for CFO=0, 0.25, and 0.4

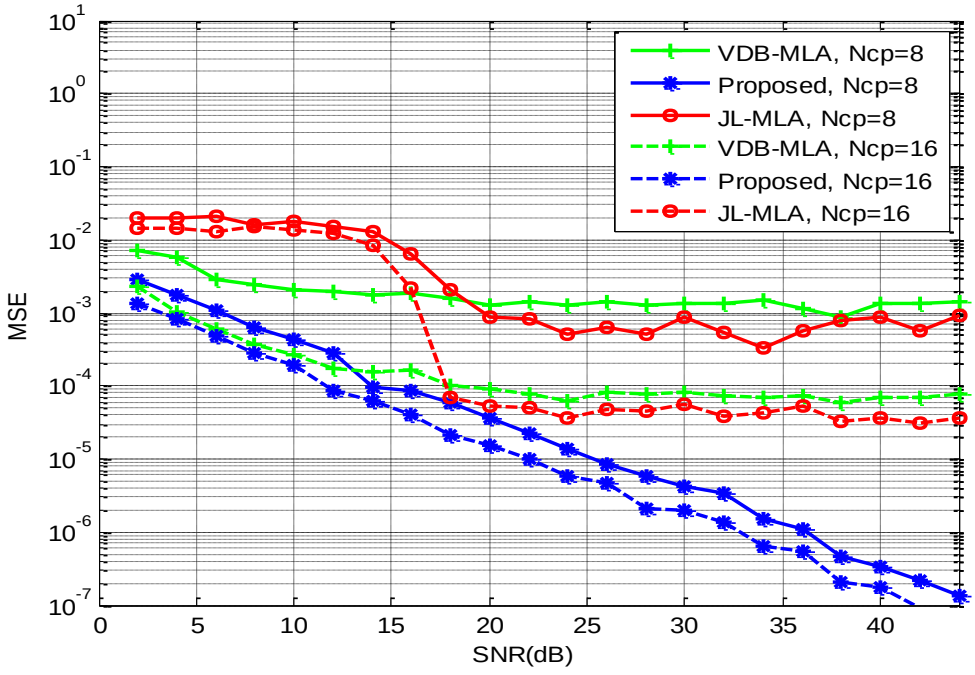

Figure 4.4. The MSEs of the proposed estimator, VDB-MLA estimator and JL-MLA under AWGN channel, frequency offset is 0.25

In order to evaluate the effectiveness of the proposed estimator, several simulations are conducted for different approaches with Ncp=16 and Ncp=8. As has been noticed in Figure 4.4, the proposed

estimator outperforms the VDB-MLA estimator and the JL-MLA (Lee et al., 2004) estimator for all SNR values. It can also be seen that the MSE of the proposed estimator decreases gradually as the SNR increases. In addition, for an SNR <16 db, the VDB-MLA estimator gives better results than the JL-MLA estimator. However, for an SNR >16db, the JL-MLA estimator outperforms the VDB-MLA estimator. It can also be deduced that both estimators VDB-MLA (Van de Beek et al., 1997)[36] and JL-MLA (Lee et al., 2004)[58] provide better results when the SNR >16 db. It has been observed that MSE diminishes as Ncp increases for the proposed estimators, VDB-MLA and JL-MLA. However, as Ncp increases, the computational complexity increases.

4.4. Evaluation of the Proposed Method over Rayleigh Fading Channel

In order to demonstrate the robustness of our proposed estimator, we used different Rayleigh fading channel parameters. Table 4.2 below presents the path gains, path delays and the delay spread of each channel.

Table 4.2. Channel parameters

	Path Gains	**Path Delays**	**Delay Spread**
Channel 1	0.34, 0.28, 0.23, 0.11, 0.04	0, 1, 2, 6, 11	6.37
Channel 2	0.35, 0.25, 0.18, 0.13, 0.09	0, 1, 2, 3, 4	1.74
Channel 3	0.25, 0.25, 0.25, 0.25	0, 4, 8, 12	20

Figures 4.5, 4.6, 4.7 below present the impulse response of Channel 1, Channel 2 and Channel 3, respectively.

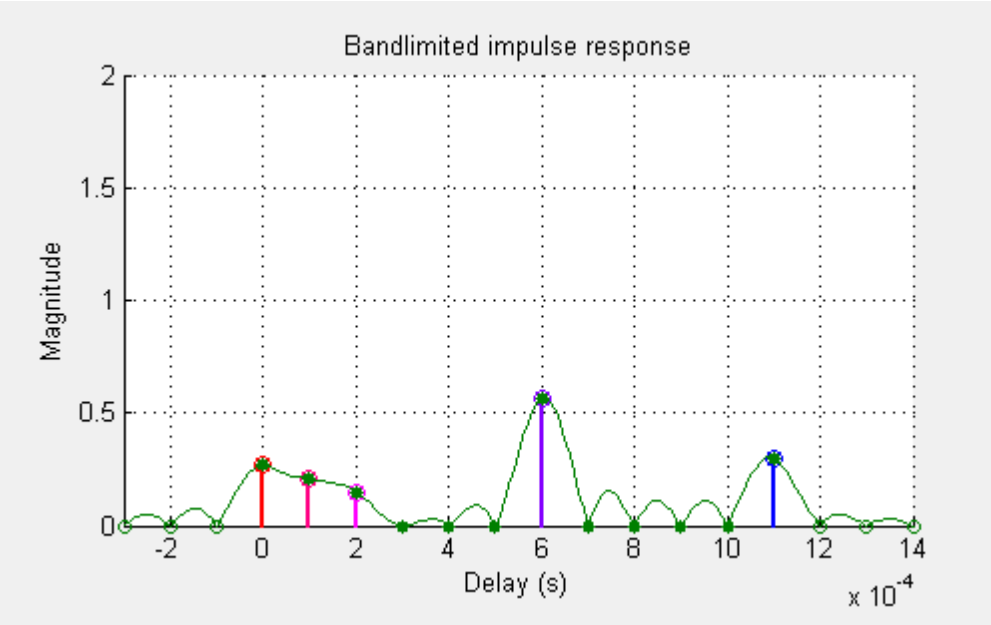

Figure 4.5. Impulse response of Channel 1

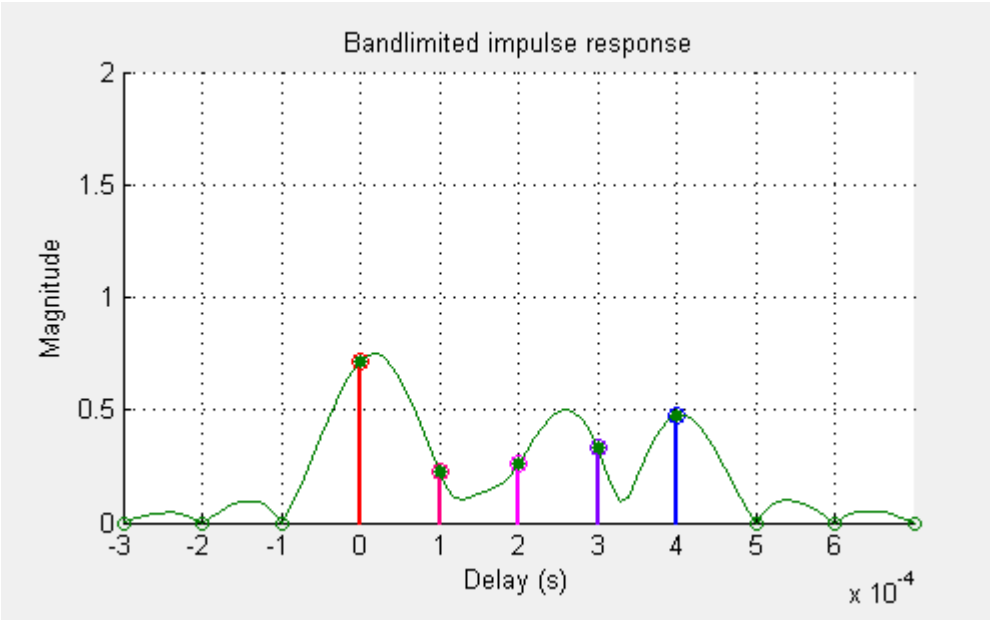

Figure 4.6. Impulse response of Channel 2

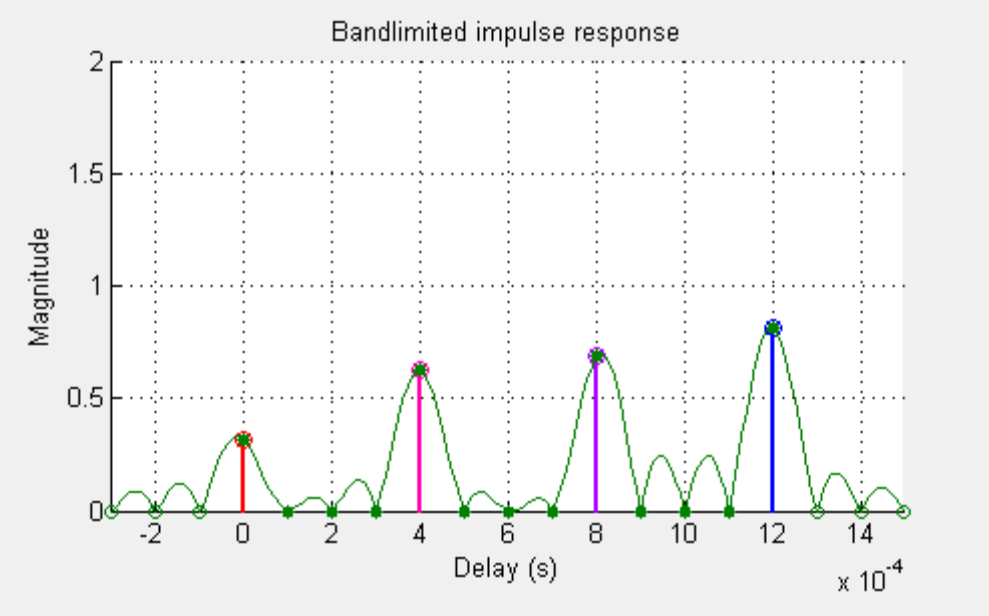

Figure 4.7. Impulse response of Channel 3

4.4.1. Evaluation of the Proposed Method over Rayleigh Fading Channel 1

The performances of our estimator are evaluated and Monte Carlo methods are employed. Different OFDM systems are used to assess the proposed estimator. The first OFDM system consists of ten symbols, the used parameters being N=128 and N=64 subcarriers for different lengths of Ncp, frequency offset CFO=0.295 and 0.25. The time offset is assumed null. The signal passes through the Rayleigh fading channel with five paths with delays of [0 1 2 6 11] and variances [0.34 0.28 0.23 0.11 0.04], respectively, as given in [54]. The channel has additive white Gaussian noise (AWGN) and is abbreviated as Channel 1. A quadrature amplitude modulation 16-QAM is utilized. The performances of the proposed estimator are evaluated by calculating the mean squared error (MSE) compared with the signal-to-noise ratio (SNR). By running the simulation for 500 trials and 10 OFDM block symbols per trial in this example, the performance of the system is measured in terms of the MSE of the channel estimation. The MSE for the m^{th} subcarrier is defined as

$$MSE(m) = \frac{E\left\{\left\|Y_n(m) - \hat{Y}_n(m)\right\|^2\right\}}{E\left\{\left\|Y_n(m)\right\|^2\right\}} \tag{4.1}$$

The MSEs of the proposed estimator (MSE-Proposed-2), the Lin estimator (Lin-coarse and Lin-fine)[54] and the Beek estimator (VDB-MLA) [36] versus an SNR for N=64 and Ncp=16 are presented in the figure below. The obtained results in Figure 4.8 show clearly the effectiveness of the proposed estimator compared with the Lin and Beek estimators. Lin-coarse and VDB-MLA

have closer results. The proposed estimator gives lower MSE than the others for all SNR values. These results can be explained by the choice of the correlation interval which is taken when the correlation coefficient is high (close to 1). In addition, the proposed estimator has low computational complexity compared to the Lin estimator which divides the estimation into two steps and thus increases the complexity of the computation.

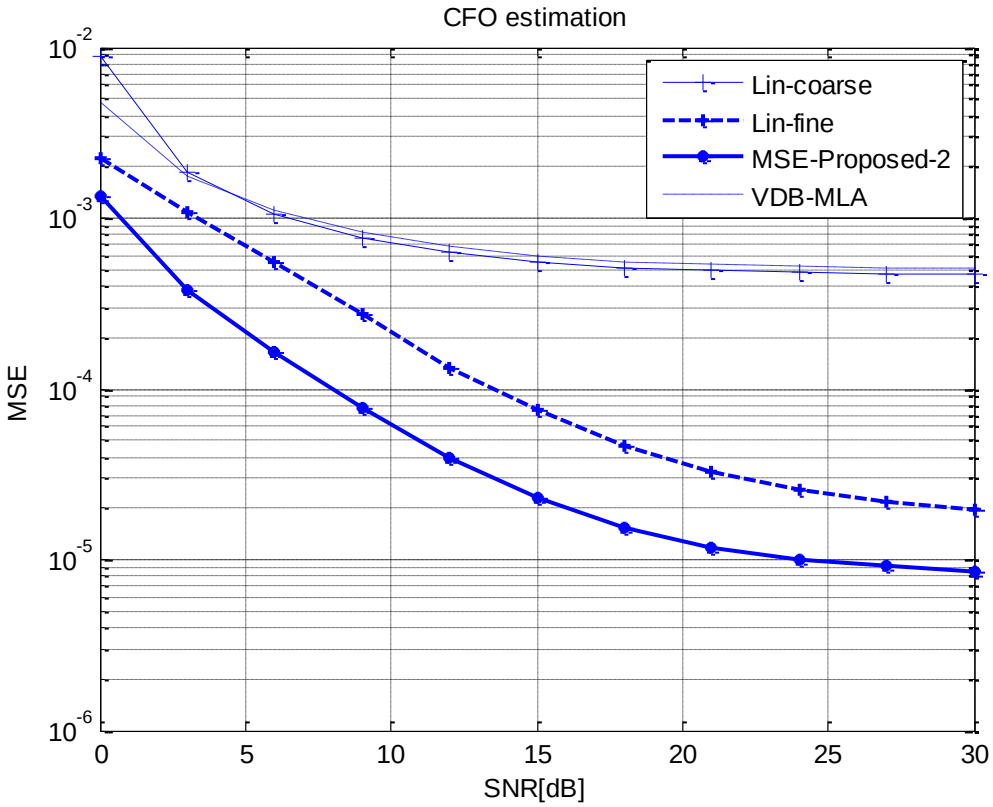

Figure 4.8. The MSE of the proposed estimator, the Lin estimator and the Beek estimator under Rayleigh fading Channel 1 for Ncp=16 and CFO=0.295

Our goal is to adapt the OFDM symbol so that it can be used for the fifth generation, i.e., how to deal with frequency offset without decreasing the bandwidth efficiency.

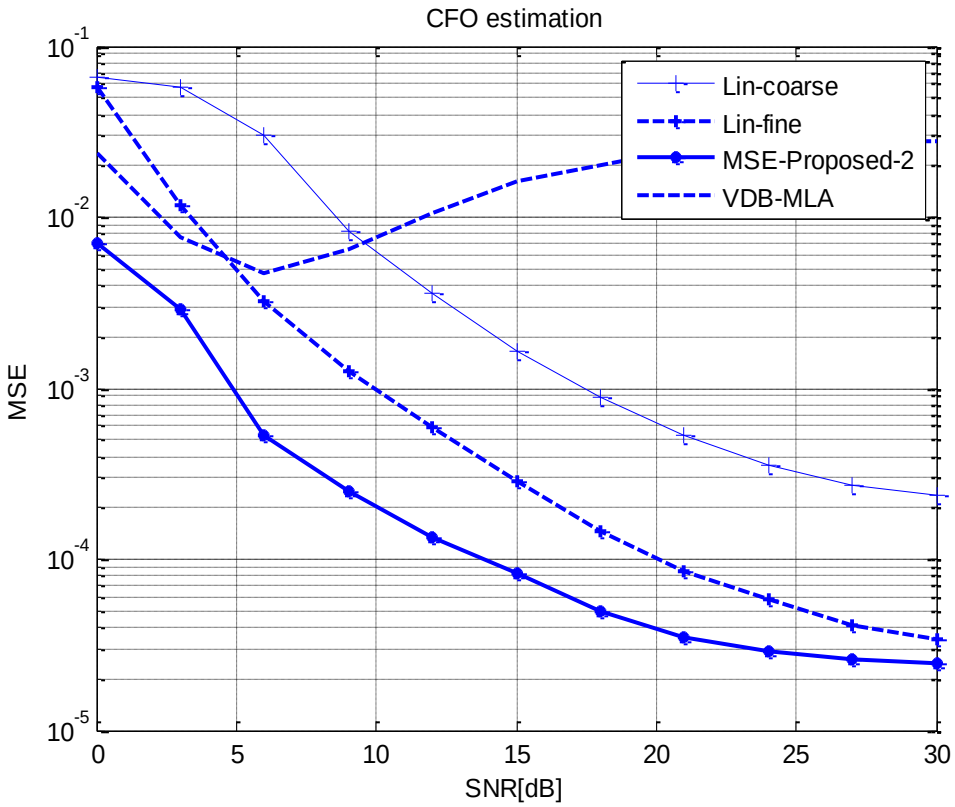

Figure 4.9. The MSE of the proposed estimator, the Lin estimator and the Beek estimator under Rayleigh fading Channel 1 for Ncp=8 and CFO=0.25

We employ different lengths of cyclic prefix (CP) to show the robustness of the proposed estimator with lower lengths of the guard interval. Figures 4.9 and 4.10 give the MSE of the frequency offset versus SNR under a Rayleigh channel for Ncp=8 and Ncp=6, respectively. It can be seen clearly that the proposed estimator outperforms Lin and Beek estimators for all SNR values and for all CP lengths. We can notice that as Ncp increases, the efficiency increases.

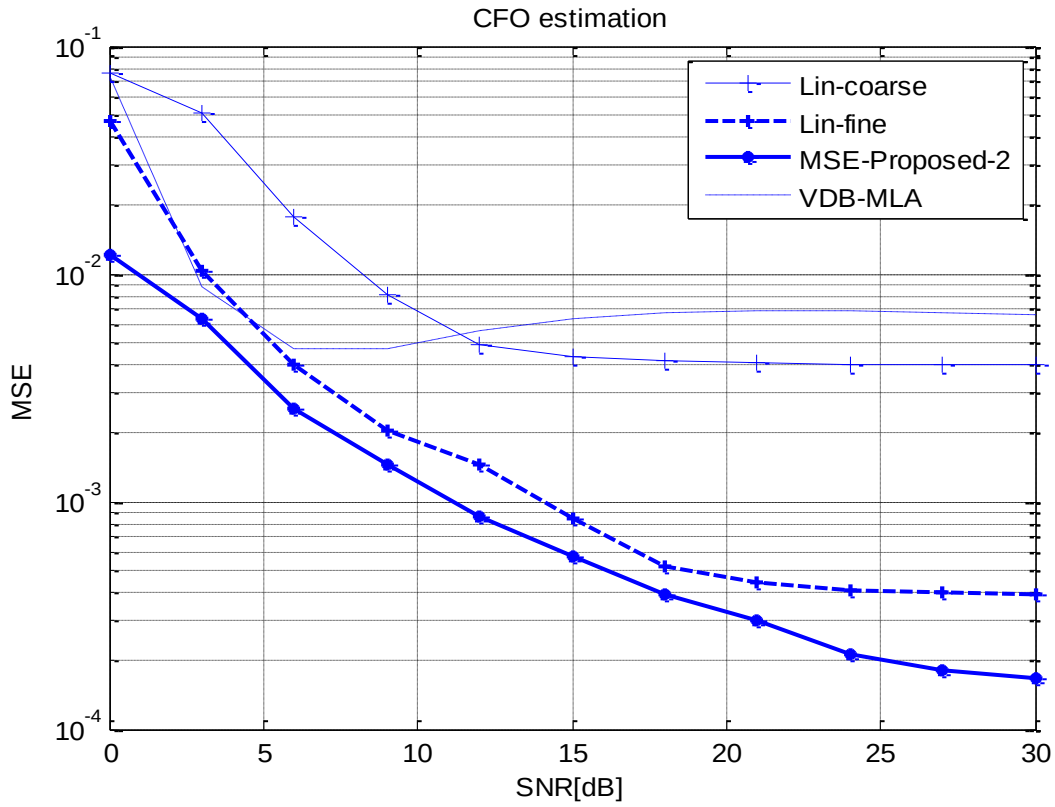

Figure 4.10. The MSE of the proposed estimator, the Lin estimator and the Beek estimator under Rayleigh fading Channel 1 for Ncp=6

Figure 4.11 displays the MSE of the proposed estimator and the Lin fine estimator over Rayleigh fading Channel 1 for different lengths of CP. For Ncp=32, the proposed estimator gives better results than the Lin fine estimator for an SNR inferior to 22dB and gives close results for an SNR between 22.5dB and 24dB. However, its performances decrease for an SNR superior to 24dB compared to the Lin fine estimator. For Ncp=8, Ncp=16, the proposed estimator outperforms the Lin fine estimator [54] for all SNR values. Thus, this estimator can effectively decrease the effect of ICI and can enhance the performance of OFDM systems.

According to the obtained results, when the CP decreases, the undesirable MSE increases. However, the unwanted MSE is decreased as compared to the previous study [54].

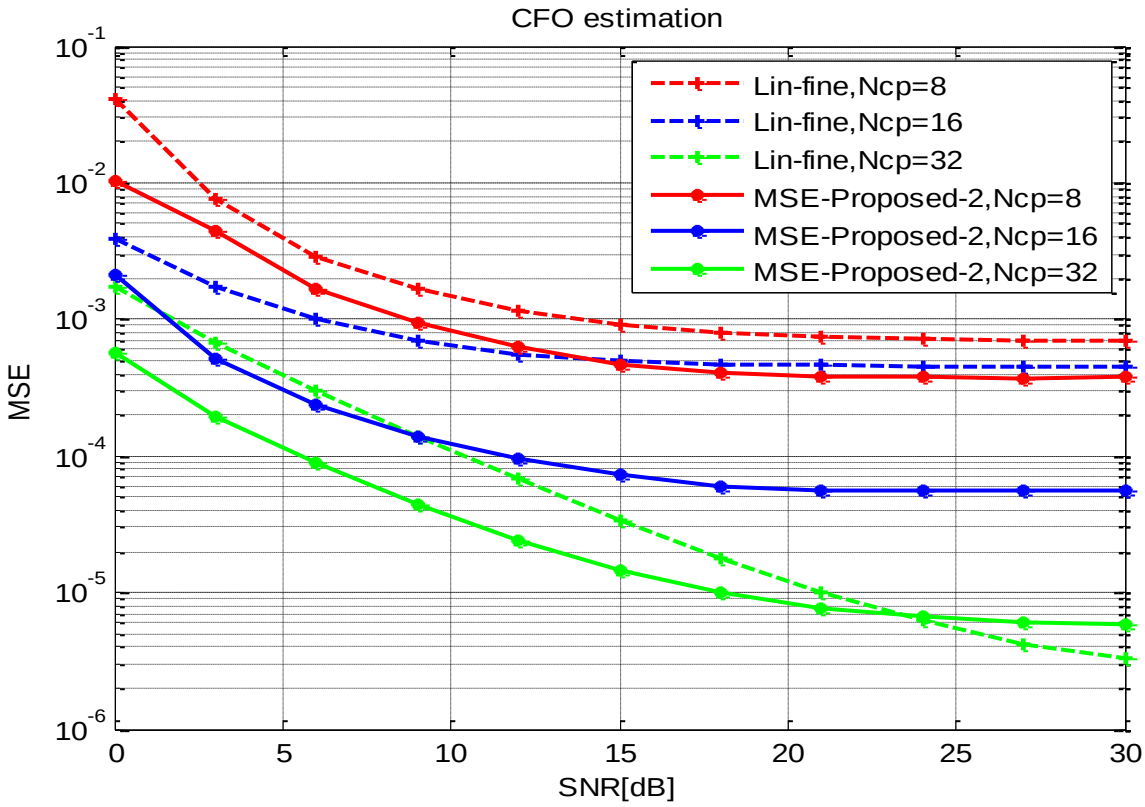

Figure 4.11. The MSE of the proposed estimator Lin-fine estimator for N=128, Ncp=8, 16 and Ncp=32, CFO=0.25

4.4.1.1. Evaluation of the Proposed Estimator for Different Orders of QAM

We can achieve high data rates by using a high order of quadrature amplitude modulation QAM. Thus, we assess our proposed estimator for different orders of QAM, 8QAM, 16QAM, 32QAM and 64QAM to show the behavior of our estimator in combating ICI on one side and keeping a high data rate on the other side. For this, an OFDM system with N= 64 subcarriers, Ncp=16 the length of CP is used to provide protection from ISI due to the channel multipath delay spread, and frequency offset CFO=0.295. The performances of the proposed estimator are evaluated by calculating the MSE compared with the SNR under a Rayleigh fading channel.

As is presented in Figures 4.12-4.15 below, the MSEs of the proposed estimator (MSE-Proposed), the Lin estimators (Lin-coarse and Lin-fine)[54] are given. We notice that the OFDM system with a low QAM order (8QAM and 16QAM) give better results than the OFDM systems with a high QAM order (32QAM and 64QAM) under the same OFDM parameters and the same channel conditions for both the proposed estimator and the Lin estimators (coarse and fine). In addition, the proposed estimator with a 16QAM order offers better results. For SNR=27dB, the MSE is to the order of 10^{-6} whereas the Lin fine estimator is to the order of 10^{-5}.

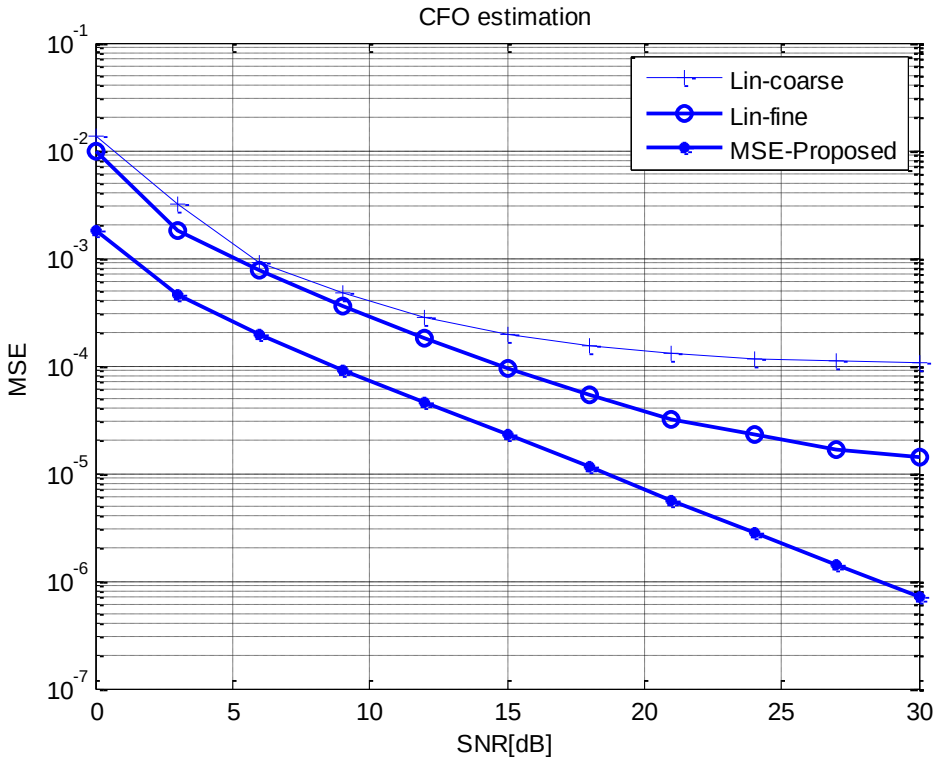

Figure 4.12. The MSE of the proposed estimator and the Lin estimator under Rayleigh fading Channel 1 for 2QAM

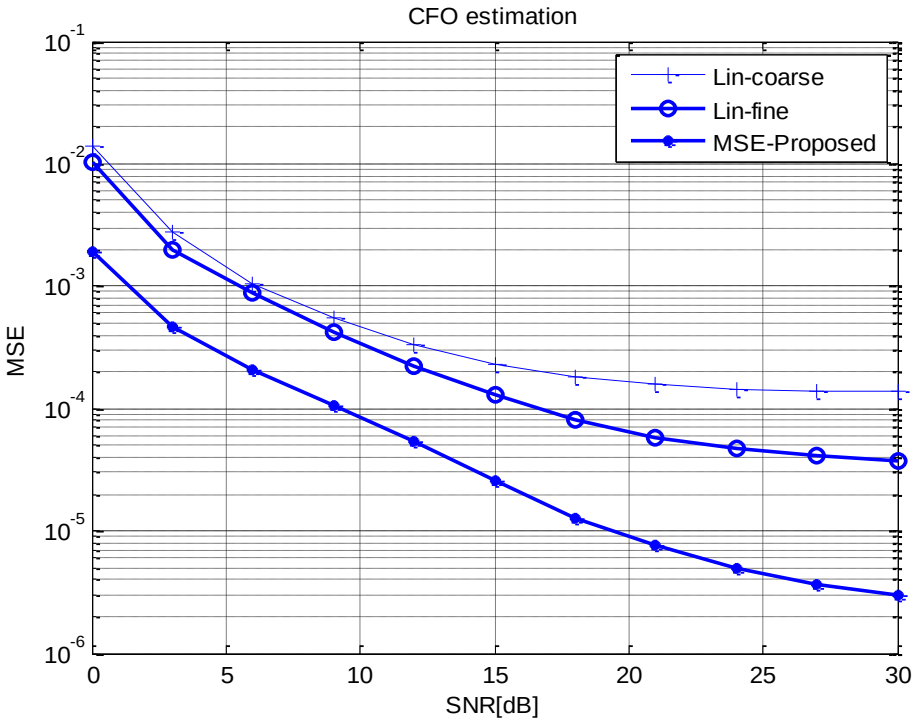

Figure 4.13. The MSE of the proposed estimator and the Lin estimator under Rayleigh fading Channel 1 for 4QAM

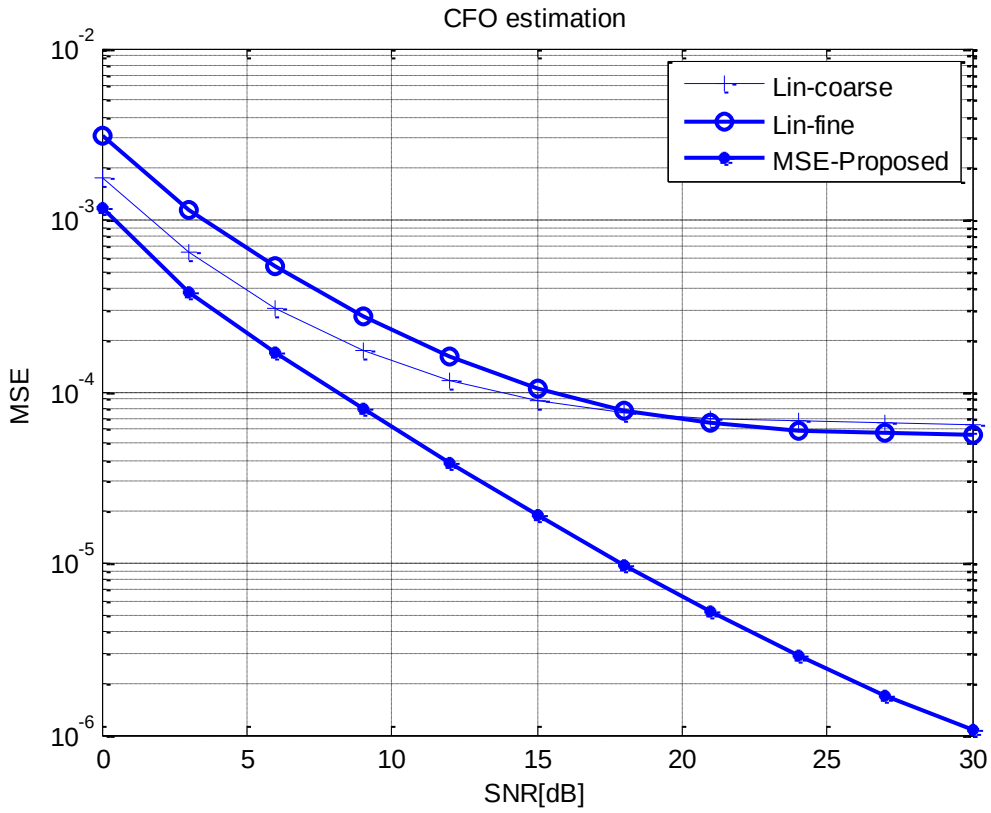

Figure 4.14. The MSE of the proposed estimator and the Lin estimator under Rayleigh fading Channel 1 for 8QAM

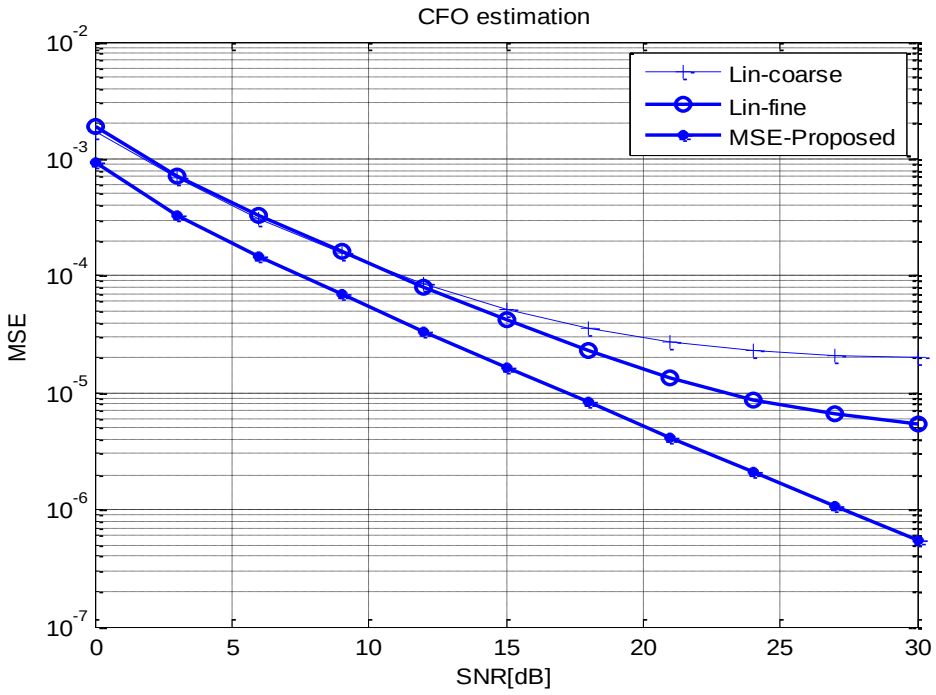

Figure 4.15. The MSE of the proposed estimator and the Lin estimator under Rayleigh fading Channel 1 for 16QAM

Figures 4.16 and 4.17 prove the effectiveness of our proposed estimator compared to the Lin estimators in the coarse and the fine estimation. Figure 4.16 shows that our proposed estimator can combat ICI even over fading channels with high bit rate transmissions. Figure 4.17 notices that the MSEs are between 10^{-25} and 10^{-4} for an SNR (dB) inferior to 10dB. For SNR (dB) between 10dB and 25dB the MSEs are between 10^{-4} and 10^{-5}. For an SNR superior to 25dB, the MSEs saturate at 10^{-5}. However, the MSEs of the Lin estimator are between 10^{-1} and 10^{-3} for an SNR (dB) inferior to 10dB. For an SNR (dB) between 10dB and 25dB the MSEs are between 10^{-4} and 10^{-5}. For an SNR superior to 25dB, the MSEs saturate at 10^{-5}.

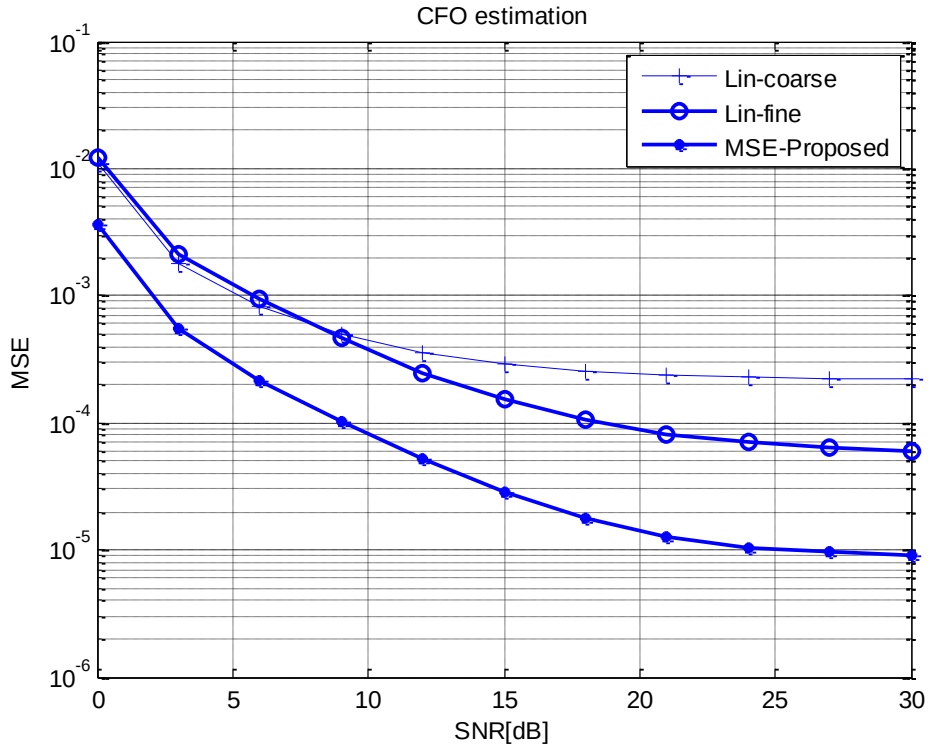

Figure 4.16. The MSE of the proposed estimator and the Lin estimator under Rayleigh fading Channel 1 for 32QAM

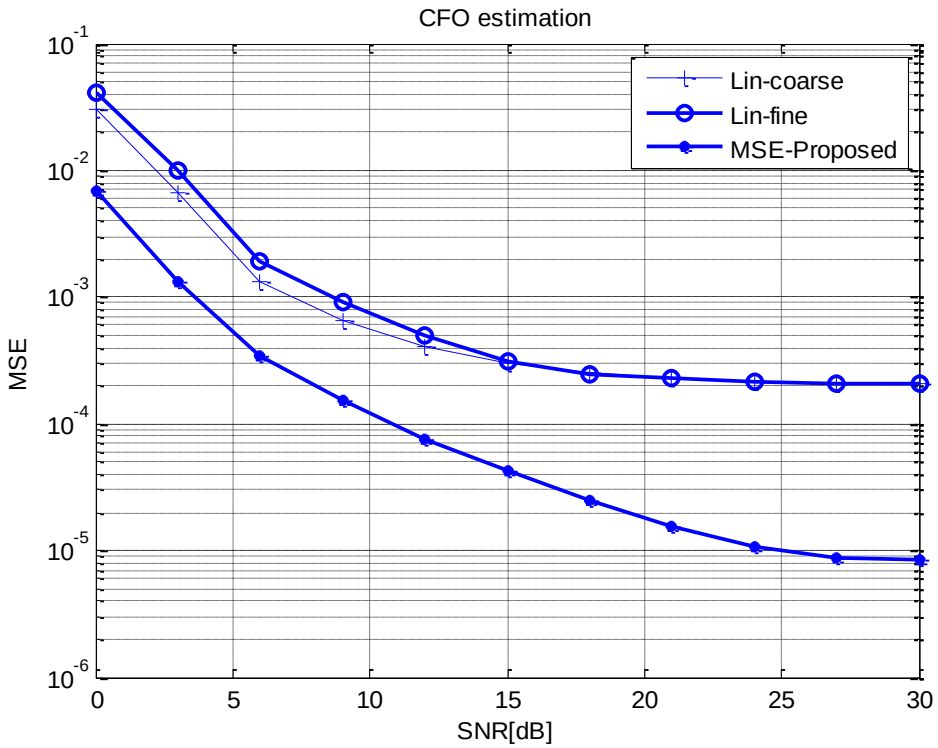

Figure 4.17. The MSE of the proposed estimator and the Lin estimator under Rayleigh fading Channel 1 for 64QAM

4.4.1.2. Evaluation Performance of the Proposed Estimator for Different Value of the Carrier Frequency Offset under Channel 1

In order to assess our proposed estimator for different values of CFO, we used an OFDM system with 64 subcarriers and Ncp =16 as the length of CP. By taking the same order of quadrature amplitude modulation (16QAM) and transmitting our OFDM system over Rayleigh fading Channel 1, the OFDM symbol will have a fair comparison. The mean squared error is calculated for frequency offset values: 0.1, 0.2, 0.4, and 0.49. The results presented in Figures 4.18, 4.19, 4.20 and 4.21 show that our estimator outperforms the Lin estimator for all the values of frequency offset. In addition, for the high frequency offset =0.49, the performances of the Lin estimator (coarse and fine estimation) degrade severely; however the proposed estimator maintains its performances as is presented in Figure 4.21 below.

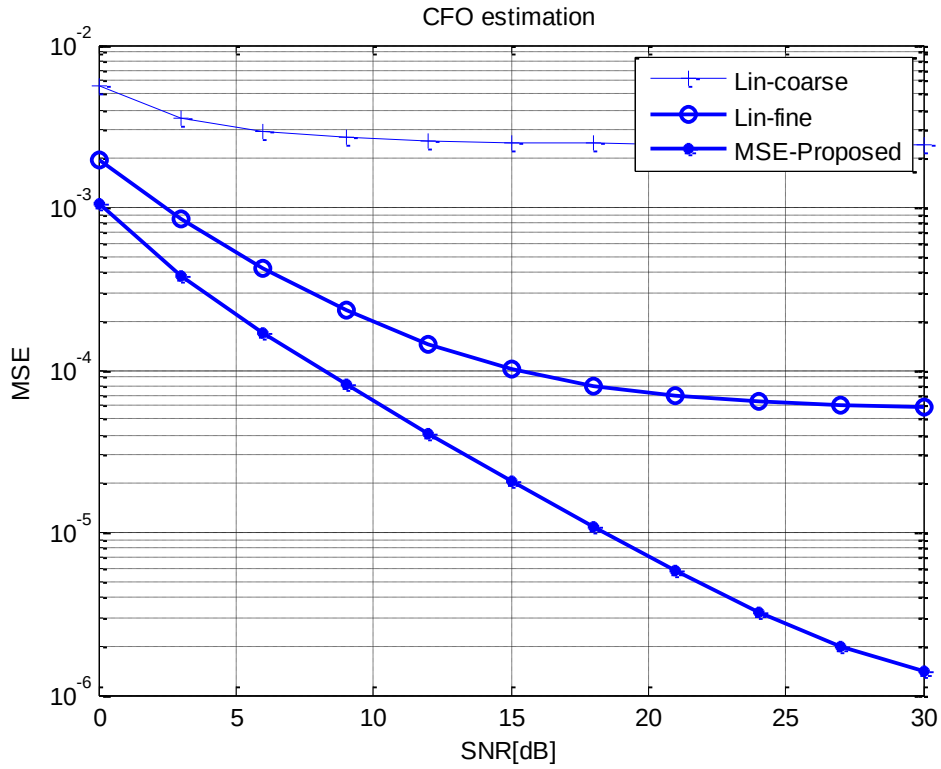

Figure 4.18. The MSE of the proposed estimator and the Lin estimator under Rayleigh fading Channel 1 for frequency offset =0.1

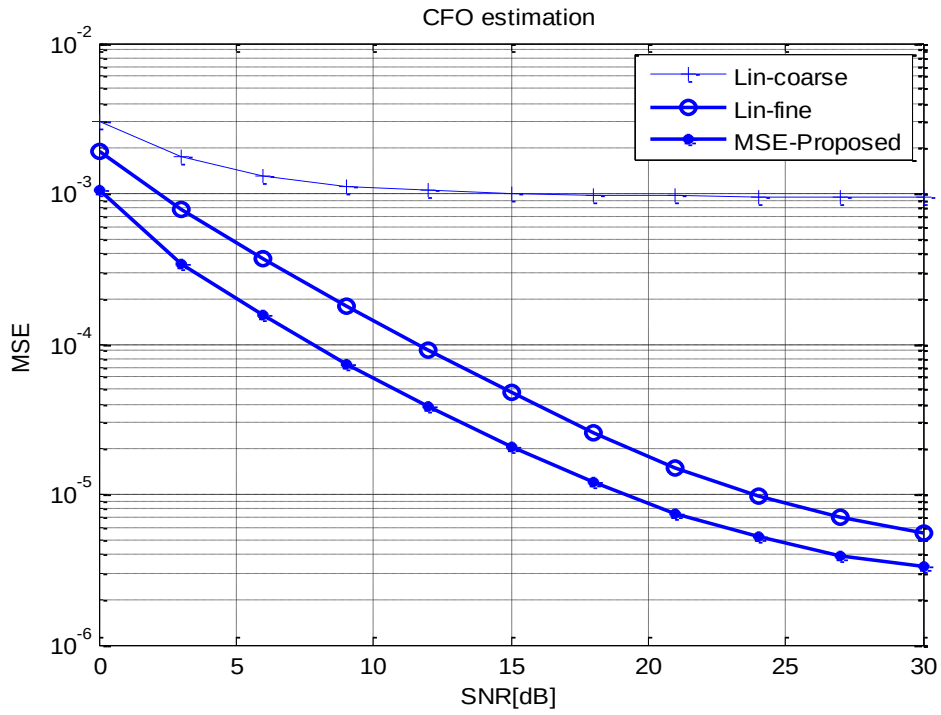

Figure 4.19. The MSE of the proposed estimator and the Lin estimator under Rayleigh fading Channel 1 for frequency offset =0.2

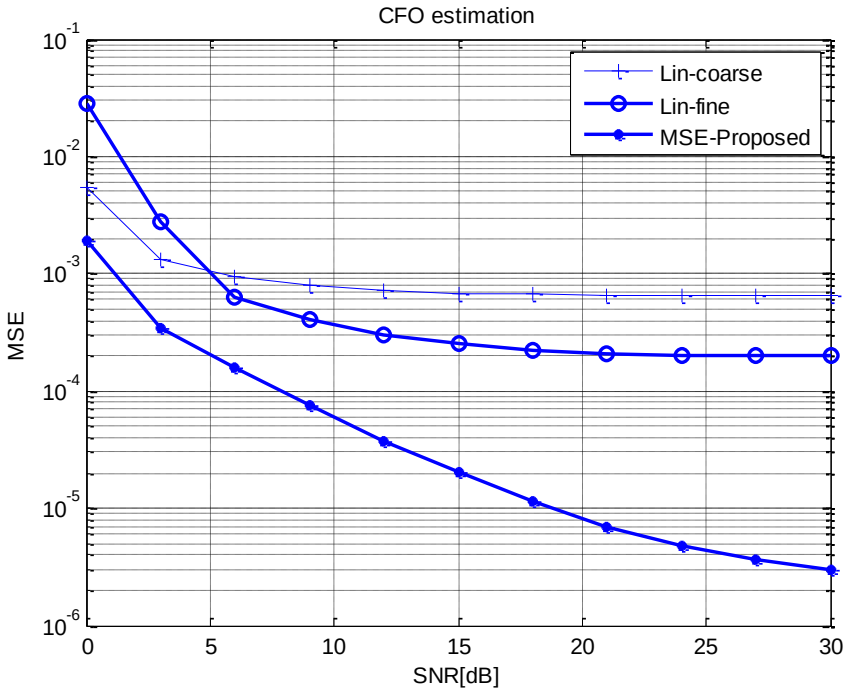

Figure 4.20. The MSE of the proposed estimator, Lin estimator under Rayleigh fading Channel 1 for frequency offset =0.4

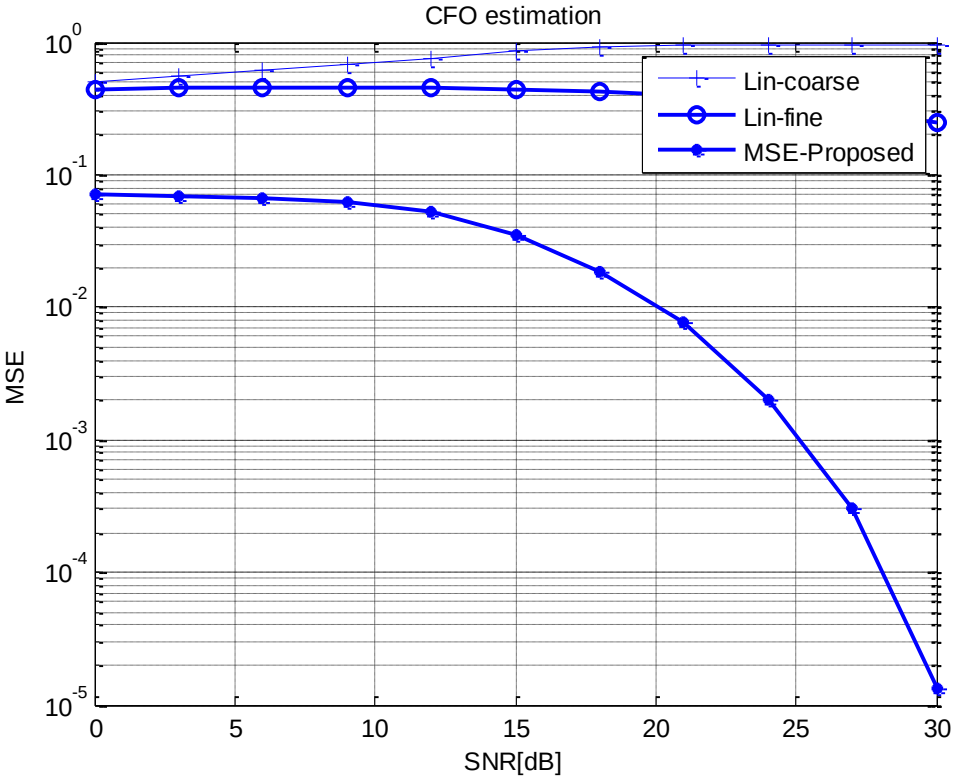

Figure 4.21. The MSE of the proposed estimator and the Lin estimator under Rayleigh fading Channel 1 for frequency offset =0.49

4.4.2. Evaluation of the Proposed Method over Rayleigh Fading Channel 2

We used another Rayleigh fading channel to show the strength of our estimator under different channel transmissions and to prove the effectiveness of our estimator in combating carrier frequency offset. We used an OFDM system with 64 subcarriers and 16 subcarriers for the cyclic prefix. The signal passes through the Rayleigh fading channel with five paths with delays of [0 1 2 3 4] and variances [0.35, 0.25, 0.18, 0.13, 0.09], respectively. The channel has additive white Gaussian noise (AWGN) and is abbreviated as Channel 2. Monte Carlo simulation is used with 500 iterations.

Figure 4.22 below presents the MSE versus the SNR for both the proposed estimator and the Lin estimator. We used 8QAM for the constellation and CFO=0.295 for the carrier frequency offset. As is described in Figure 4.22, the MSE of the Lin coarse estimation varies between 3×10^{-2} and 2×10^{-2} when the SNR is inferior to 15 dB and stabilizes at 2×10^{-2} for an SNR superior to 15 dB. So, this estimator gives the worst estimation compared to both the Lin fine and the proposed estimators. The Lin fine estimator has a better estimation than the Lin coarse estimator, the MSE varying between 10^{-2} and 4×10^{-6} for the SNR variation between 0 and 30dB with linear pace. The proposed estimator outperforms both the Lin estimator and the MSE varying from 10^{-3} to 10^{-6} for an SNR varying from 0 to 30dB. It gives the minimum number of errors.

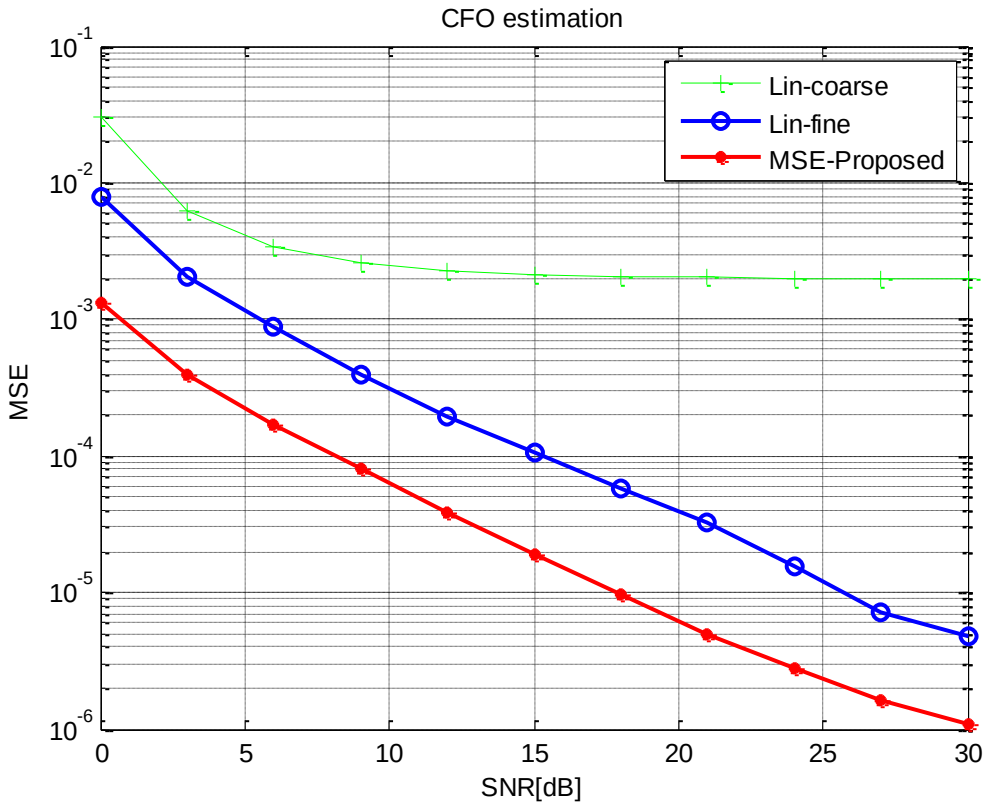

Figure 4.22. The MSE of the proposed estimator and the Lin estimator (coarse and fine estimation) under Rayleigh fading Channel 2 for frequency offset =0.295, 8QAM

The same characteristics are used for Figure 4.23 below except we used 16QAM for the constellation. The results show that both the proposed and Lin estimators present a degradation compared to Figure 4.22 above because we used a higher order of QAM. However, the Lin coarse estimator has better results than before (Figure 4.22). The MSE of our estimator is between 1.9×10^{-3} and 2.9×10^{-6} for 0 dB< SNR<30dB. So, the proposed estimator gives the best results.

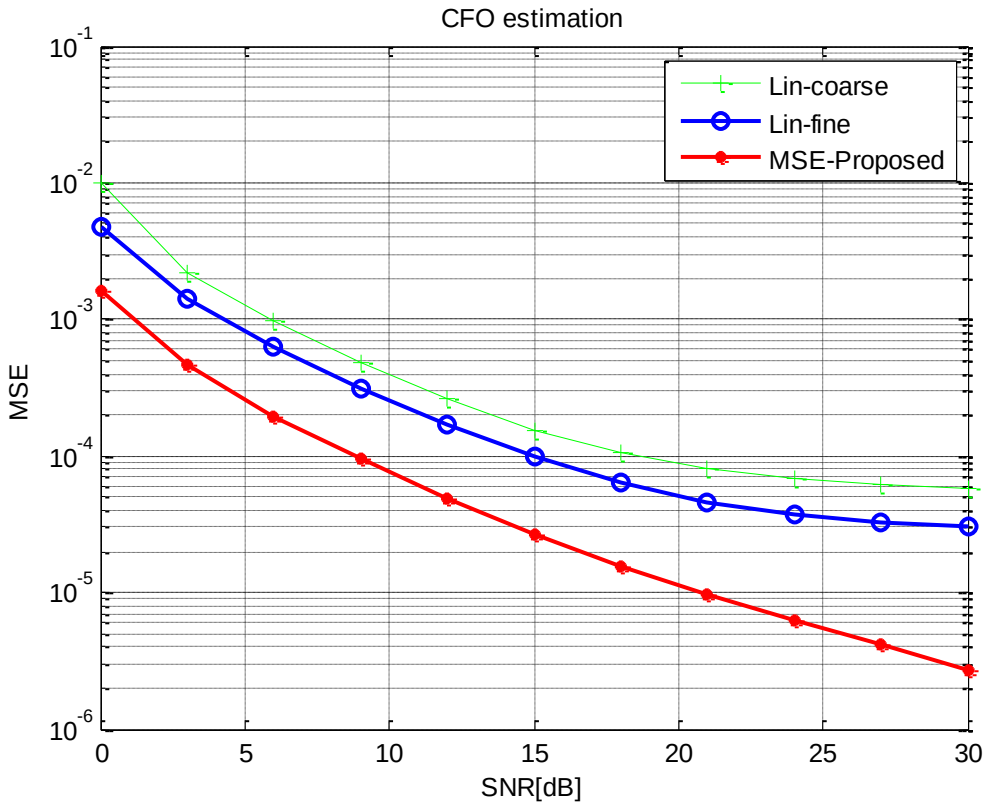

Figure 4.23. The MSE of the proposed estimator and the Lin estimator (coarse and fine estimation) under Rayleigh fading Channel 2 for frequency offset =0.295, 16QAM

Figures 4.24 and 4.25 present the results for 32QAM and 64QAM, respectively. These figures prove the robustness of our estimator even for high QAM orders. The MSE of the proposed estimator varies from 3×10^{-3} to 10^{-5} for an SNR between 0dB and 30dB, whereas the MSE of the Lin fine estimator varies from 10^{-2} to 2.9×10^{-5} as is presented in Figure 4.24. The MSE of the Lin coarse estimator varies from 10^{-2} to 3×10^{-4} for 0dB<SNR<15dB and stabilizes at 2.7×10^{-4} for SNR>15dB. In Figure 4.25, we notice that both the proposed estimator and the Lin coarse estimator outperform the Lin fine estimator for a low SNR (SNR<10dB). For an SNR >10dB , the Lin fine estimator gives better results than the Lin coarse estimator and gives lower results than the proposed estimator. As a result, the proposed estimator offers the best results for different QAM orders under Rayleigh Channel 2.

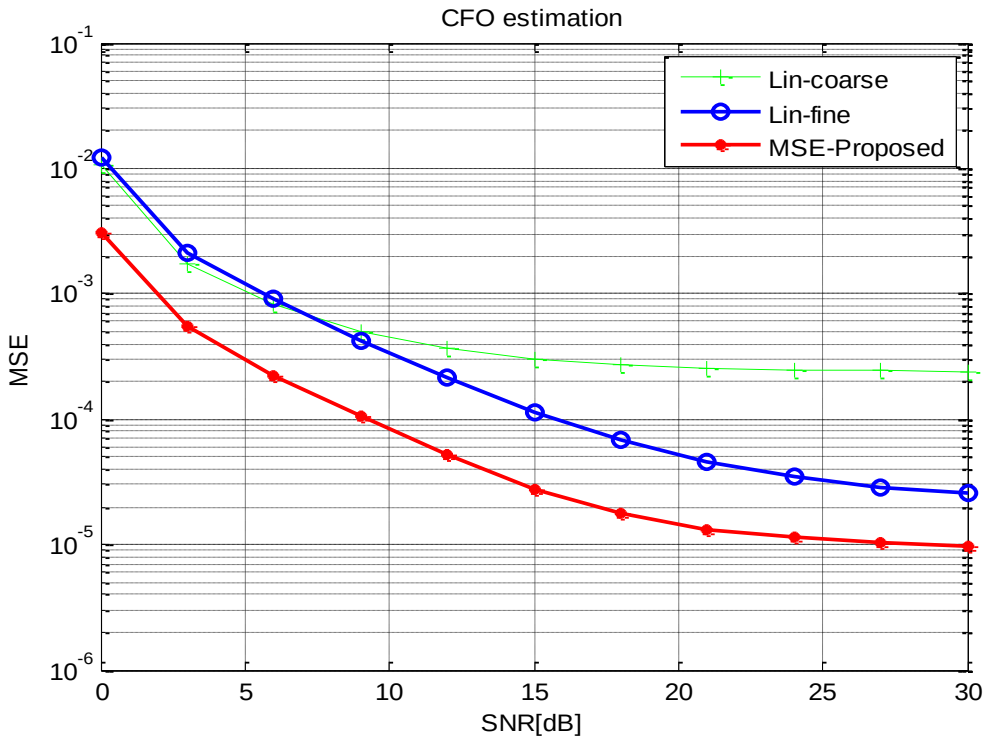

Figure 4.24. The MSE of the proposed estimator and the Lin estimator (coarse and fine estimation) under Rayleigh fading Channel 2 for frequency offset =0.295, 32QAM

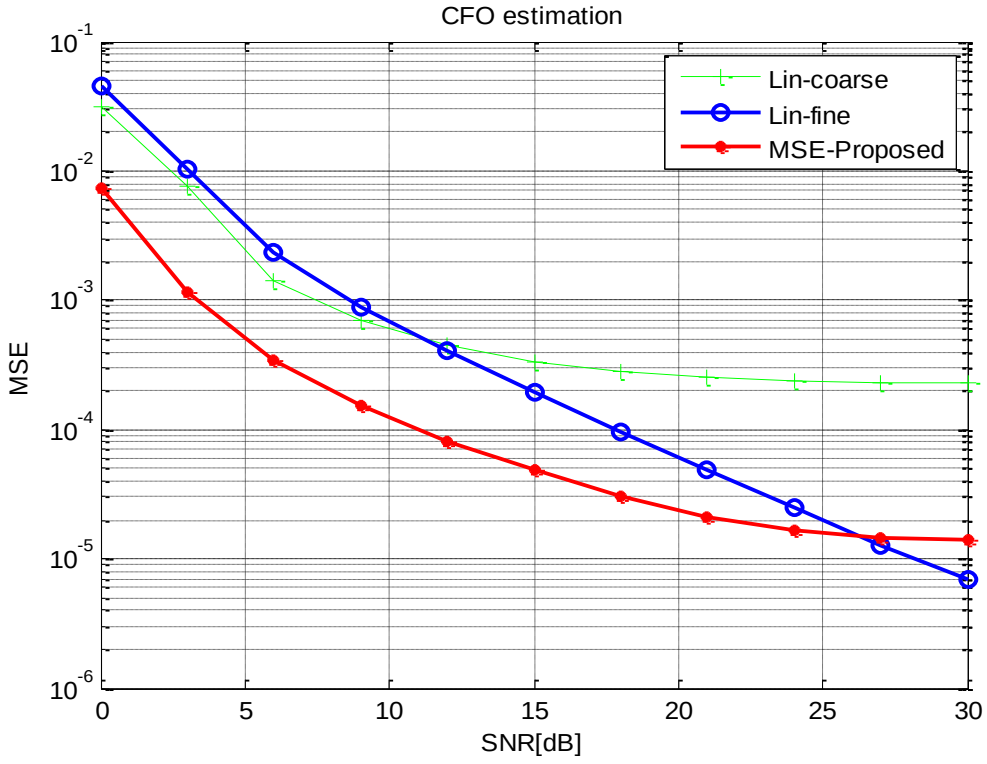

Figure 4.25. The MSE of the proposed estimator and the Lin estimator (coarse and fine estimation) under Rayleigh fading Channel 2 for frequency offset =0.295, 64QAM

4.4.3. Evaluation of the Proposed Method over Rayleigh Fading Channel 3

The Monte Carlo simulation is adopted and the quadrature amplitude modulation (QAM) is used for the constellation of transmission symbols. The size of the DFT matrix is $N = 64$, and the length of CP is $L = 16$. From Figure 4.26 to Figure 4.29, we use the channel model in Table 4.2 abbreviated as Channel 3. The channel is a multipath Rayleigh fading channel with additive white Gaussian noise (AWGN). There are four paths with delays of [0 4 8 12] samples. The variances of these taps are given by [0.25, 0.25, 0.25, 0.25], and the mean square delay spread is 20. The channel does not change while the CFO estimation is being performed. At the beginning, the normalized CFO is set to 0.295. The mean square error (MSE) of the normalized CFO estimation is adopted as the figure of merit. For comparison, we also include the results of Lin [54] and Beek [36].

The simulation results validate the effectiveness of the novel estimator under a Rayleigh fading channel, and show that with a higher SNR, a lower MSE is obtained. We plot the performance of our proposed estimator for different orders of QAM.

We see that our proposed estimator could outperform the Lin estimator especially when using 32QAM for the constellation. In addition, we can observe a performance degradation when using 32QAM and 64QAM for our estimator as compared to the results obtained by 8QAM and 16QAM for the low SNR. In addition, we should emphasize that our proposed estimator offers significant improvement when compared to both the Lin coarse estimator and the Lin fine estimator. It is observed that our proposed estimator and the Lin estimator have closer results, around 10^{-4} ,when using 16QAM for the constellation.

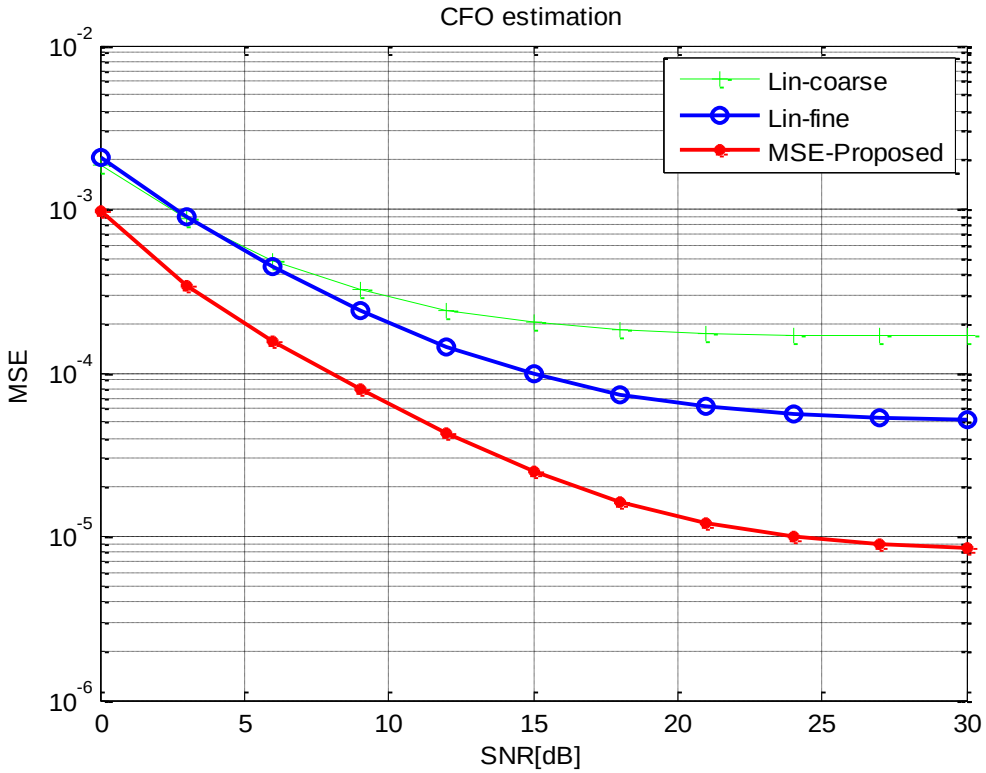

Figure 4.26. The MSE of the proposed estimator and the Lin estimator (coarse and fine estimation) under Rayleigh fading Channel 3 for frequency offset =0.295, 8QAM

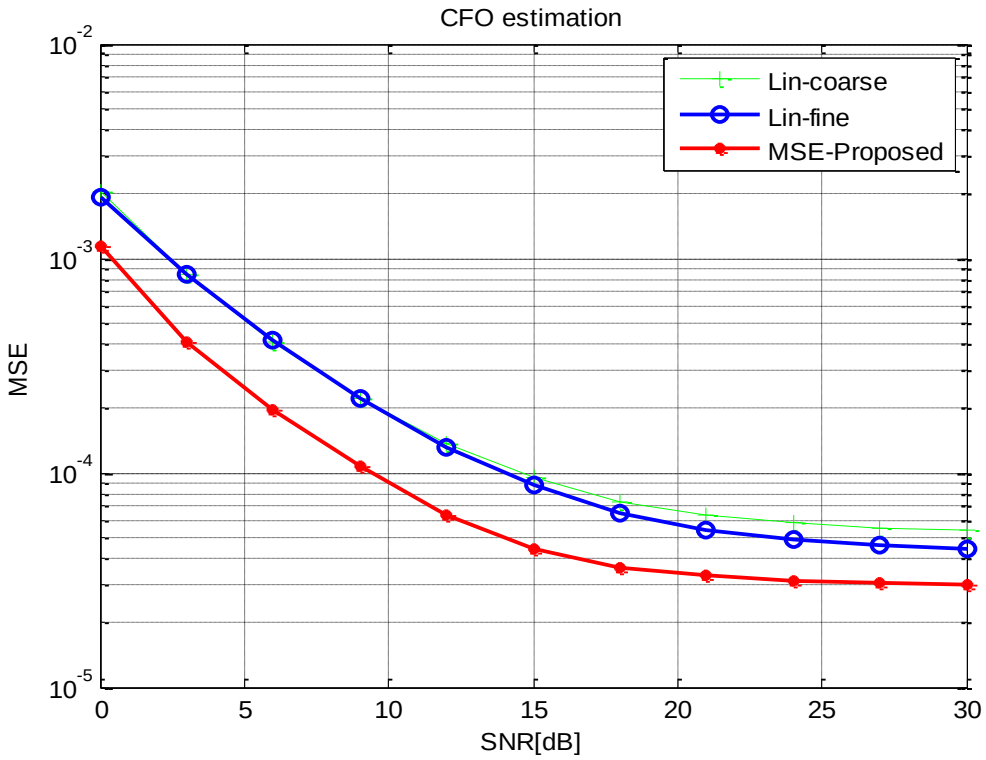

Figure 4.27. The MSE of the proposed estimator and the Lin estimator (coarse and fine estimation) under Rayleigh fading Channel 3 for frequency offset =0.295, 16QAM

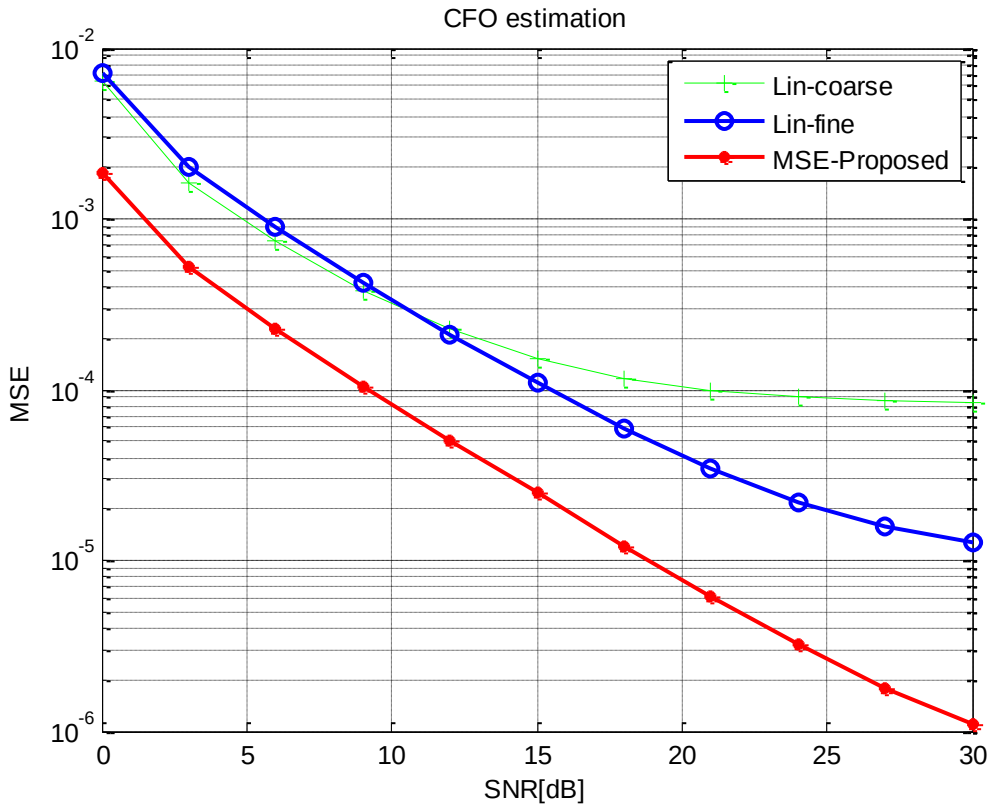

Figure 4.28. The MSE of the proposed estimator and the Lin estimator (coarse and fine estimation) under Rayleigh fading Channel 3 for frequency offset =0.295, 32QAM

In Figure 4.29 the MSEs of our estimator vary from 8×10^{-3} to 3×10^{-5} for an SNR inferior to 20dB and stabilize at 3×10^{-5} for an SNR superior to 20dB. However, the MSEs of the Lin fine estimator is between 6×10^{-2} to 4×10^{-5} for an SNR between 0dB and 30dB. The MSEs of the Lin coarse estimator vary from 4×10^{-2} to 5×10^{-4} for an SNR inferior to 20dB and saturate at this value for an SNR superior to 20dB.

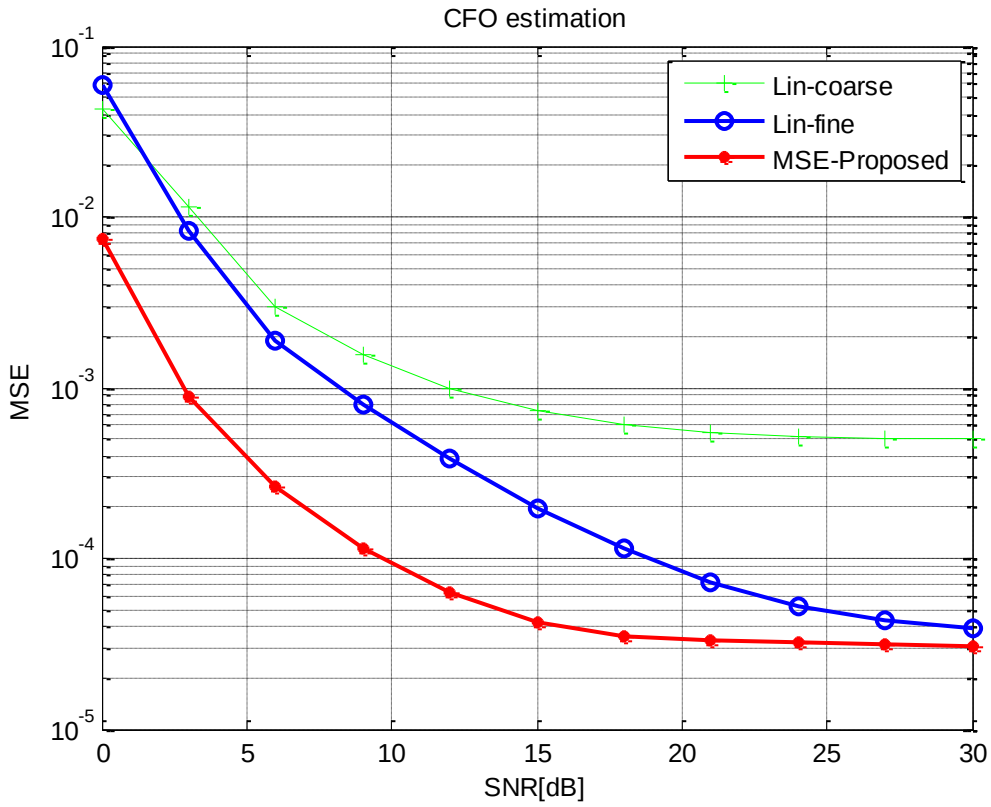

Figure 4.29. MSE of the proposed estimator and the Lin estimator (coarse and fine estimation) under Rayleigh fading Channel 3 for frequency offset =0.295, 64QAM

4.5. Assessment of the Proposed Estimator using Different Carrier Frequency Offset (CFO)

Figures 4.30, 4.31, 4.32, 4.33 and 4.34 are drawn to verify the effectiveness of the proposed estimator for different values of the carrier frequency offset. They show the estimation accuracy against the SNR for various estimators: the proposed estimator, and the Lin coarse and fine estimators. The 16QAM constellation and Channel 3 are used and don't change while the CFO estimation is being executed.

Figures 4.30, 4.31 and 4.32 present the MSEs versus the SNR (dB) for CFO=0.15, 0.245, 0.345, respectively. It is clear that our proposed estimator outperforms the Lin estimators for all CFO values. We notice in Figure 4.29 that the MSEs of the Lin coarse estimator vary from 8×10^{-3} to 8×10^{-4} for an SNR inferior to 13dB and saturated at 8×10^{-4} for an SNR superior to 13dB. The MSE of the Lin fine estimator vary between 4×10^{-3} and 1.5×10^{-4} for 0dB<SNR<30dB. However, the proposed estimator has lower MSEs, ranging from 1.9×10^{-3} to 7×10^{-7} for an SNR between 0dB and 30dB. Thus, the results of our estimator are considered accurate.

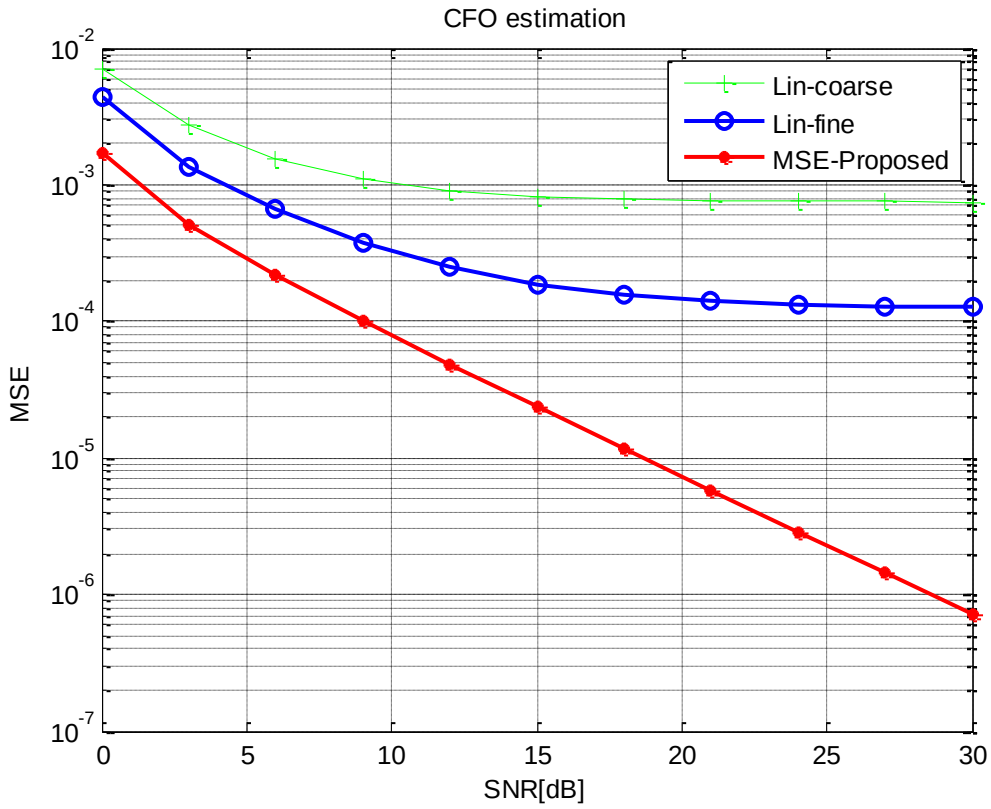

Figure 4.30. The MSE of the proposed estimator and the Lin estimator (coarse and fine estimation) under Rayleigh fading Channel 3 for frequency offset =0.15, 16QAM

Figures 4.31 and 4.32 show the resistance of the proposed estimator against the ICI. The range of the MSEs of our estimator are between 10^{-3} and 10^{-6} for 0dB<SNR<30dB. Our method still is much better than the others. Also, the Lin fine estimator outperforms the Lin coarse estimator for all SNR values.

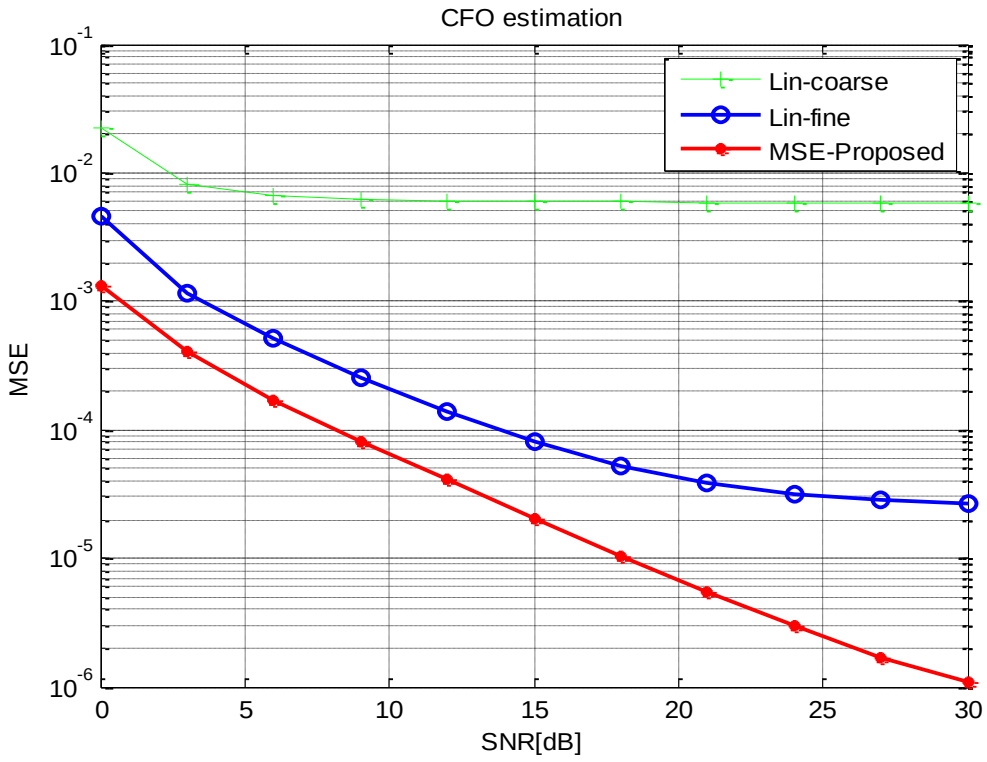

Figure 4.31. The MSE of the proposed estimator and the Lin estimator (coarse and fine estimation) under Rayleigh fading Channel 3 for frequency offset =0.245, 16QAM

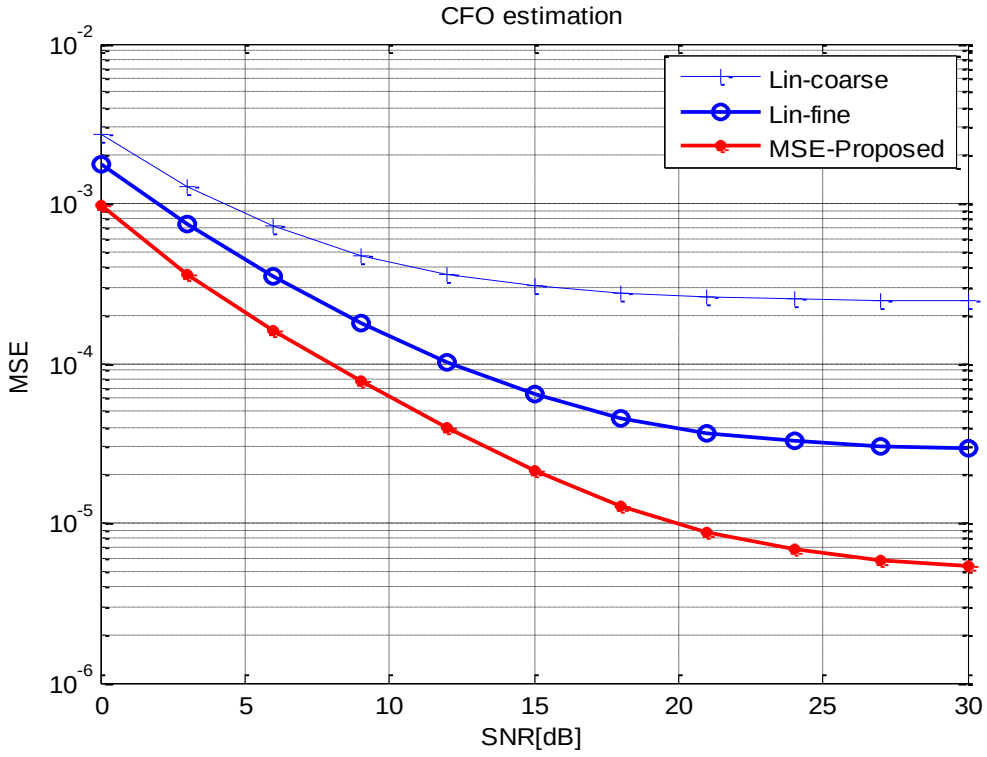

Figure 4.32. The MSE of the proposed estimator and the Lin estimator (coarse and fine estimation) under Rayleigh fading Channel 3 for frequency offset =0.345, 16QAM

As is presented in Figure 4.33, our estimator performs well even for CFO=0.445, while the performance of the Lin fine estimator degrades remarkably for an SNR between 0dB and 12dB and saturates at 3×10^{-4} dB for an SNR superior to 12dB.

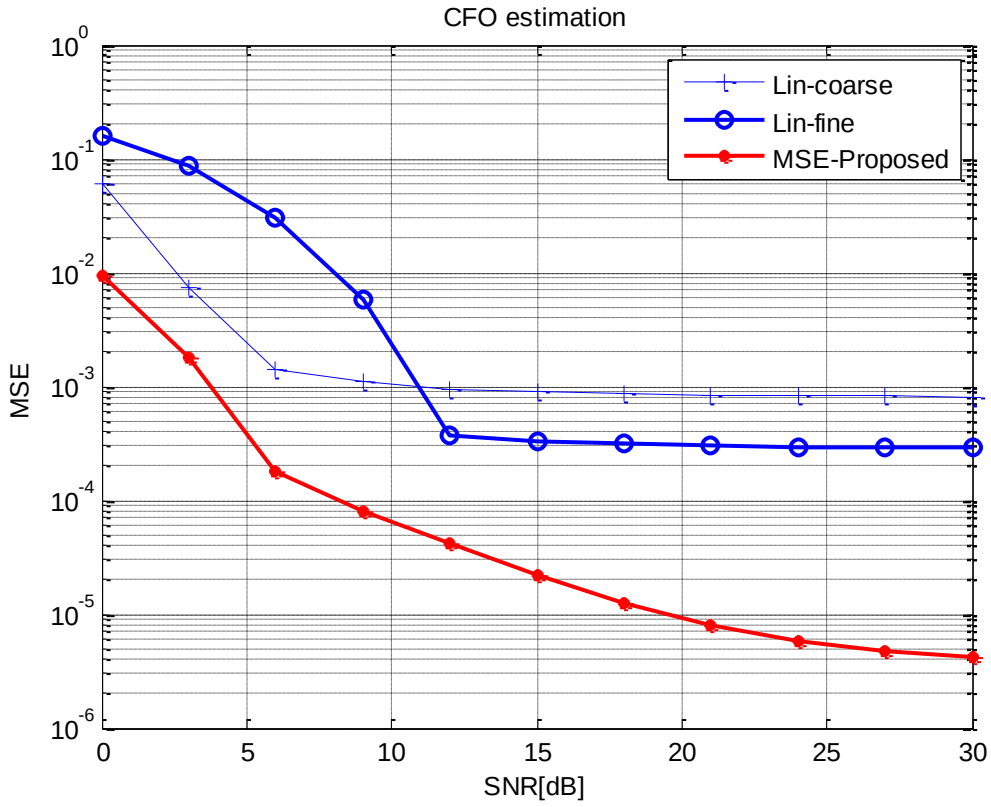

Figure 4.33. The MSE of the proposed estimator and the Lin estimator (coarse and fine estimation) under Rayleigh fading Channel 3 for frequency offset =0.445, 16QAM

The MSE versus the SNR plots for CFO=0.5 and the Rayleigh fading channel referred to as Channel 3 is shown in Figure 4.34 below. Even though the proposed method shows better performance than the other methods, the results are not effective. The performance of our estimator degrades significantly. This is because the range of frequency offset for our estimator is -0.5<CFO<+0.5. The Lin coarse and fine estimators do not perform well and their MSEs increase.

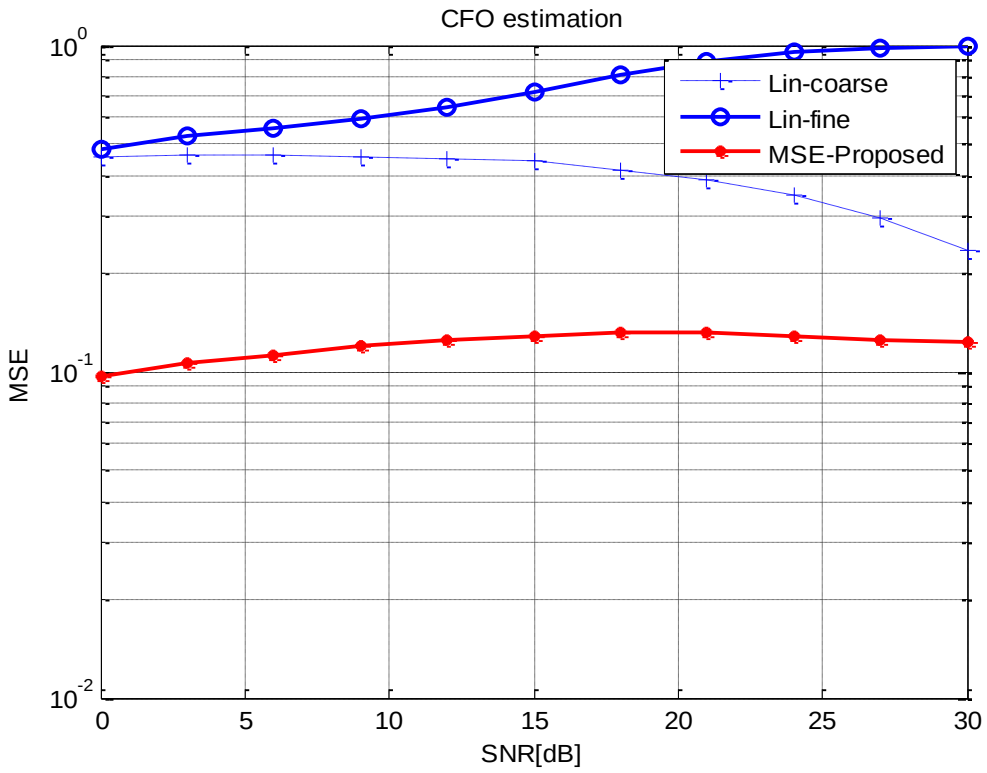

Figure 4.34. The MSE of the proposed estimator and the Lin estimator (coarse and fine estimation) under Rayleigh fading Channel 3 for frequency offset =0.5, 16QAM; k=100

4.6. Assessment of the Proposed Estimator using Different Cyclic Prefix Lengths (Ncp)

The simulations were carried out in MATLAB in order to study the effect of the cyclic prefix length and the IFFT length on the error in estimating the offset.

We investigated the performance of our method for different lengths of cyclic prefix L. Figures 4.35, 4.36 and 4.37 present the MSE versus the SNR under Rayleigh fading Channel 1, Channel 2 and Channel 3, respectively. We can see that our method always has the best performance for different lengths of cyclic prefix L under the different Rayleigh fading channels. This is evident from the simulation results as shown in Figure 4.35 for a low SNR that as the Ncp increases, the MSE decreases for both the proposed and the Lin fine estimators. As Ncp determines the effective throughput of the system, the prefix should be kept as small as possible. But, the length of the CP should be greater than the channel delay spread to minimize the symbol timing offset error. Hence, there is a tradeoff between the length of the CP and the reliability in the reception of data. Thus, to guard the efficiency of the bandwidth, the Ncp is maximized at N/4.

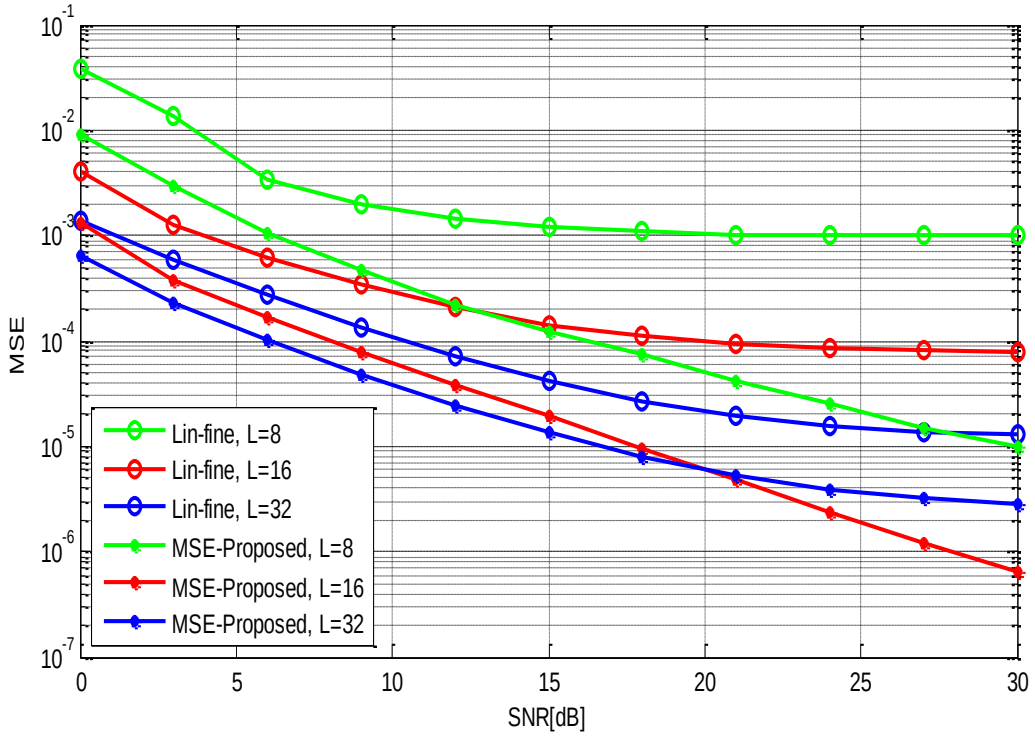

Figure 4.35. The MSE of the proposed estimator and the Lin fine estimator under Rayleigh fading Channel 1 for different Ncp frequency offset =0.25, 16QAM; N=128

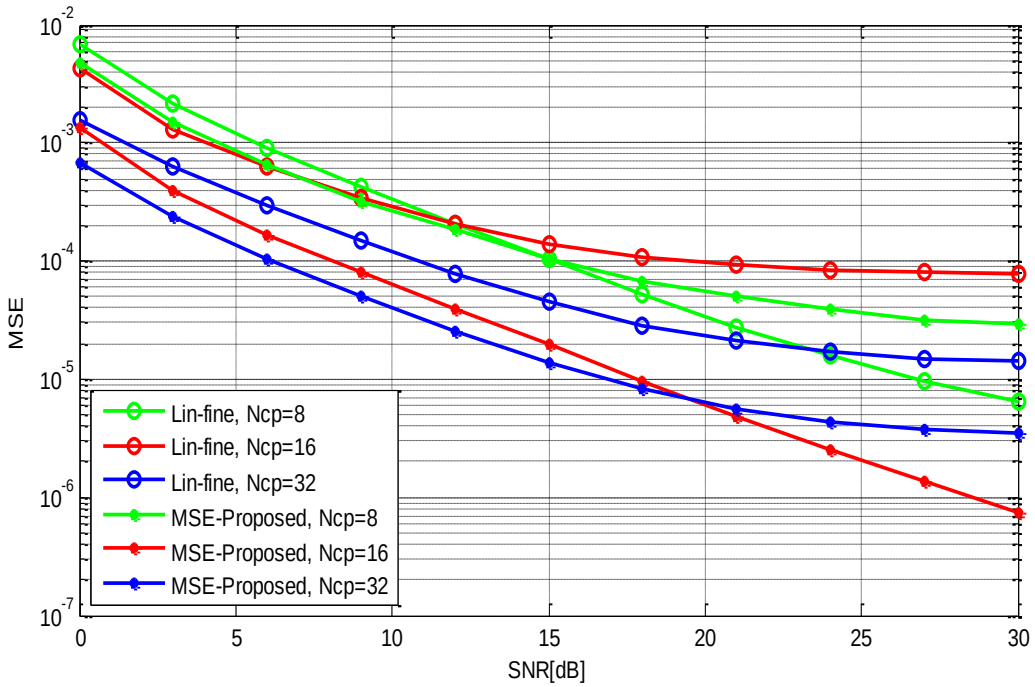

Figure 4.36. The MSE of the proposed estimator and the Lin estimator under Rayleigh fading Channel 2 for different Ncp, frequency offset =0.25, 16QAM; N=128

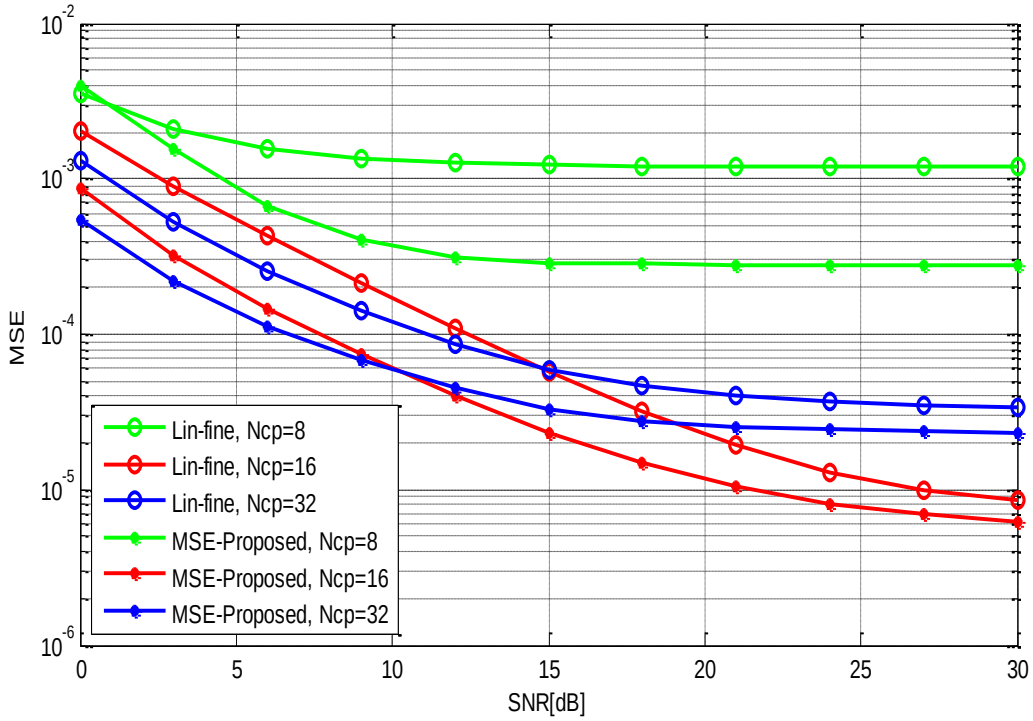

Figure 4.37. The MSE of the proposed estimator and the Lin estimator under Rayleigh fading Channel 3 for different Ncp, frequency offset =0.25, 16QAM; N=128

4.7. Assessment of the Proposed Estimator using Different FFT lengths (Nfft)

We used different lengths of subcarriers in the OFDM symbol in order to assess our proposed estimator. The results are given in Figure 4.38 below. We took different lengths of subcarriers N=32, 64, 128 for OFDM system, the length of the cyclic prefix being L=N/4. Also, in Figure 4.38, we use 16QAM for the constellation and the carrier frequency offset CFO=0.25. The signal is transmitted over Rayleigh Channel 1. It is clear that the proposed estimator is performing better than the Lin fine estimator for all values of N. As the number of subcarriers N increases, the effect of error in estimating the CFO represented by the MSE of the proposed estimator decreases. However, increasing the IFFT length also increases the complexity of the receiver.

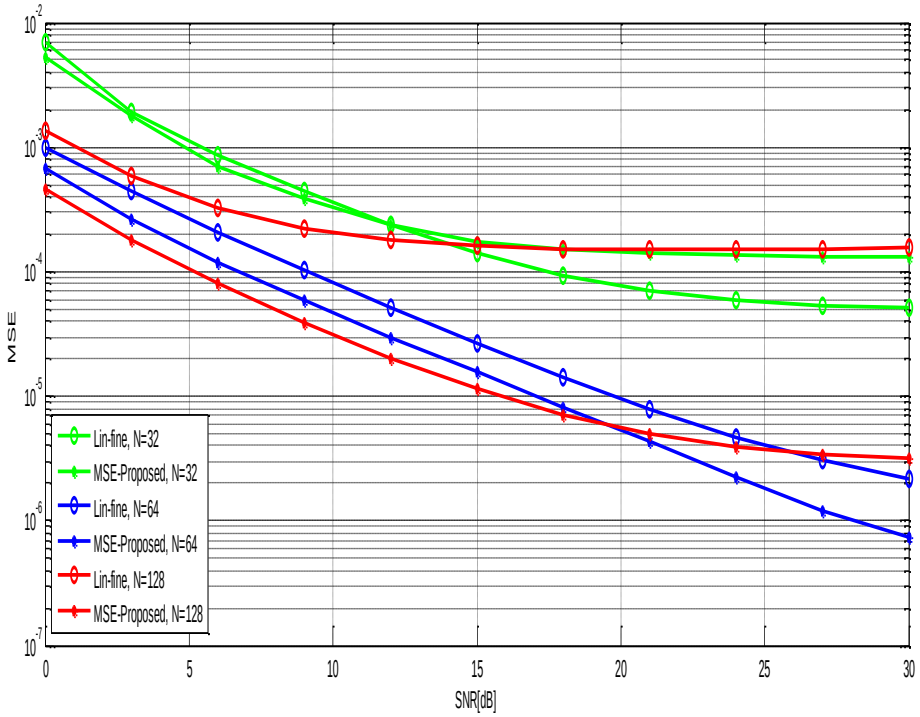

Figure 4.38. The MSE of the proposed estimator and the Lin fine estimator under Rayleigh fading Channel 1 for Ncp=N/4, frequency offset =0.25, 16QAM; N=32, 64,128

4.8. Computational Complexity

Computation requirements are important in evaluating an algorithm. We briefly analyze the computations required for these algorithms. Assume we are sending an OFDM frame with K symbols. The FFT size is N, CP is L, so a total frame has $(N + L)$ discrete samples. Assuming the algorithm starts from the detection of signal power received that passes a threshold at the receiver and ends at the estimation of the timing index for a protocol frame, and also, assuming that one complex multiplication equals four real multiplications(1 CMUL = 4 RMUL), then the proposed algorithm has the lower number of CMUL compared to Lin's estimator. The comparison between the three algorithms is presented in the table below:

Table 4.3. Comparison of the number of complex multiplications (CMUL) for CFO estimation

Blind CFO Estimation	CMUL in terms of N, L, and K
Beek's estimator [36]	LK
Lin's estimator[54]	6LK-9L/2
Proposed estimator	3LK/2

4.9. Conclusion

A proposed ML estimator of CFO for OFDM systems over Rayleigh channels is presented. This estimator is based on the correlation between the remodulated and received samples on the receiver side. The results prove the effectiveness of the proposed estimator compared to the Beek estimator and the Lin coarse and fine estimators . In addition, the results prove that the proposed estimator can achieve a much lower MSE using a short guard interval with lower computational complexity. Although the results indicate an improvement in terms of reducing the length of the cyclic prefix and increasing the OFDM performance, additional research is needed to further reduce the Ncp, completely eliminate ICI and thus be able to better increase the performance of OFDM systems.

CONCLUSION AND PERSPECTIVES

In this thesis, we studied in detail the effect of frequency offset in OFDM communication systems. Frequency offset will introduce ICI to the demodulated signal and will degrade the performance of OFDM systems. First we simulated some existing estimators to determine whether estimates produced by previous algorithms serve our project. We introduced two previous frequency estimation algorithms (Classen, Moose), and compared them. The analysis shows that data-based estimators offer better solutions in terms of mean squared errors while reducing bandwidth, which is not helpful in achieving our goal. In addition, ICI self cancellation performs much better than standard OFDM systems. Although this technique is useful for combating the impact of ICI and easy to implement, it decreases the bandwidth of the system by half. Thus, the methods that serve our work are the methods that preserve the bandwidth efficiency like Beek's estimator. This latter estimator uses redundant information contained within the cyclic prefix to mitigate the frequency offset under additive white Gaussian noise (AWGN) channel. For Beek's estimator, we expand the range of frequency offset detection, and we use a Rayleigh fading channel to evaluate the performance of the system under this channel. However, this method has limitations under multipath fading channels. Another estimator based on the cyclic prefix for blind carrier frequency offset estimation in orthogonal frequency division multiplexing OFDM transmission over multipath channels is propose by Lin and Phoung. This algorithm uses remodulated receive vectors and achieves higher estimation accuracy than other CP-based methods. In our study, we propose a new estimator that uses the redundant data within the cyclic prefix and the remodulated receive vectors to improve the performance of OFDM system for future use in the fifth generation. We compare our estimator and the existing methods. Our results outperform the existing ones in terms of mean squared errors on the one hand, and offer better bandwidth efficiency on the other.

Orthogonal frequency division multiplexing (OFDM) family is well suited for fifth generation communications. OFDM offers a series of attractive properties and features that make it widely popular. However, despite its popularity, the defects and drawbacks of OFDM, along with its high peak to average power ratio (PAPR), need to be addressed and overcome.

By increasing the velocity of the 5G and 6G mobiles in the future; we will experience more time varying channels effects on the received OFDM signals. Therefore, futur work for estimating multipath fading channels should have more attention.

In addition, combining Blind CFO estimator and training based CFO estimator need further works to achieve accurate estimate of CFO.

Bibliography

[1] Y. Bar-Ness, J. Carlin, and M. Steinberger, "Bootstrapping adaptive interference cancelers: Some practical limitations," in *Proc. IEEE GLOBE-COM,* 1982, pp. 1251–1255.

[2] B. Ans, J. Hérault, and C. Jutten, "Adaptive neural architectures: Detection of primitives," in *Proc. COGNITIVA,* Paris, France, June 1985, pp. 593–597.

[3] Wireless coverage complaint database, "what does 1G, 2G, 2.5G, 3G, 3.5G, 4G, 5G mean," Thursday, June 4, 2010: deadcellzones.com.

[4] Zhang Jian, The Development Trends of 4G Technology, Guangdong Communication Technology,2004

[5] Akhilesh Kumar Pachauri 1 and Ompal Singh ,"5G Technology – Redefining wireless Communication in upcoming years" , International Journal of Computer Science and Management Research ,Vol 1 Issue 1,Aug 2012.

[6] Ms. Anju Uttam Gawas, An Overview on Evolution of Mobile Wireless Communication Networks: 1G-6G, JRITCC, volume 3 issue 5, may2015.

[7] Ms. Lopa J. Vora, Evolution of Mobile Generation Technology: 1G to 5G and Reviewof Upcoming Wireless Technology 5G, *International Journal of Modern Trends in Engineering and Research (IJMTER) Volume 02, Issue 10, 2015.pp: 281-290.*

[8] Ms. ReshmaS ,5G Mobile Technology JARCET, Volume 2, Issue 2, February 2013.

[9] Sucheta and Yadav K. P., 2013, "A Comparative Study of 1G, 2G, 3G and 4G" International Journal of Advances in Engineering Research, Vol.No.3, no. 3.

[10] Nikhil Bhandari, Shivinder Devra, Karamdeep Singh, Evolution of Cellular Network: From 1G to 5G, International Journal of Engineering and Techniques - Volume 3 Issue 5, Sep - Oct 2017, pp:98—105.

[11] 5G radio access, Ericsson White paper, Uen 284 23-3204 Rev C, April 2016.

[12] https://www.tutorialspoint.com/5g/5g_technology.htm

[13] Introducing 5G networks –Characteristics and usages. 2016.Gemalto.Com.

[14] Charan Langton, Orthogonal frequency division multiplexing (OFDM) tutorial. http://www.complextoreal.com/chapters/ofdm2.pdf.

[15] L. Hanzo, M. Munster, B. J. Choi and T. Keller, *OFDM and MC-CDMA for broadband multi-user Communications,* New York, IEEE press, 2000.

[16] BRAHMAJI T.A.R.K., an efficient ICI cancellation technique for OFDM communication systems, thesis, Department of Electrical Engineering National Institute of Technology Rourkela 2009.

[17] R.E. Ziemer, W.H. Tranter, and D.R. Fannin, Signals and Systems: Continuous and Discrete, Fourth Edition, New Jersey: Prentice-Hall, 1998.

[18] W.Y. Zou, Y. Wu, "COFDM, an Overview", IEEE Transactions on Broadcasting, Vol. 41, no 1, pp. 1-8, 1995.

[19] Sedki Younis, Synchronization Algorithms and Architectures for Wireless OFDM Systems, thesis of Doctor of philosophy, School of Electrical, Electronic and Computer Engineering, Faculty of Science, Agriculture and Engineering, Newcastle University, UK.

[20] Natalia Revuelto, PAPR reduction in OFDM systems, Master of Science in Telecommunication Engineering & Management, polytechnic university of Catalonia.

[21] Wei Zhang, Channel and frequency offset estimation for OFDM-based systems, Phd thesis Electrical and Computer Engineering Department, Edmonton, Alberta, 2011.

[22] Steven Charles Hemple, Analysis and Simulation Of Wireless OFDM Communicaions, Master Thesis of Science in Applied Mathematics with a Concentration in Mathematical Theory of Communication Systems.

[23] Arun Gangwar1, Manushree Bhardwaj2, An Overview : Peak to Average Power Ratio in OFDM system & its Effect, International Journal of Communication and Computer Technologies, Vol:01, N°02, pp. 22-25, 2012.

[24] R.F.H. Fischer, "Widely-Linear Selected Mapping for Peak-to-Average Power Ratio Reduction in OFDM," IEEE Electronics Letters, pp. 766- 767, July 2007.

[25] Gupta K et al. PAPR reduction of OFDM using a new phase sequence in SLM technique, IEE. 2013; 2(2):125–9.

[26] Kim D-K, Shi D-J, Park Y-S, Song B-G. New peak-windowing for PAPR reduction of OFDM systems. APWCS. 2005 Aug; 169–73.

[27] SeungHee Han and Jae Hong Lee. An overview of peak-to-average power ratio reduction techniques for multicarrier transmission. IEEE Wireless Communications, 12(2):56 – 65, 2005.

[28] Praveen Pawar, Deepak Pancholi, A Review Paper on OFDM and PAPR, International Journal of Science and Research IJSR, Vol :5 N°:6, pp: 394- 396, 2016.

[29] TevfikYücek, Self-interference Handling in OFDM Based Wireless Communication Systems, Master thesis, Department of Electrical Engineering, College of Engineering, University of South Florida, 2003.

[30] Supplement to IEEE standard for information technology telecommunications and information exchange between systems - local and metropolitan area networks - specific requirements. Part 11: wireless LAN Medium Access Control (MAC) and Physical Layer (PHY) specifications: high-speed physical layer in the 5 GHz band, The Institute of Electrical and Electronics Engineering, Inc. Std. IEEE 802.11a, Sept. 1999.

[31] K. Sathananthan and C. Tellambura, \Performance analysis of an OFDM system with carrier frequency offset and phase noise," in Proc. IEEE Veh. Technol. Conf., vol. 4, Atlantic City, NJ, Oct. 2001, pp. 2329- 2332.

[32] Rajet Krishnan, On the Impact of Phase Noise in Communication Systems - Performance Analysis and Algorithms, Phd Thesis, Communication Systems Group, Department of Signals and Systems, Chalmers University of Technology, Gothenburg 2015.

[33] Luca Rugini, Paolo Banelli, Geert Leus. OFDM Communications over Time Varying Channel. Chapter 07, University of Perugia, Perugia, Italy, 2011, pp: 285- 336. http://dx.doi.org/10.1016/B978-0-12-374483-8.00007-8

[34] X. Wang and B. Hu, "A Low-Complexity ML Estimator forand Sampling Frequency Offsets in OFDM Systems, " IEEE Commun. Lett., vol. 18, no. 3, pp. 503–506, Mar. 2014.

[35] P. H. Moose, " A technique for orthogonal frequency division multiplex ing frequency offset correction," IEEE Trans. Commun., vol. 42, pp2908–2914, 1994.

[36] J. J. Van de Beek, et al, " ML estimation of time and frequency offset in OFDM systems," IEEE Trans. Signal Process., vol. 45, no. 7, pp. 1800–1805, 1997.

[37] P. S. Wang and D. W. Lin, " Maximum-Likelihood Blind Synchronization for GFDM Systems" IEEE Signal Process.Lett., vol. 23, no. 6, pp. 790–794, June. 2016.

[38] M. Liu, B. Li, and J. Ge, " Blind Estimation for OFDM Fractional frequency offset Over Multipath Channels," Wireless Pers. Commun., 2014.

[39] T. Fusco and M. Tanda, " Blind synchronization for OFDM systems in multipath channels," IEEE Trans. Wireless Commun., vol. 8, no. 3. pp. 1340–1348, 2009.

[40] Biao Chen, Hao Wang, Maximum Likelihood Estimation of OFDM Carrier Frequency Offset. 0-7803-7400-2/02/$17.00 © 2002 IEEE.pp : 49—53.

[41] H. Liu and U. Tureli, "A high-efficiency carrier estimator for OFDM communications," *IEEE Communications Letters*, vol.2, pp.104-106, April 1998.

[42] Lin, J. C. (2003) 'Maximum-likelihood frame timing instant and frequency offset estimation for OFDM communication over a fast Rayleigh-fading channel', *IEEE Transactions on Vehicular Technology*, Vol. 52, No.4, pp.1049 – 1062.

[43] TiejunLv, Hua Li, and Jie Chen, Joint Estimation of Symbol Timing and Carrier Frequency Offset of OFDM Signals Over Fast Time-Varying Multipath Channels, IEEE Transactions on Signal Processing, VOL. 53, NO. 12, DECEMBER 2005, pp: 4526—4535.

[44] W. L. Chin, " ML estimation of timing and frequency offsets using distinctive correlation characteristics of OFDM Signals over dispersive fading channels," IEEE Trans. Veh. Technol., vol.60, no. 2, pp. 444–456, 2011.

[45] M. Liu, B. Li, and J. Ge, " Blind Estimation for OFDM Fractional frequency offset Over Multipath Channels," Wireless Pers. Commun., 2014.

[46] Mo,R.,&Chew,Y. H. (2006).Ajoint blind timing and frequency offset estimation forOFDMsystems over frequency selective fading channels. *IEEE Transaction on Wireless Communications*, *47*(5), 2604–2614.

[47] K. Pushpa, C. N. Kishore, and Y. Yoganandam, "A new method for frame synchronization in OFDMA mode of WMAN," in *Proc. 2008 TENCON - IEEE Region 10 Conf.*

[48] Michele Morelli, Leonardo Marchetti, Macro Moretti. Maximum Likelihood Frequency Estimation and Preamble Identification in OFDMA-based WiMAX Systems. IEEE Trans Wireless Commun. 2014 Mar;13(03):1582–1592.

[49] M. Ruan, M. C. Reed, and Z. Shi, "A universal frequency offset estimator for OFDM applications," in *Proc. 2009 IEEE Global Commun. Conf.*, pp. 1–5.

[50] Qi Zhan, Hlaing Minn. New Integer Normalized Carrier Frequency Offset Estimators. IEEE Transactions on SignalProcessings. 2015;63(14):3657–3670.

[51] BaileXie, WenxunQiu, Hlaing Minn. Exact signal model and new carrier frequency offset compensation scheme for OFDM. IEEE Transactions on Wireless Communications. 2012;11(02):550 – 555.

[52] Po-Sen Wang, David W Lin. On Maximum-Likelihood Blind Synchronization Over WSSUS Channels for OFDM Systems. IEEE Transactions on Signal Processings. 2015;63(19):5045–5059.

[53] J. A. López-Salcedo, E. Gutiérrez, G. Seco-Granados, and A. L. Swindlehurst, "Unified framework for the synchronization of flexible multicarrier communication signals," *IEEE Trans. Signal Process.*, vol. 61, no. 4, pp. 828–842, Feb. 15, 2013.

[54] Tzu-Chiao Lin, See-May Phoong. A New Cyclic-Prefix Based Algorithm for Blind CFO Estimation in OFDM Systems. IEEE Trans Wireless Commun. 2016 Jun;15(06):3995–4008.

[55] Feifei Gao, Yonghong Zeng, Arumugam Nallanathan, Tung-Sang Ng. Robust subspace blind channelestimationforcyclicprefixed MIMO OFDM systems:Algorithm, identifiabilityandperformanceanalysis. IEEE J Sel Areas Commun. 2008 Feb;26(02):378–388.

[56] Yong-Hwa Kim, and Jong-Ho Lee, Joint Maximum Likelihood Estimation of Carrier and Sampling Frequency Offsets for OFDM Systems,IEEE TransactionsonBroadcasting, vol. 57, no. 2, june 2011, pp: 277—283.

[57] Tilde Fusco, Ferdinando Marrone, Mario Tanda, Semiblind techniques for carrier frequency offset estimation in OFDM systems. Science Direct, Signal Processing 88 (2008) 704–718.

[58] Lee, J., Lou, H. and Toumpakaris, D. (2004) 'Maximum likelihood estimation for time and frequency offset for OFDM systems', *Electronics Letters*, Vol. 40, No. 22, pp.1428–1429.

[59] Classen, F., Meyr, H. Frequency synchronization algorithms for OFDM systems suitable for communication over frequency selective fading channels. In *Proceedings of the 44th IEEE Vehicular Technology Conference*. 1994, vol. 3, p. 1655–1659. DOI: 10.1109/VETEC.1994.345377.

[60] Sandeep Kaur, Harjinder Singh, Amandeep Singh Sappal, Carrier Frequency Offset Estimation for OFDM Systems Using Time/Frequency-Domain Techniques, *International Journal of Advanced Research in Computer Science and Electronics Engineering Volume 1, Issue 2, April 2012, pp:154—160.*

[61] Timothy M. Schmidl and Donald C. Cox, Robust Frequency and Timing Synchronization for OFDM. IEEE Transactions on Communications, vol. 45, no. 12, december 1997, pp:1613—1621.

[62] Claus Muschallik, Improving an OFDM Reception Using An Adaptive Nyquist Windowing. IEEE Transactions on Consumer Electronics, Vol. 42, No. 3, august 1996, pp:259—269.

[63] Ken Gentile, Design a PLL Filter When Only the Zero Resistor and Capacitor Are Adjustable, Analog Dialogue 49-02, February 2015, pp:1—6.

[64] LalithaPakala and Bernhard Schmauss, Applications of Kalman Filters for Coherent Optical Communication Systems. In book: Kalman Filters - Theory for Advanced Applications, 2017, pp: 205—231. DOI: 10.5772/intechopen.71617

[65] Alejandro Ribeiro, Ioannis D. Schizas, Stergios I. Roumeliotis, And Georgios B. Giannakis. Kalman filtering in Wireless Sensor Networks : Reducing Communication Cost In State Estimation Problems. IEEE Control Systems Magazine ,April 2010, pp: 66—86.

[66] K Nosrati, AS Rostami, A Azemi, F MohannaA Private Secure Communication Scheme Using UKF-based Chaos Synchronization. Journal of Engineering Science & Technology Review 8 (2), 2015, pp: 96 – 105.

[67] Yuping Zhao, Sven-Gustav Häggman, Intercarrier Interference Self-Cancellation Scheme for OFDM Mobile Communication Systems. IEEE Transactions On Communications, Vol. 49, No. 7, July 2001, pp: 1185—1191.

[68] Y. Zhao and S.-G. Häggman, "Sensitivity to Doppler shift and carrier frequency errors in OFDM systems—The consequences and solutions," in *Proc. IEEE 46th Vehicular Technology Conf.*, Atlanta, GA, Apr. 28–May 1, 1996, pp. 1564–1568.

[69] ---, "A general coding method to minimize intercarrier interference in OFDM mobile communication systems," in *Proc. Int. Wireless and Telecommunications Symp./Exhibition (IWTS'97)*, vol. 1, Shah Alam, Malaysia, May 14–16, 1997, pp. 231–235.

[70] J. Armstrong, "Analysis of new and existing methods of reducing intercarrier interference due to carrier frequency offset in OFDM," *IEEE Trans. Commun.*, vol. 47, pp. 365–369, Mar. 1999.

[71] K. A. Seaton and J. Armstrong, "Polynomial cancellation coding and finite differences," *IEEE Trans. Inform. Theory*, vol. 46, pp. 311–313, Jan. 2000.

[72] Y. Zhao, J.-D. Leclercq, and S.-G. Häggman, "Intercarrier interference compression in OFDM communication systems by using correlative coding," *IEEE Commun. Lett.*, vol. 2, pp. 214–216, Aug. 1998.

[73] BehrouzFarhang-Boroujeny , Hussein Moradi. OFDM Inspired Waveforms for 5G. *IEEE Communications Surveys&Tutorials*. 2016;18(4):2474–2492.

[74] Recommendation ITU-R M.2083. IMT Vision .Framework and overall objectives of the future development of IMT for 2020 and beyond [Internet]. 2015. Available from: https://www.itu.int/dms_pubrec/itu-r/rec/m/R-REC-M.2083-0-201509-I!!PDF-E.pdf

[75] C H. M. R. Nurul, Z. Mansor, M. K. A. Rahim. Dual element MIMO planar inverted-F antenna (PIFA) for 5G millimeter wave application. *TELKOMNIKA*. 2019 Aug;17(4):1648–55.

[76] Ali A. Nasir, Salman Durrani, Hani Mehrpouyan, Steven D. Blostein and Rodney A. Kennedy. Timing and carrier synchronization in wireless communication systems: a survey and classification of research in the last 5 years. *EURASIP Journal on Wireless Communications and Networking*. 2016;180.

[77] Bo AiZhi-xing Yang, Chang-yong Pan, Jian-huaGe, Yong Wang, Zhen Lu. On the Synchronization Techniques for Wireless OFDM Systems. *IEEE Transactions on Broadcasting*. 2006;52(02):236– 244.

[78] ShagunSharma ,Khushal Thakur. *Carrier frequency Offset in OFDM Systems*. Second International Conference on Inventive Systems and Control (ICISC 2018). Coimbatore. 2018;369–373.

[79] Ankita Yadav Akanksha Dixit. A Review on Carrier Frequency Offset Estimation in OFDM Systems. *Journal of Emerging Technologies and Innovative Research*. 2017 Jul;04(07):108–112.

[80] Gaofeng Cui, Cheng Wang, Weidong Wang, Yinghai Zhang. Frequency Offset Compensation for Satellite Communication System with CE-OFDM. *China Communications*. 2017;14(8):93–104.

[81] P. Muneer , S. M. Sameer. Pilot-Aided Joint Estimation of Doubly Selective Channel and Carrier Frequency Offsets in OFDMA Uplink With High-Mobility Users. *IEEE Transactions on VehicularTechnology*. 2015 Jan;64(1):411–417.

[82] Yong-An Jung, Joon-Yub Kim, Young-Hwan You. Complexity Efficient Least Squares Estimation of Frequency Offsets for DVB-C2 OFDM Systems. *IEEE Access*. 2018;6:35165–170.

[83] Po-Sen Wang, David W Lin. Maximum-Likelihood Blind Synchronization for GFDM Systems. *IEEE SignalProcessLett*. 2016 Jun;23(06):790–794.

[84] Sucharita Chakraborty, Debarati Sen. Joint Estimation of Time, Frequency Offsets, and Channel Gains With ICIs in EF Multi-relay DMIMO-OFDM System.*IEEE Transactions on Vehicular Technology*. 2017 Jul;66(07):5822–5838.

[85] Jeffrey G. Andrews, Stefano Buzzi, Wan Choi, Stephen Hanly, Angel Lozano, Anthony C.K. Soong, Jianzhong Charlie Zhang,. What Will 5G Be? *IEEE Journal on Selected Areas in Communications*. 2014 Jun;32(6):1065–1082.

[86] Sameer A Dawood, F. Malek, MS Anuar, HA Rahim. Enhancement the Performance of OFDM based on Multiwavelets Using Turbo Codes. *TELKOMNIKA Indonesian Journal of Electrical Engineering*. 2015 Dec;13(4):1225–1232.

[87] JianchengAn , Lu Gan , Hongshu Liao. *A non-data-aided algorithm based on ML for OFDM synchronization*. 2018 International Conference on Electronics Technology (ICET). Chengdu. 2018 Jul;1–6.

[88] Rawaa J. Hasan, Hikmat N. Abdullah. Comparative study of selected subcarrier index modulation OFDM schemes. *TELKOMNIKA Indonesian Journal of Electrical Engineering*. 2019 Feb;17(1):15–22.

[89] R. V. Nee and R. Prasad, OFDM for Wireless Multimedia Communications, Boston: Artech House, 2000.

[90] R. Gustafsson, A. Mohammed, Simulation of Wireless Fading Channels, Department of Telecommunications and Signal Processing Blekinge Institute of Technology Ronneby, Sweden, May 2003.

[91] W. Stallings. *Wireless Communications and Networks*. Prentice-Hall, New Jersey, 2002.

[92] Bernard Sklar, “Rayleigh fading channels in mobile digital communication systems”, IEEE communications Magazine, July 1997, pp: 90—100.

[93] A. Tkac, V. Wieser and S. Pollak, "Calculation of impulse response in Rician and Rayleigh channel," *2012 ELEKTRO*, Rajeck Teplice, 2012, pp. 99-102. doi: 10.1109/ELEKTRO.2012.6225580

[94] Yang-Seok Choi, P. J. Voltz and F. A. Cassara, "On channel estimation and detection for multicarrier signals in fast and selective Rayleigh fading channels," in *IEEE Transactions on Communications*, vol. 49, no. 8, pp. 1375-1387, Aug. 2001. doi: 10.1109/26.939860

International Publication

Atoui Sakina, Doghmane Noureddine, Afifi Sadek, “ Blind Frequency Offset Estimator for OFDM Systems”, *TELKOMNIKA Telecommunication, Computing, Electronics and Control.* Vol. 17, No. 6**.** Décembre 2019, pp. 2722-2728.